RATIONAL DESIGN OF RATIOMETRIC CHEMOSENSOR VIA MODULATION OF ENERGY DONOR EFFICIENCY

A THESIS SUBMITTED TO
THE GRADUATE SCHOOL OF NATURAL AND APPLIED SCIENCES
OF
MIDDLE EAST TECHNICAL UNIVERSITY

BY

RUSLAN GULIYEV

IN PARTIAL FULFILLMENT OF THE REQUIREMENTS
FOR
THE DEGREE OF MASTER OF SCIENCE
IN
CHEMISTRY

AUGUST 2008

Approval of the thesis:

RATIONAL DESIGN OF RATIOMETRIC CHEMOSENSOR VIA MODULATION OF ENERGY DONOR EFFICIENCY

submitted by **Ruslan Guliyev** in partial fulfillment of the requirements for the degree of **Master of Science in Chemistry Department, Middle East Technical University** by,

Prof. Dr. Canan Özgen _____
Dean, Graduate School of **Natural and Applied Sciences**

Prof. Dr. Ahmet M. Önal _____
Head of Department, **Chemistry**

Prof. Dr. Engin U. Akkaya _____
Supervisor, **Chemistry Dept., METU**

Examining Committee Members:

Prof. Dr. Ayhan S. Demir _____
Chemistry Dept.,METU

Prof. Dr. Engin U. Akkaya _____
Chemistry Dept., METU

Prof. Dr. Özdemir Doğan _____
Chemistry Dept., METU

Assist. Prof. Fatih Danışman _____
Chemistry Dept., METU

Dr. Ö. Altan Bozdemir _____
Chemistry Dept., Bilkent University

Date:

I hereby declare that all information in this document has been obtained and presented in accordance with academic rules and ethical conduct. I also declare that, as required by these rules and conduct, I have fully cited and referenced all material and results that are not original to this work.

Name, Last name: Ruslan Guliyev

Signature:

ABSTRACT

RATIONAL DESIGN OF RATIOMETRIC CHEMOSENSOR VIA MODULATION OF ENERGY DONOR EFFICIENCY

Guliyev, Ruslan
M.S., Department of Chemistry
Supervisor: Prof. Dr. Engin U. Akkaya

August 2008, 75 pages

Rational design of fluorescent chemosensors is an active area of supramolecular chemistry, photochemistry and photophysics. Ratiometric chemosensors are even more important, as they have an internal system for self-calibration. In order to develop a new methodology for a ratiometric chemosensor design, we proposed coupling of energy transfer phenomenon to ion sensing.

In this study, we targeted energy transfer cassette type chemosensors, where the efficiency of transfer is modulated on the donor side, by metal ion binding which changes the spectral overlap. This work involves the synthesis of a number of EET systems with varying degrees of EET efficiency.

The results suggest that this strategy for ratiometric ion sensing is a promising one, enabling a modular approach in chemosensor design.

Keywords: Supramolecular chemistry, boradiazaindacene, fluorescent chemosensor, energy transfer system, ion sensing

ÖZ

ENERJİ DONÖR ETKİNLİĞİ MODÜLASYONU İLE
ORANTISAL MOLEKÜLER ALGILAYICILARIN RASYONEL TASARIMI

Guliyev, Ruslan
Yüksek lisans, Kimya Bölümü
Tez yöneticisi: Prof. Dr. Engin U. Akkaya

Ağustos 2008, 75 sayfa

Floresan moleküler algılayıcıların rasyonel tasarımı supramoleküler kimya, fotokimya ve fotofiziğin aktif bir araştırma alanıdır. Self kalibrasyon için dahili bir sisteme sahip olduklarından orantısal algılayıcılar daha da önemlidirler.

Bu çalışmada orantısal bir moleküler algılayıcı tasarımı için yeni bir metodoloji geliştirmek amacıyla enerji transfer olayı ve iyon algılanmasının birleştirilmesi önerilmiştir. Donör kısmında spektral örtüşmeyi değiştiren metal iyon bağlanması ile transfer etkinliğinin modüle edildiği enerji transfer kaseti tipinde moleküler algılayıcılar hedeflenmiştir. Bu çalışma değişen derecelerde EET etkinliğine sahip çeşitli EET sistemlerinin sentezini içermektedir.

Elde edilen sonuçlar orantısal iyon algılanması için geliştirilen bu stratejinin umut vaat ettiğini ve moleküler algılayıcı tasarımı için modüler bir yaklaşım sağladığını ortaya koymuştur.

Anahtar kelimeler: Supramoleküler kimya, boradiazaindasen, floresan moleküler algılayıcı, enerji transfer sistem, iyon algılanması

Dedicated to my parents

ACKNOWLEDGEMENTS

I would like to express my gratitude to my supervisor Prof. Dr. Engin U. Akkaya for his guidance, support, patience and for teaching us how to become a good scientist. I will never forget his support throughout my life.

I owe a special thank to Dr.Ali Coşkun, Dr.Altan Bozdemir, Serdar Atılgan and Deniz Yilmaz for their support, guidance as well as their unlimited knowledge and experience that I have benefited from greatly.

I would like to thank to our group members Yusuf, Onur, Gökhan, Ilker, Bora, Suriye, Tuğba, Sündüs, Sencer, Safacan for valuable friendships, wonderful colloborations, and great ambiance in the laboratory. They are very precious for me. It was wonderful to work with them.

My special thanks go to my family for their endless support, trust and encouragement.

I wish to express my sincere appreciation to the NMR technicians Fatoş Doğanel Polat and Seda Karayılan for NMR spectra and for their patience.

TABLE OF CONTENTS

LIST OF FIGURES

LIST OF ABBREVIATIONS

PET:	Photoinduced electron transfer
EET:	Excited Energy Transfer
PCT:	Photoinduced charge transfer
RET:	Resonance Energy Transfer
ICT:	Internal Charge Transfer
Et_3N:	Triethylamine
TMS:	Trimethyl Silyl
TMR:	Tetramethyl Rhodamine
ROX:	Carboxy-X-Rhodamine
TAMRA:	Carboxytetramethyl Rhodamine
BODIPY:	Boradizaindacene
AcOH:	Acetic acid
$CHCl_3$:	Chloroform

CHAPTER 1

INTRODUCTION

1.1 Supramolecular Chemistry

Supramolecular chemistry is a new research field that has developed very rapidly in the last three decades.[1-5] Lying on the crossroads among chemistry, biochemistry, physics and technology makes it a highly interdisciplinary field. It is an almost impossible task to write a useful definition of supramolecular chemistry. Since the field is ever changing as it advances, scientists prefer having their own understanding and set of terminolgy rather than trying to limit the field by claiming certain definitions. Paul Ehrlich's receptor idea, Alfred Werner's coordination chemistry, and Emil Fischer's lock-and-key image play a significant role in the development of supramolecular chemistry.[6] Traditionally, some phrases such as ''chemistry beyond the molecule'', ''the chemistry of the non-covalent bond'', and ''non-molecular chemistry'' were also used to discribe the field. The modern concept of supramolecular chemistry was introduced by Jean-Marie Lehn, which he defined as the ''chemistry of molecular assemblies and of the intermolecular bond''.[7]

From the above mentioned descriptions, it can be easily inferred that contrary to the traditional chemistry, supramolecular chemistry concerns the weaker and reversible noncovalent interactions between molecules. These interactions are hydrogen bonding, metal coordination, hydrophobic forces, Van der Waals forces, π-π interactions and electrostatic effects.

In the beginning, supramolecules mainly comprised two components, a host and a guest, which interact with one another in a noncovalent manner (Figure 1). However, the field developed very rapidly, such that it encompassed molecular devices and molecular assemblies. More recently (2002), Lehn added a further functional definition: ‘‘Supramolecular Chemistry aims at developing highly complex chemical systems from components interacting by non-covalent intermolecular forces.’’[7]

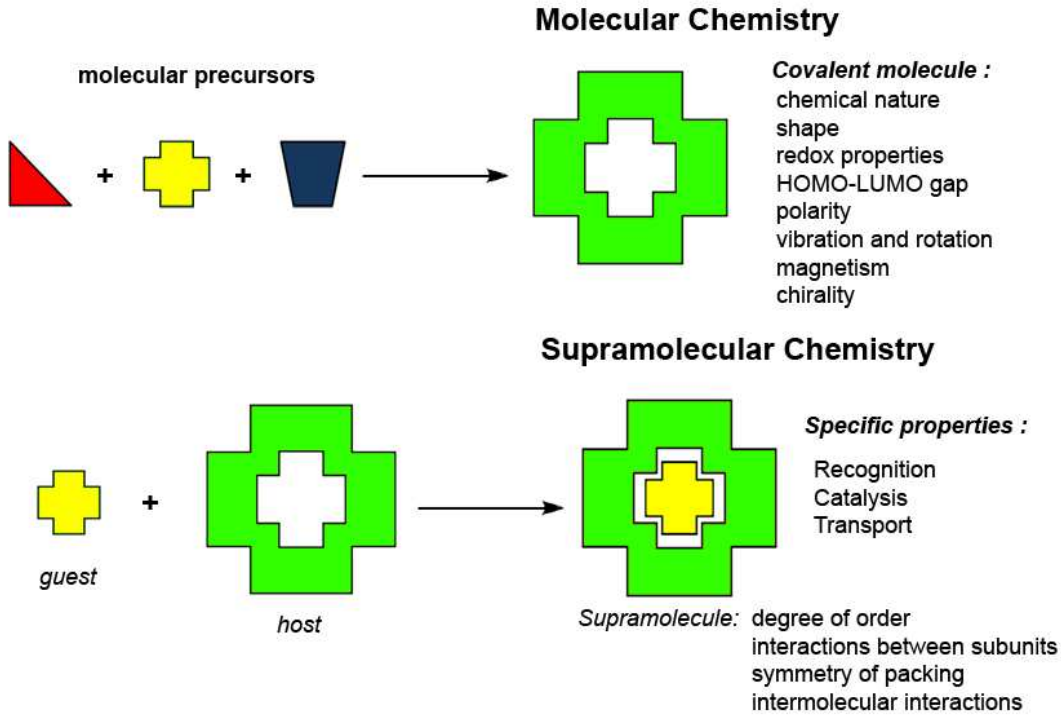

Figure 1. Comparison between molecular and supramolecular chemistry

From the early days of supramolecular chemistry the field has been associated with possible applications. The directed assembly of supramolecular arrays is a topic of significant interest with tremendous potential in the areas of catalysis, sensor design, molecular electronics, and nanotechnology.

There are several examples in the recent literature where the internal cavity of covalently linked supramolecular structures has been used as catalyst to arrange reactants and stabilize reactive intermediates involved in organic transformations.[8-10]

A wide range of chromophores, fluorophores, and redox-active functionalities have been successfully incorporated into supramolecular frameworks. Combined with the rich host-guest chemistry, they are well-suited for sensing applications. Many number of work is done in which guest binding is detected through luminescence[11,12] and electrochemistry.[13,14]

Additionally molecular level devices were successfully synthesized with certain functions.[15,16] Nanoscience and nanotechnology is receiving great attention in view of both their basic interest and their potential applications. Here again, supramolecular chemistry contribute a fundamentally novel outlook of deep impact. There are great developments in surface studies with the assistance of supramolecular concepts.[17]

Using supramolecular methods in the design and sythesis of artificial biological agents[18,19] and developing new therapeutic agents[20] is a very hot and novel application of this field.

The next decade will see rapid advances in the development and utilization of supramolecular concepts. These improvements will turn out as small and intermediate-sized molecular receptors in sensor devices, molecular transport agents, new materials for molecular electronics, novel light-harvesting structures for solar energy conversion, and perhaps even molecular machines.[21]

1.2 Fluorescence

Most elementary particles are in their ground state at room temperature. When these particles are irradiated by photons with proper energies, the electrons move to a higher energy state, which can also be termed as excited state. Once a molecule is excited by absorption of a photon, it can return to the ground state with emission of fluorescence, but many other pathways for de-excitation are also possible (Figure 2). These are internal conversion, intersystem crossing, intramolecular charge transfer and conformational change. Moreover, interactions in the excited state with other molecules such as electron transfer, energy transfer, excimer formation may compete with de-excitation.[22]

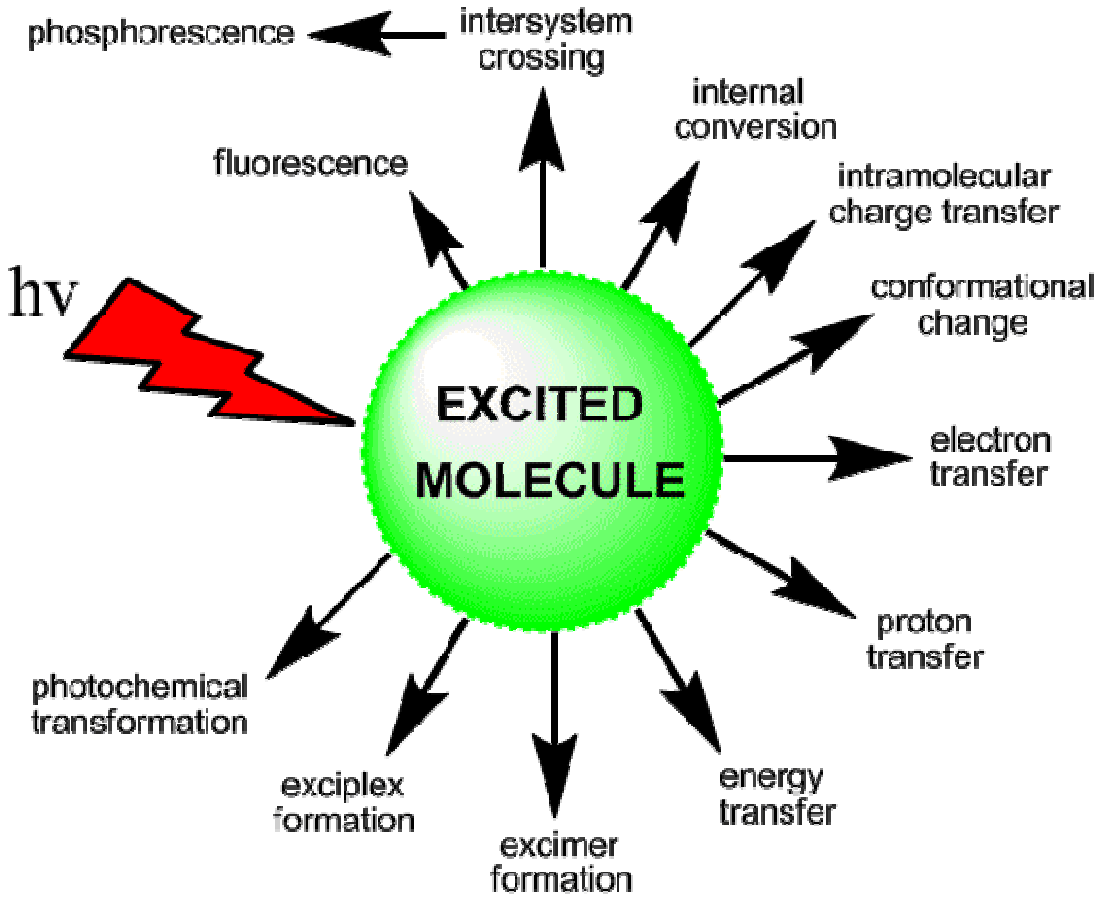

Figure 2. Possible de-excitation pathways of excited molecules

The Perrin-Jablonski diagram (Figure 3) is convenient for visualizing in a simple way the possible processes that occurs after photon absorption. The singlet electronic states are denoted S_0 (ground state), S_1, S_2,…. and the triplet states T_1, T_2,…. Vibrational levels are associated with each electronic state. The vertical arrows corresponding to absorption start from the lowest vibrational energy level of S_0. Absorption of a photon brings a molecule to one of the vibrational levels of S_1, S_2,… Excited molecule then relaxes (non-radiatively) to the lowest vibrational level of S_1, a process which is called internal conversion. Emission of photons during the S_1 to S_0 relaxation is called fluorescence. The third possible de-excitation process from S_1 is intersystem crossing. In this mechanism transition of electron from singlet excited state S_1 to the triplet excited state T_1 occurs (non-radiatively). In solution at room temperature, non-radiative de-excitation from the triplet state T_1 is dominant over radiative relaxation which is called phosphorescence. On the contrary, at low temperatures and in rigid medium phosphorescence can be measured easily.

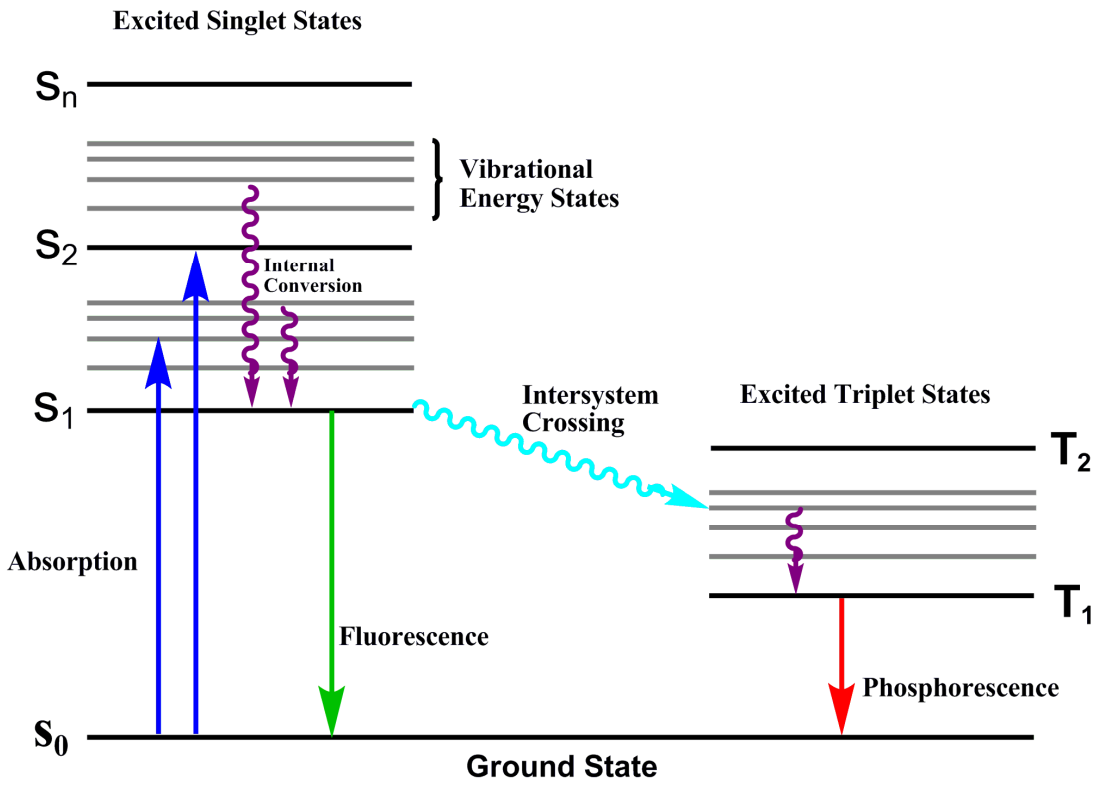

Figure 3. Jablonski diagram

As it can be seen in the Jablonski diagram, emitted light always has a longer wavelength (less energetic) than the absorbed light due to limited energy loss by the molecule prior to emission. The difference (usually in frequency units) between the spectral positions of band maxima of the absorption and luminescence is called Stokes' shift (Figure 4). So the main cause of Stokes' shift is the rapid decay to the lowest vibrational level of S_1. In addition to this effect, fluorescent molecules can display further Stokes' shift due to solvent effects, excited-state reactions, complex formation and energy transfer.[23]

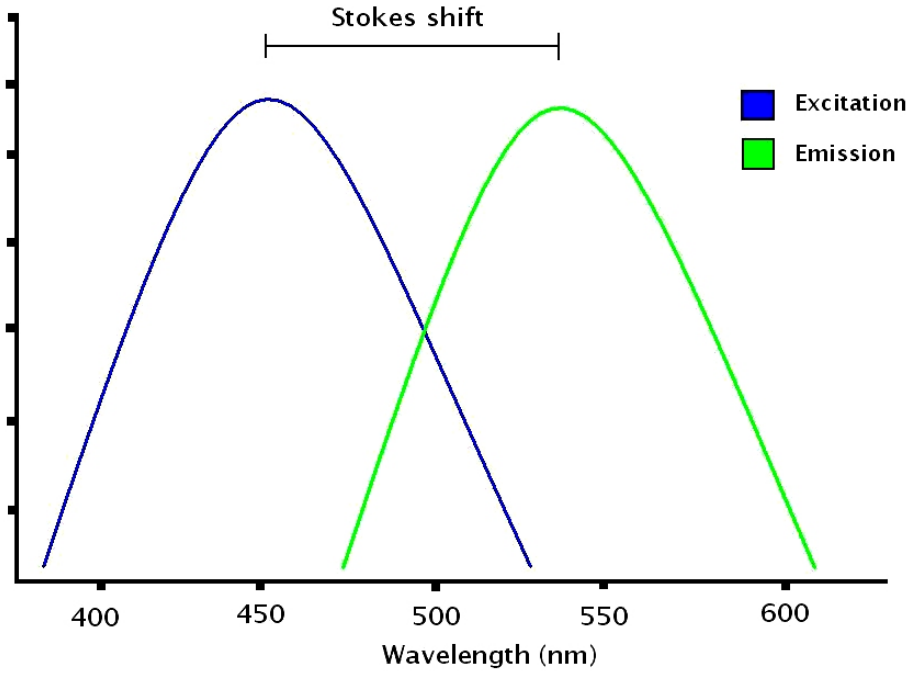

Figure 4. Stokes' shift

1.3 Fluorescent dyes

A common feature of almost all traditional dyes is that they absorb particular wavelengths of visible light, leaving the remaining wavelengths to be reflected and seen as color by the observer. For example, a traditional yellow dye absorbs blue light and thus appears yellow. The energy coming from the absorbed light is stored in the electron structure of the dye molecule and given off in the form of heat. The unique feature of a fluorescent dye is that they not only absorb light in the traditional sense, but this resulting energy is then dissipated in the form of emission of light.

Organic dyes that emit ultraviolet (UV), visible (Vis), and near infrared (IR) regions are of great interest, and have wide application fields. The most common dyes whose emissions span the UV to IR spectrum are shown in Figure 5.

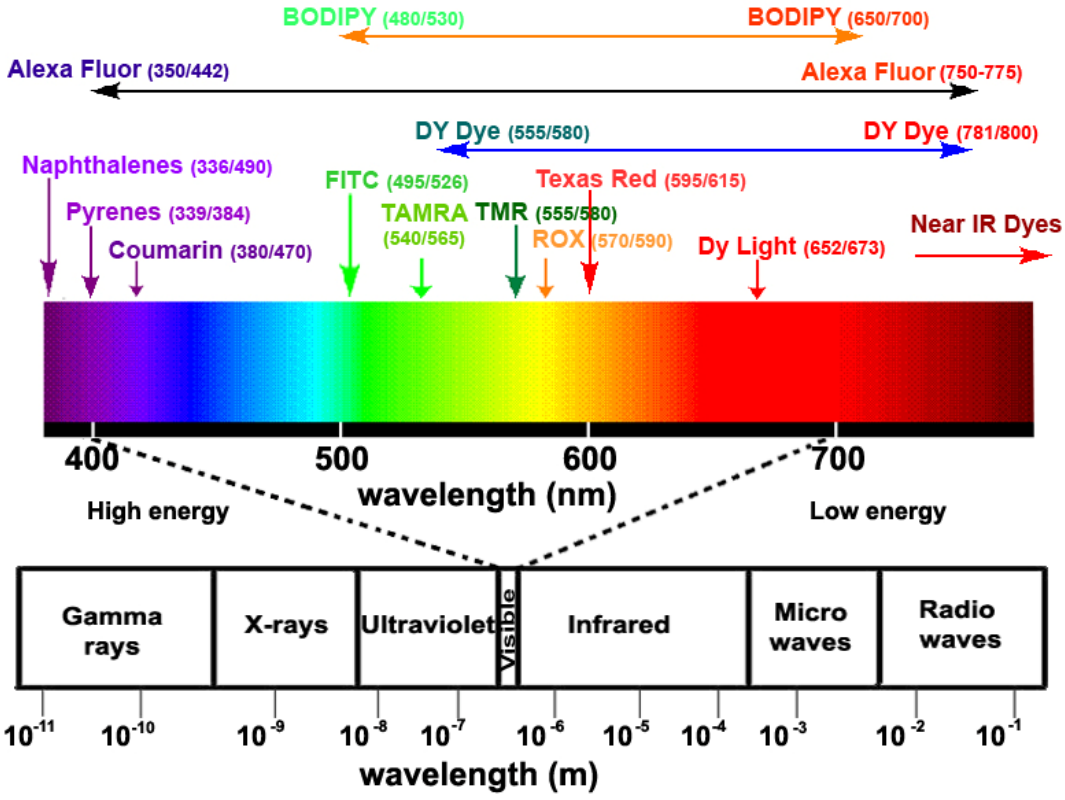

Figure 5. Distribution of dye families in the visible region

In the above figure, absorbance and emission maxima along with spectral regions covered by a particular dye family are highlighted. Tetramethyl rhodamine (TMR), carboxytetramethyl rhodamine (TAMRA), and carboxy-X-rhodamine (ROX) are all rhodamine based dyes. The UV dyes are typically pyrene-, naphthalene-, coumarin- based structures, while the Vis/near IR dyes include fluorescein-, rhodamine-, and cyanine- based derivatives (Figure 6).

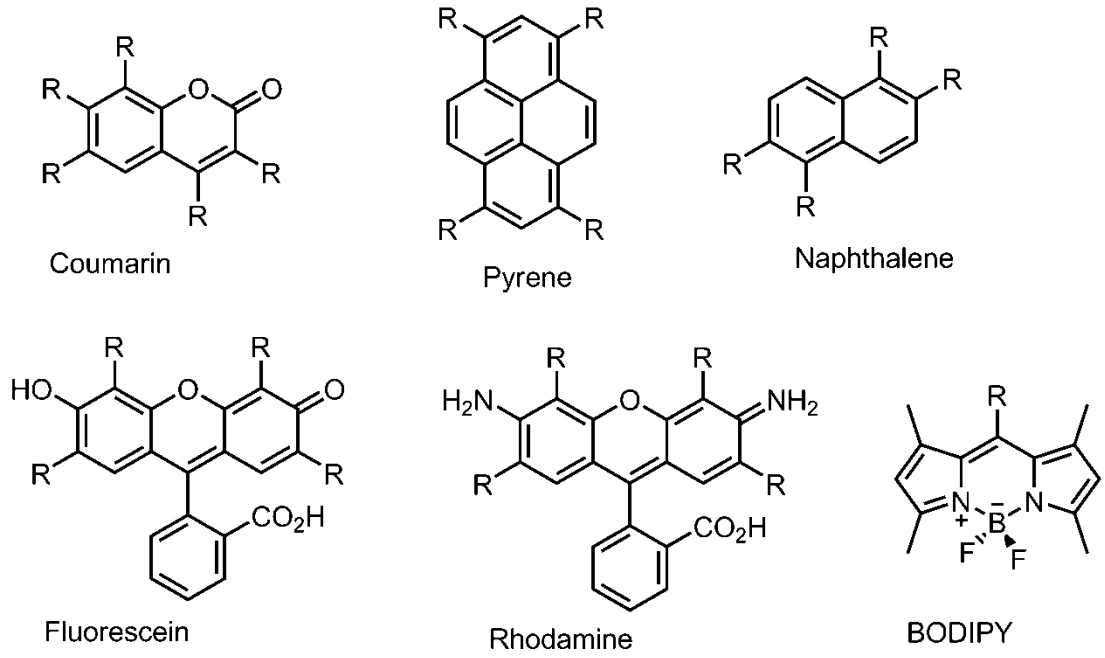

Figure 6. Structures of common UV/Vis fluorescent dyes

Members of some dye families, such as cyanines (Cy), are closely related in structures, whereas others, such as the AlexaFluor compounds, are quite diverse. All dye families have both advantages and disadvantages depending on the intended application. For example, fluorescein dyes are popular because of their high quantum yields, solubility, and ease of bioconjugation. However, fluorescein has a high rate of photobleaching, is pH sensitive, and can self-quench at high degrees of substitution. Another important family of dyes that are BODIPY based will be discussed in detailed in the following sections.

1.4 Molecular Sensors

A receptor may be used as a sensor if it can report the presence of the guest by some physical means. Sensor should ideally be selective for a particular guest and not only report the presence of the guest molecule, but should also allow the chemist to monitor its concentration. This is important medically (for monitoring indicators of physical function) and environmentally (monitoring pollutant levels).[24]

There are numerous analytical methods that are available for the detection of various analytes, however they are expensive and often require samples of large amount. So, the molecular sensors gain primary importance in this area. Molecular sensors can be split into two major categories; these are electrochemical sensors and optical sensors. Electrochemical sensors can be obtained with the attachment of a redox active unit to the receptor moiety. A change in the redox properties of the receptor can be detected by an electrochemical technique such as cyclic voltametry (CV).

The most common type of the optical sensors is fluorescent sensors. Because the fluorescence detection has three major advantages over other light-based investigation methods: high sensitivity, high speed, and safety. In relation to the use of fluorescence for sensing, the principal advantage over other light-based methods such as absorbance is its high sensibility. This is so because the emission fluorescence signal is proportional to the substance concentration whereas in absorbance measurements the substance concentration is proportional to the absorbance, which is related to the ratio between intensities measured before and after the beam passes through the sample. Thus, in fluorescence, an increase of the intensity of the incident beam results in a larger fluorescence signal whereas this is not so for absorbance. As a result, using fluorescence, one can monitor very rapid changes in concentrations. They are, therefore, very sensitive and suitable for use in biological systems. The point of safety refers to the fact that samples are not affected or destroyed in the process, and no hazardous by products are generated.

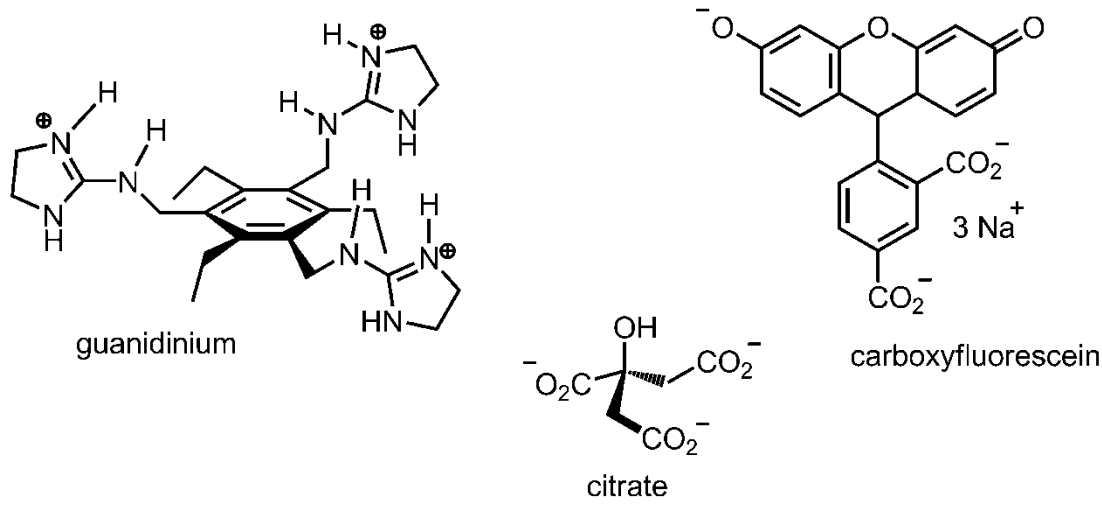

Figure 7. Displacement assay for citrate anion

An excellent example is provided by a sensor for citrate anions developed in the research group of Eric Ansyln shown in Figure 7.[25] Tridentate guanidinium based receptor shows a high affinity and selectivity for tricarboxylate citrate anion. Neither of these two components are fluorescent, and in order to convert the receptor into a sensor, a clever strategy was utilized. A mixture of guanidinium and carboxyfluorescein was prepared. Substrate which is fluorescent binds to the receptor, but quite weakly. When tricarboxylate citrate is added to the mixture it displaces the substrate. The fluorescent properties of substrate changes considerably on its release from the complex, and in this way sensory response to the addition of citrate is obtained.

1.5 Fluorescent chemosensors

The recognition and signaling moieties are the most important parts in the design of sensors. Thus, fluorescent sensors are usually constructed by attaching a receptor (synthetic or biological) to a fluorophore. The fluorescence properties of a fluorophore can be affected by the binding of an analyte to the receptor part. These changes can be monitored to determine the presence or the concentration of a given

analyte. Binding of the target analyte to the synthetic sensor can result in either amplification or quenching of the fluorescence.[26] These fluorescent probes are either constructed as fluorophore-spacer-receptor or as integrated fluorescent probes (Figure 8). In the former case, the receptor and fluorophore are separated by an alkyl chain, whereas in the latter case the receptor is part of a π-electron system of the fluorophore.[27]

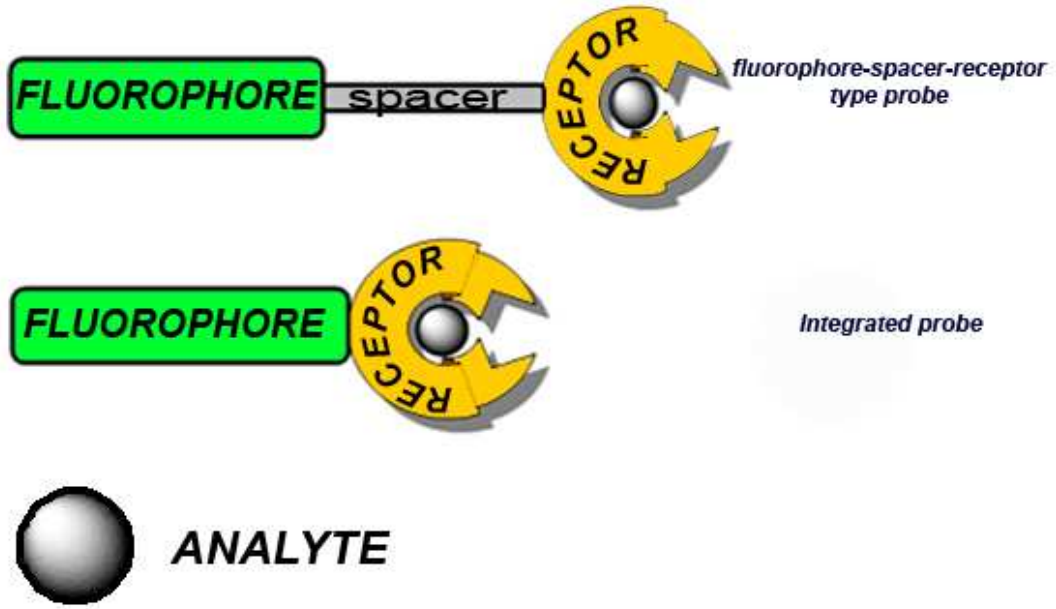

Figure 8. Schematic representations for the types of fluoroionophores

1.5.1 Photoinduced electron transfer (PET)

In flourophore-spacer-receptor systems only long range electronic interactions are possible, the most common is PET. Photoinduced electron transfer (PET) is a signaling event which relies on emission quenching or enhancement. Due to this reason it is widely used in sensors for the fluorescent sensing of various analytes such as cations, anions, and neutral molecules. Figure 9 shows working principal of the PET mechanism in the fluoroionophores. The receptor part contains an electron donating group such as amino group. Upon excitation of the fluorophore, an electron in the highest occupied molecular orbital (HOMO) of fluorophore is

promoted to the lowest unoccupied molecular orbital (LUMO). PET from the HOMO of the free receptor to that of the fluorophore causes fluorescence quenching of fluorophore. However, analyte binding makes the HOMO of receptor lower in energy than that of fluorophore, consequently PET cannot happen any more and fluorescence enhancement occurs.[28]

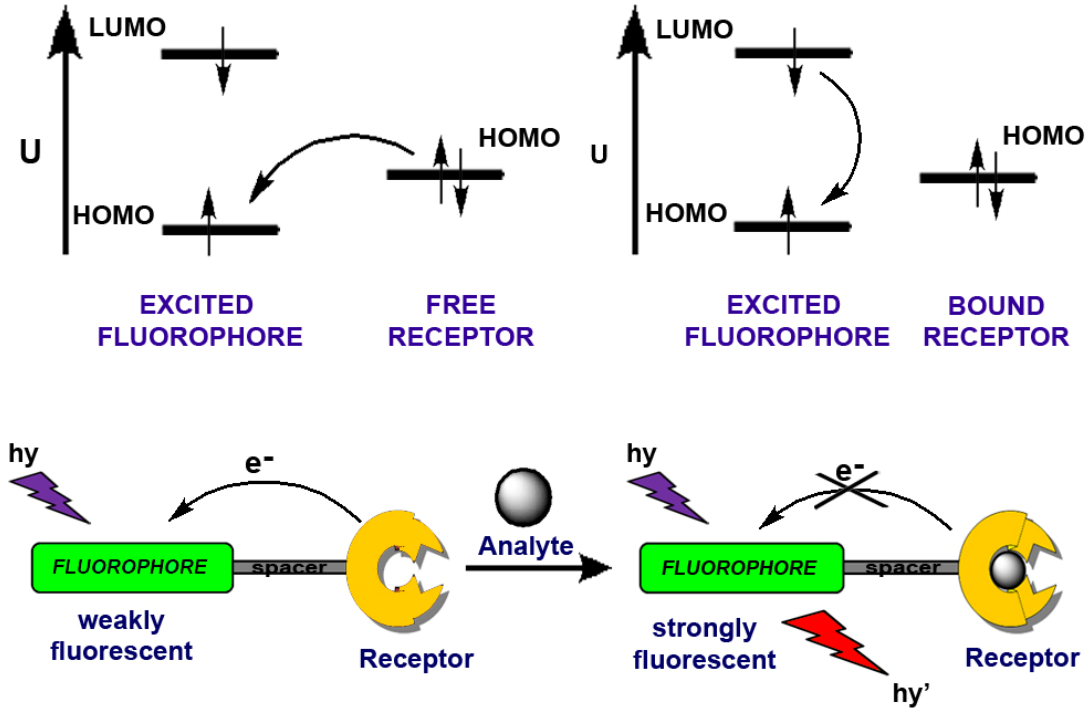

Figure 9. PET mechanism

Many of the fluorescent chemosensors work with this principle. Selectivity for ions is achieved by the correct choice of recognition moiety for the desired ion. A classical example is compound 1[29] (Figure 10). The recognition moiety is not necessary to be a crown ether. There are many examples of cryptand- (2),[30] podand- (3),[31] 2,2-dipyridyl-,[32] and calixarene-based[33] PET sensors as selective for sodium, magnesium, potassium, calcium, and transition metal ions. In these sensors photoinduced electron transfer quenches the luminescence in the absence of the analyte. Binding the analyte inhibits the PET and switches on the emission.

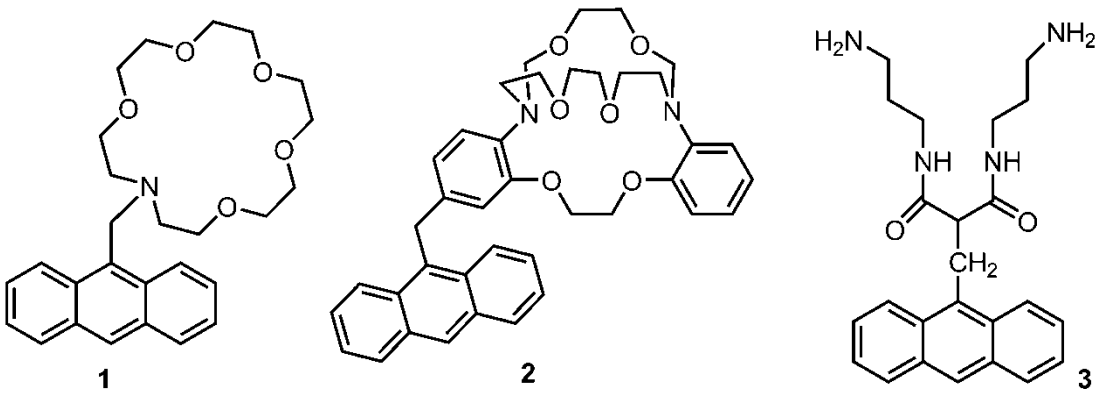

Figure 10. Some examples of PET based fluorescent chemosensors

PET may sometimes occur from fluorophore part to receptor unit. If the energy states are such that the excited state of the fluorescent group can donate electrons to the LUMO of receptor, then oxidative PET or reverse PET occurs (Figure 11).

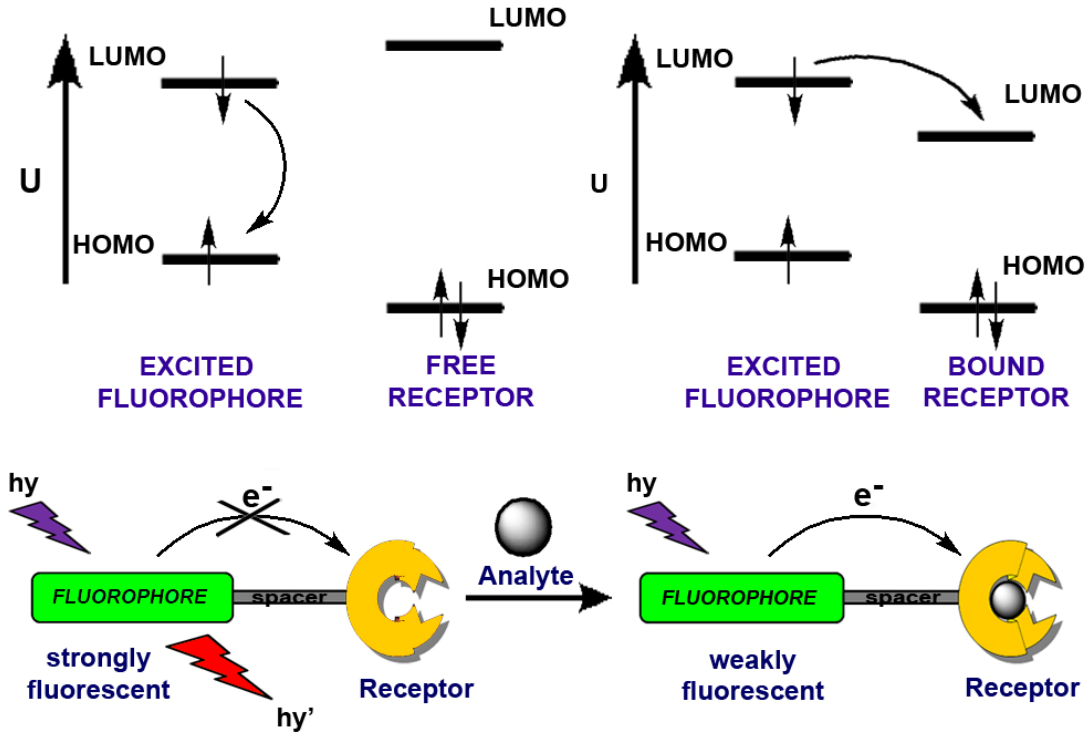

Figure 11. Oxidative PET mechanism

Compound **4**[34] is a nice example exhibiting this mechanism. In that particular case depicted in Figure 12, BODIPY dye was chosen as a fluorophore and 2, 2-bipyridine for the receptor part. In the absence of zinc cation fluorophore has bright-green fluorescence, and upon addition of mentioned ion fluorescence is quenched via oxidative PET mechanism.

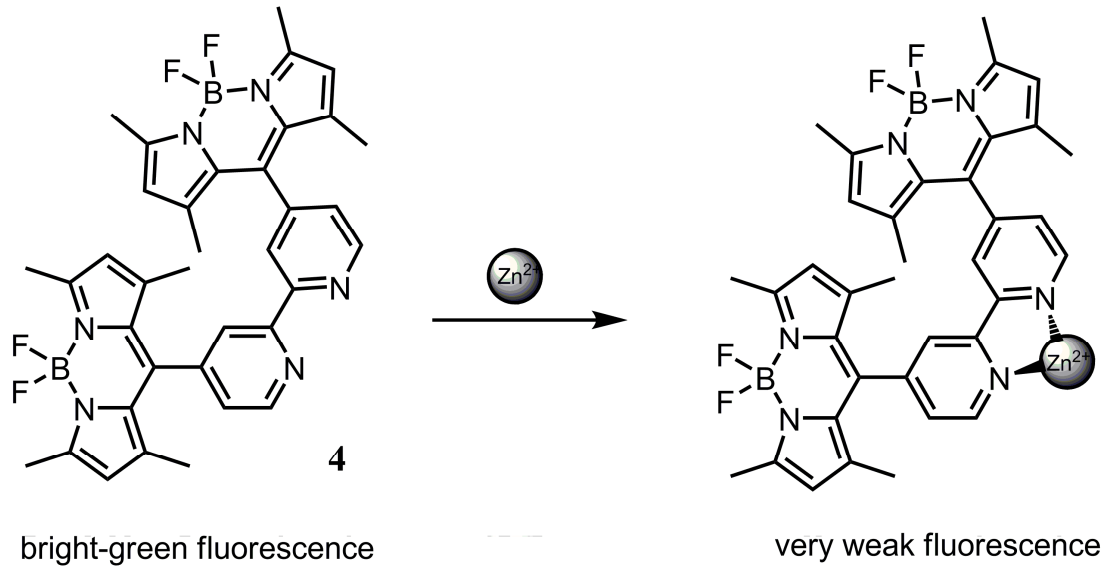

Figure 12. Coordination of zinc triggers the oxidative PET mechanism

1.5.2 Photoinduced charge transfer (PCT)

There is no spacer unit between the receptor and fluorophore moieties in the fluoroionophores working with PCT mechanism. The receptor unit is part of a π-electron system of the fluorophore. Then, one terminal tends to be electron rich and the other electron poor. Upon excitation of such a system, redistribution of electron density occurs, so that a substantial dipole is created, resulting in intramolecular charge transfer from donor to the acceptor. Binding of analyte to the receptor, causes an interaction with this excited state dipole, and this interaction can be followed in the emission spectrum.

If there's an electron donating group (such as amino group) within the fluorophore, interaction with a cation reduces electron donor character of it, which results in the reduction of the conjugation. A blue shift in the absorption spectrum is expected. The photophysical changes upon cation binding can also be described in terms of charge dipole interactions. In the excited state amino group will be positively charged. The interaction between this moiety and the cation will destabilize the excited state (Figure 13). Thus, an increase in the energy gap between S_0 and S_1 energy levels will take place. As a result blue shift is observed and the desired analyte can be signaled in this way.

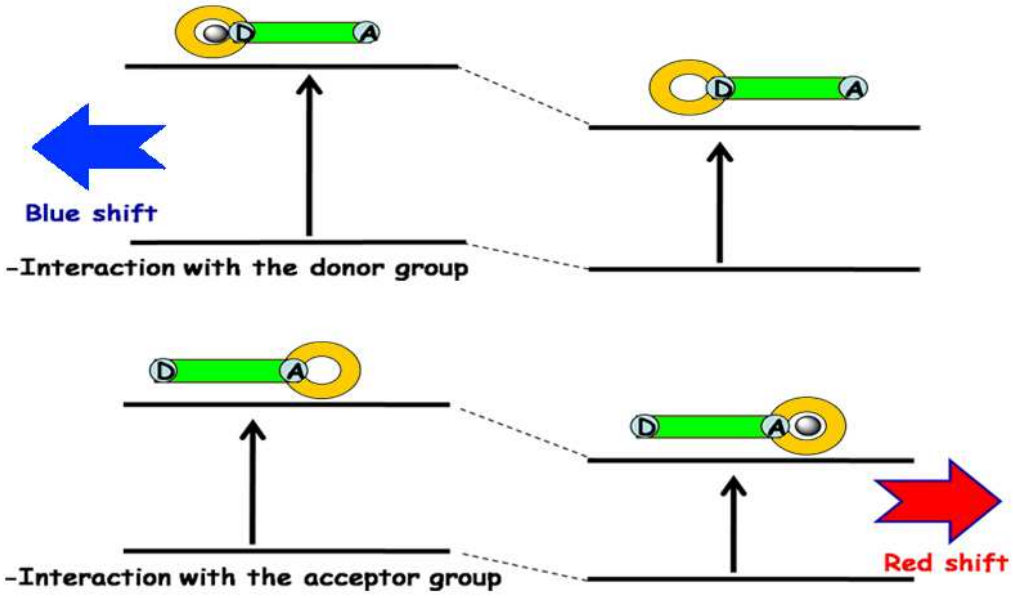

Figure 13. Spectral displacements of PCT type sensors

On the contrary, a cation interacting with the acceptor group (like a carbonyl group) enhances the electron-withdrawing character of this group. It is easily explained in terms of a charge-dipole interaction. When the cation interacts with the acceptor group, the excited state is more stabilized by the cation, and the energy gap between S_0 and S_1 will decrease, causing a red-shift in the spectrum (Figure 13).

Many fluoroionophores have been designed according to this (PCT) mechanism. Compounds **5**[35] and **6**[36] (Figure 14) exhibit blue shift in both absorption and emission spectra upon cation binding.

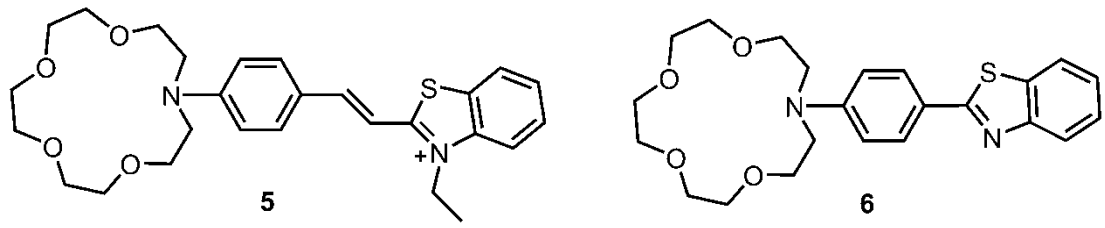

Figure 14. Crown containing PCT sensors

1.6 BODIPY dyes

Among the large variety of known fluorescent dyes, the boradiazaindacene (BODIPY) family has a significant place and has found great popularity with chemists, biochemists and physicists. BODIPY dyes were first discovered by Treibs and Kreuzer in 1968.[37] Since then many applications of BODIPY were reported in a wide range of fields. Biomolecular labeling, ion sensing, drug delivery reagents, molecular logic, light harvesting systems, sensitizers for solar cells are some of them.

BODIPY dyes have high molar extinction coefficients, generally present strong absorption and fluorescence bands in the visible region, and high fluorescence quantum yields, in many cases close to the unity, depending on their structure and the environmental conditions.[38] Its lower sensitivity to solvent polarity and pH make it a stable compound to physical conditions. Good solubility, intense absorption profile, tunable emission range (500–800),[39,40] negligible triplet state formation and ease of doing chemistry on it are additional advantages of BODIPY dyes. Making structural modifications brings out new members of BODIPY family with shifted photophysical properties. In fact all positions (1–8) of a BODIPY skeleton (Figure 15) are labile to chemical modifications. Especially, modifications on positions 2, 3, 5, 6 extend the conjugation and make it possible to obtain new dyes having

absorption and emission maxima in red and near IR regions of the electromagnetic spectrum. Furthermore, functional units can also be attached with modifications to positions 4 and 8. Derivatization and functionalization of BODIPY dyes is still a challenge and research studies to that end are continuing. There are several renown research groups working on this issue, which are those of Akkaya, Burgess, Nagano, Rurack, and Ziessel.

1.6.1 Application of BODIPY dyes

Due to the chemical and photochemical properties of BODIPY dyes mentioned above, it has found wide applications in many hot research areas (Figure 15) such as the development of photosensitizers for solar energy conversion[41,42] and the synthesis of molecular devices.[43] BODIPY dyes have been also widely applied as fluorescent sensors and probes to study biological systems containing lipids, nucleic acids or proteins,[44,45] as well as light harvesting arrays to develop antenna systems.[46-48]

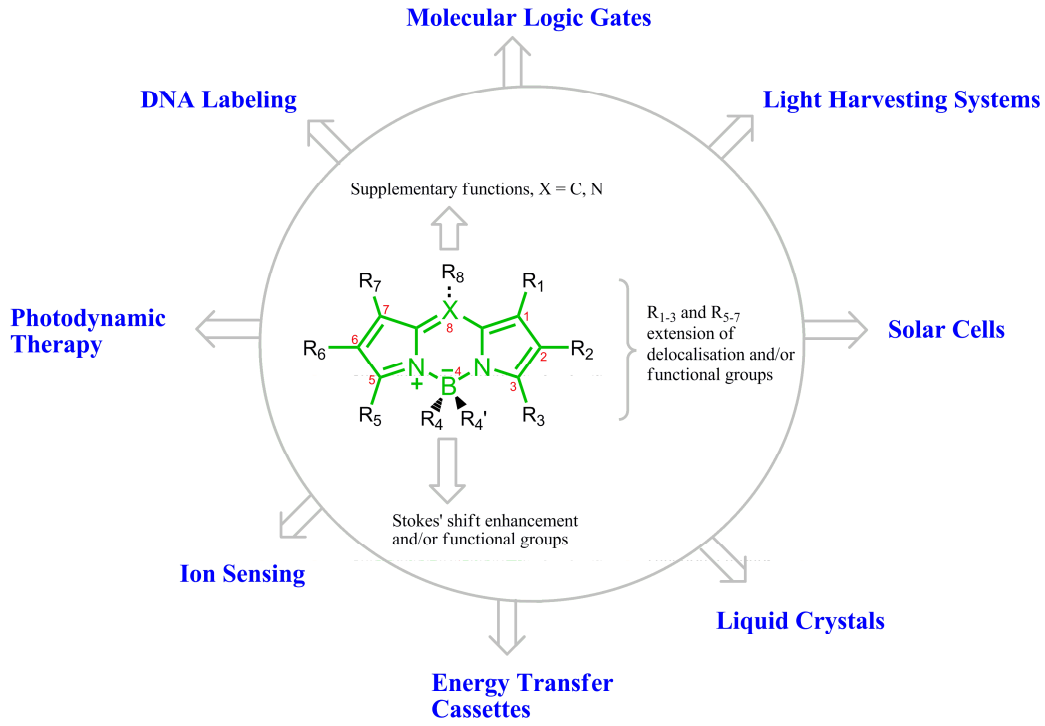

Figure 15. Potential applications of BODIPY dyes

Due to the high quantum yield and the photostability of BODIPY family, labeling of proteins was one of the first applications of these fluorophores.[49] BODIPY based chemosensors has a significant place among the ion sensors reported up to date. Many number of BODIPY chemosensors have been published in prestigious journals.

Fluorophores emitting beyond 650 nm are great candidates for sensing in biological media due to the reduced scattering of light at longer wavelengths. Making proper modifications on BODIPY skeleton may result in redshift in the absorbance and emission properties of it. Red-emitting BODIPY fluorophores and chemosensors that have been developed by Akkaya et al are shown in Figure 16 (**7, 8, 9**).[50-52]

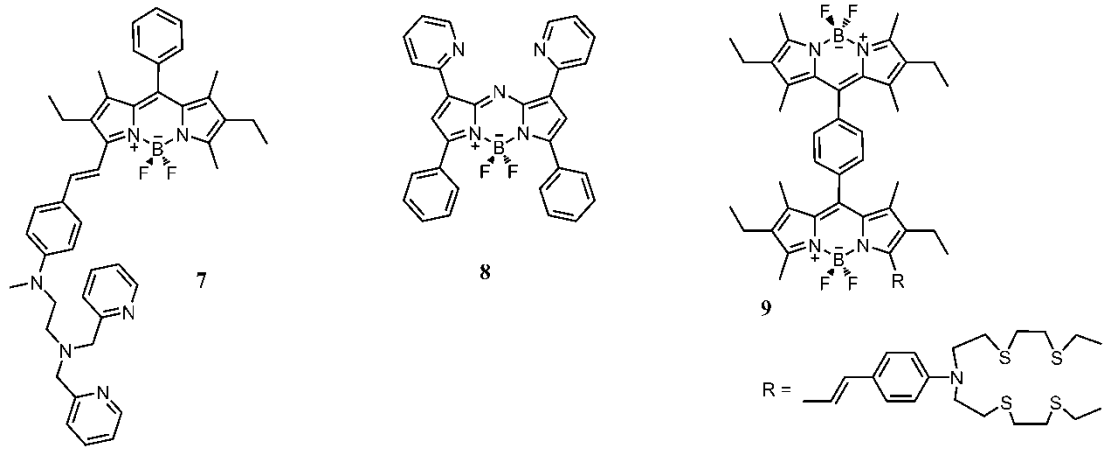

Figure 16. Red-emitting BODIPY derivatives

The core of BODIPY dyes is hydrophobic and it has no functionality to attach to biological units. Water-solubility is important in order to study living cells. Water solubility is achieved via attaching hydrophilic groups to the BODIPY skeleton. Compounds **10** and **11** and **12** are examples of water soluble BODIPYs (Figure 17).[53-55]

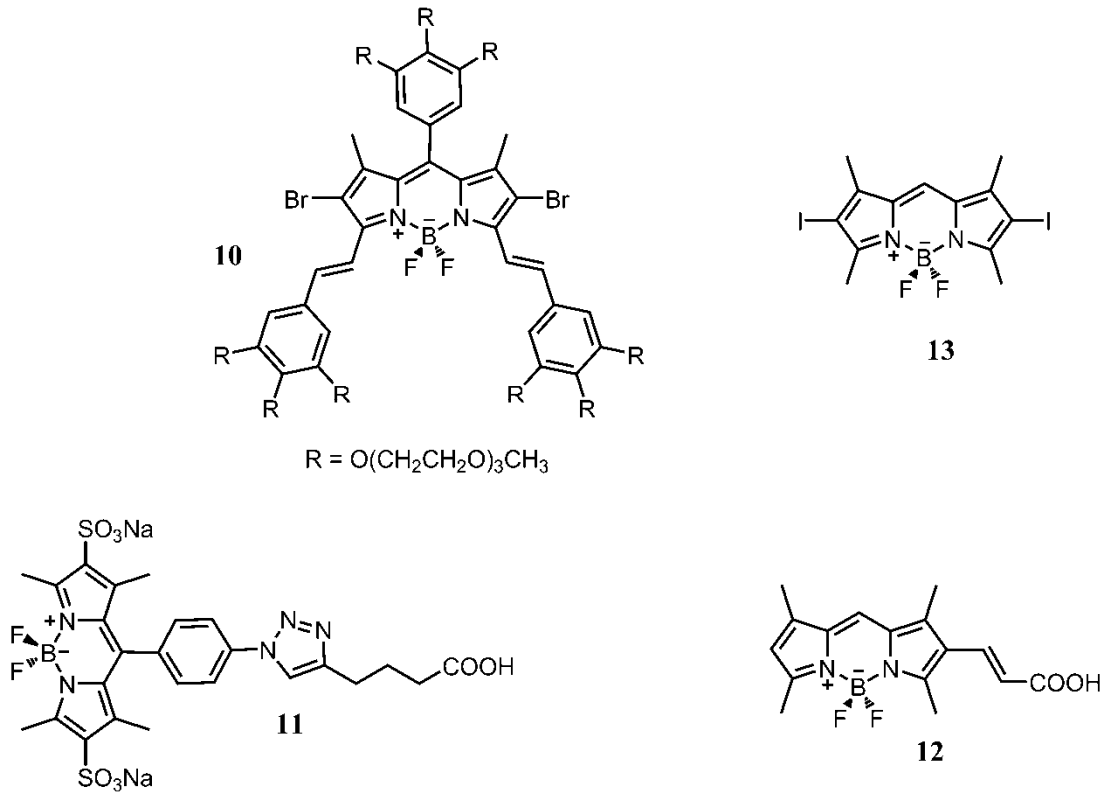

Figure 17. Photosensitizers for photodynamic therapy and water soluble derivatives

Water soluble distyryl-boradiazaindacene **10** which was developed by Akkaya et al, is a nice example illustrating the BODIPY based sensitizers for photodynamic therapy. Extension of conjugation in the bodipy framework results in longer wavelength absorption (650–680 nm). Heavy atoms attached to 2 and 6 positions of BODIPY favor the intersystem crossing, and increase the triplet yield of dye molecule. Nagano et al synthesized compound **13**, and showed that in the presence of heavy atoms the quantum efficiency of fluorescence decreased from 0.70 down to 0.02. Under aerobic conditions, singlet oxygen is generated in modest efficiency and cellular toxicity has been reported.[56]

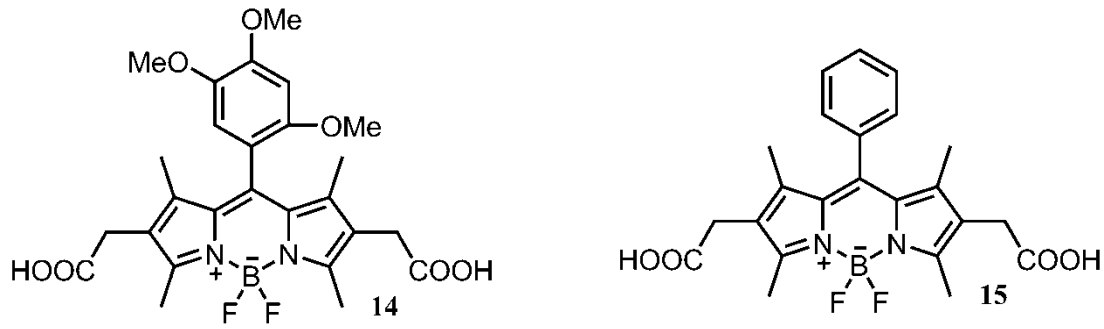

Figure 18. BODIPY photosensitizers for solar energy conversion

In recent years, it is of great interest to design organic dye sensitizers, which are not based on ruthenium complexes. Applications of BODIPY dyes in the design of photosensitizers for the solar energy conversion are very interesting. BODIPY was used as a photosensitizer firstly by Nagano et al.[42] Compounds **14** and **15** (Figure 18) was designed and synthesized. Both of them attach to the TiO_2 surface. Contrary to compound **15**, compound **14** contains three electron donor methoxy groups. The conversion efficiencies were reported as 0.13% and 0.16% for **14** and **15** respectively.

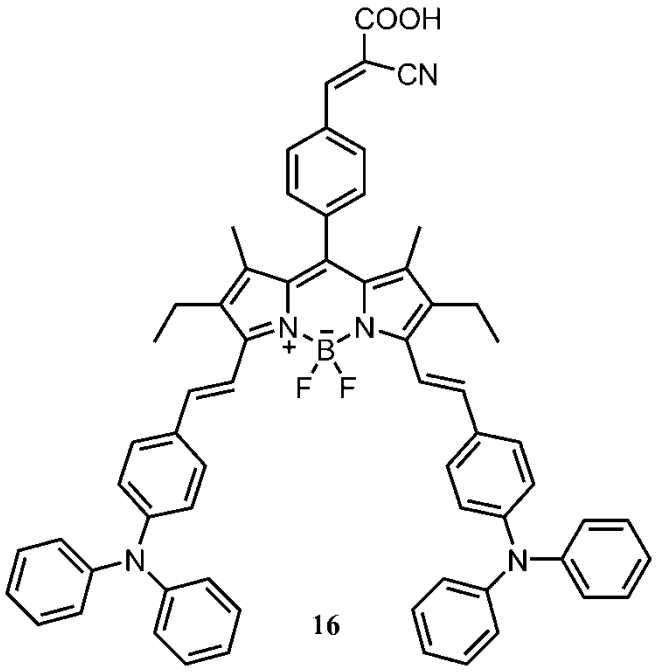

Figure 19. Novel BODIPY based photosensitizer

Recently Akkaya group also developed a novel BODIPY based photosensitizer with improved conversion efficiency.[41] They designed compound **16** (Figure 19), which has absorbance maximum especially in the longer wavelength region of the visible and near IR region of the solar spectrum. An important part of the design in this dye is placing the anchor and cyano group at the position 8 of the BODIPY core. This was also supported with the DFT calculations. It was reported that without any additives (used for the enhancement of efficiency) the obtained conversion efficiency was 1.66%.

1.7 Hg^{2+} Sensing

Heavy and transitional metals (TM) play important roles in the areas of biological, environmental and chemical systems. Therefore monitoring their activities and concentrations is of great importance for scientists. Especially the detection of Hg^{2+} is of growing interest.

Mercury exists in nature as ionic and elemental mercury. Natural sources include the weathering of cinnabar (HgS) deposits and volcanic emissions. Amalgams, pharmaceuticals, cosmetics, chloralkali plants, and other industrial activities such as manufacture of electrical products are the examples for the man made sources. Today, the major source of human exposure to Hg is through the diet from consumption of fish and fish products. Monomethymercury (MeHg) which is the most toxic species of Hg exists in the muscle tissue of marine predators.[57] Unfortunately mercury containing chemicals have been linked with a number of human health problems. Minamata, myocardial infarction, and some kinds of autism are some of them. Moreover, excessive exposure of the body to mercury can cause damage in brain, kidneys, central nervous system, immune system, and endocrin system.[58] Therefore, much attention has been focused on devoloping new methods to monitor Hg^{2+} in biological and environmental samples.

Atomic Absorption Spectroscopy[59] and Inductively Coupled Plasma Mass Spectrometry[60] are the usual methods used for the determination of total mercury in the samples. However these methods often require sophisticated and expensive instrumentation.

Recently, designing fluorescent Hg^{2+} sensors have become popular due to their capability to detect analytes by the naked eyes without resorting to any expensive instruments. Size, cost, not requiring a reference element, and the fact that the analytical signal is free of the influence of an electromagnetic field and easy to transmit over a long distance are the advantages of working with this type of sensors.[61] However, there are some important factors which limit their application in biological and environmental systems. These are poor solubility in aqueous solutions, interference problems caused by protons and other heavy metal cations such as Cu^{2+} , Co^{2+} , Pb^{2+} , Ag^{+}, short emission wavelength and weak fluorescence intensity. As a result it can be said that developing new and practical sensor systems for Hg^{2+} is still a challenge.

1.7.1 Fluorescent Hg^{2+} chemosensors

A practical fluorescent sensor for targeting ions of specific importance should at least have the following properties: simplicity, high selectivity, strong signal output, wide conditions of coordination and recognition in aqueous environments.[62] Designing the receptor part is an important step in building up the chemosensors.

According the hard and soft acids and bases theory[63] mercuric cation which is a soft acid should bond to soft bases. Therefore most of the Hg^{2+} receptors contain sulphur (S) which is a soft atom in order to increase the binding constant.

Some examples from literature are given in figure 20. Compound **17**,[64] developed by Shiguo Sun et al., is virtually non-fluorescent with a very low quantum yield (Φ=0.008), which is indicative of efficient photo-induced electron transfer

(PET) quenching from the receptor to the BODIPY fluorophore. The phenyl group is only a linker between the receptor and fluorophore. Because of the stereo effect of the methyl groups phenyl ring is not planar with BODIPY part. Upon addition of Hg^{2+} in water/ethanol system (7/3, v/v), the fluorescence intensity increases by over 160 fold. It should be due to the coordination of Hg^{2+} with the NS_2O_2 receptor and the inhibition of the PET. They have also tested the perchlorate salts of alkali and alkaline earth metal ions, transition and heavy metal ions as an analyte. But their BODIPY based chemosensor showed excellent fluorescence selectivity only towards Hg^{2+} among all other cations. Moreover, fluorescent sensors based on photo-induced electron transfer are usually disturbed by protons in the detection of metal ions. But this chemosensor displays gradually intense fluorescence only at pH<3, when pH is higher the fluorescence intensities are very low and stay constant, which means that its fluorescence emission is pH independent under a large physiological pH range. Thus it has potential applications for biological toxicities.

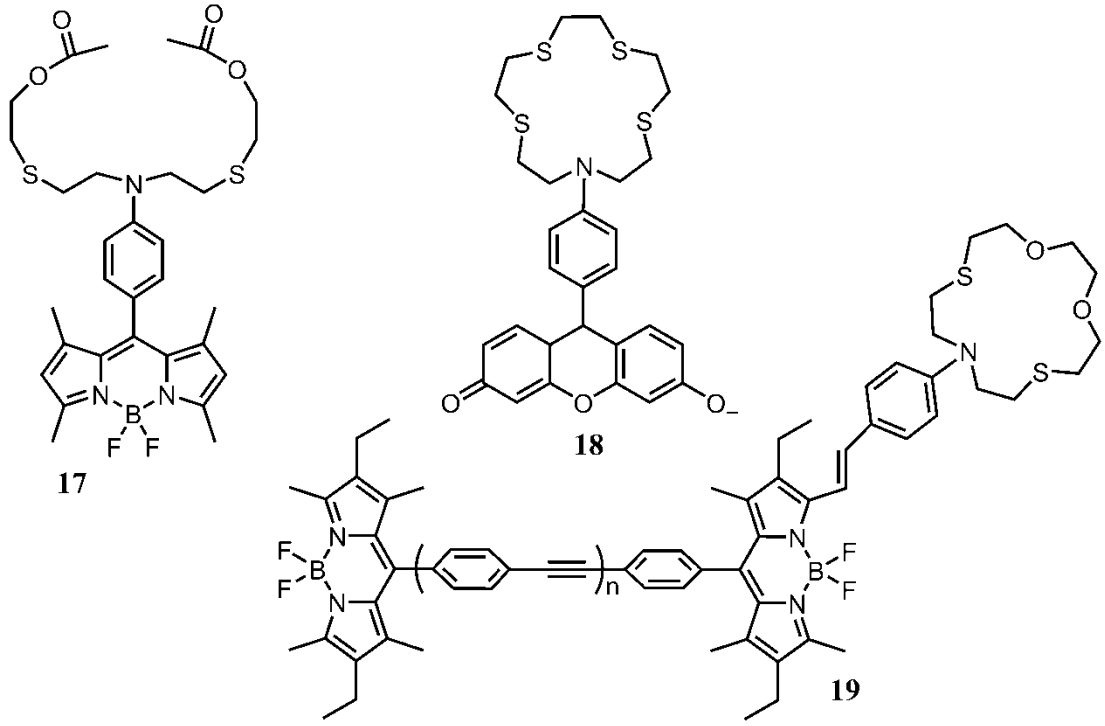

Figure 20. Hg^{2+} selective chemosensors

Chemosensor **18**[65] also behaves as a PET type chemosensor for mercuric cation in aqueous media. In this case fluorescein moiety is used as a reporter unit. Although the ligand shows quite good selectivity over other cations, it shows only a small change in the emission spectrum for Cd (II) ion.

Compound **19**[66] was developed by Akkaya et.al. By completing this work they introduced a new strategy in ratiometric chemosensor design in which the range of ratios can be significantly improved. If the chemosensor is designed as energy transfer dyad, and once the interchromophoric distance is carefully adjusted, binding of the analyte increases the spectral overlap between the donor emission and the acceptor absorption peaks. Thus, more efficient Forster type energy transfer in the bound state results in higher emission intensity for the analyte-bound chemosensor, effectively increasing the signal ratio for the two states. Binding of mercuric ion to the receptor unit shows ICT type behavior. As a result of this, absorbance of the acceptor unit blue-shifted while the emission of the donor part remains to be same. This spectral change increases the spectral overlap, thus, causes spectacular change in the efficiency of the energy transfer. In other words, Hg (II) binding increases the spectral overlap, which increases the energy transfer from donor to acceptor, and due to this, dynamic range enhancement can be done.

1.8 Energy transfer cassettes

In the dye systems that emit far from the excitation wavelength, radiationless electronic energy transfer has been used to improve emission intensities. Systems that show this characteristic, transfer energy from a donor dye that absorbs at relatively short wavelength, to an acceptor dye that fluoresces at longer wavelengths. It is most convenient if the donor and acceptor components of such systems are introduced in a single unit such as energy transfer cassette. In these cassettes energy transfer occurs by either through-space (Förster type)[67,68] mechanism or through-bond (Dexter type)[69] mechanism (Figure 21).

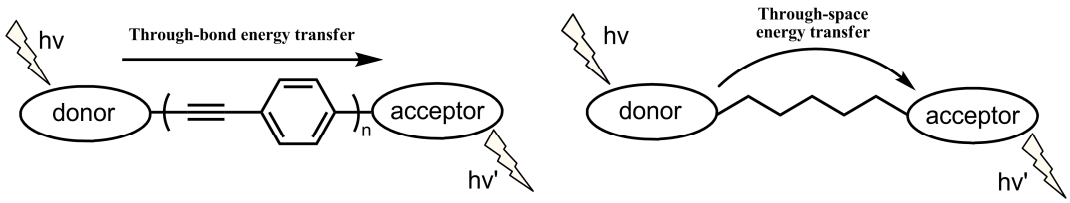

Figure 21. Through-bond and through-space energy transfer

1.8.1 Förster type

Fluorescent labels that emit light at wavelengths distant from that of the source used to excite them have many applications in biotechnology. Generally, a single florescent dye molecule has a very small Stokes' shift. When the Stokes` shift of a single dye is insufficient for a particular application, bi(multi)chromophoric systems that exploit through-space energy transfer between two dyes are frequently used. Fluorescence resonance energy transfer (FRET) occuring here is a nonradiative process whereby an excited state donor (D) transfers energy to a proximal ground state acceptor (A), and the fluorescence of the latter is observed (Figure 22). For biotechnological applications, the donor and acceptor units are usually connected via non-conjugated linker systems; therefore the predominant energy transfer mechanism here is through-space (Förster type).

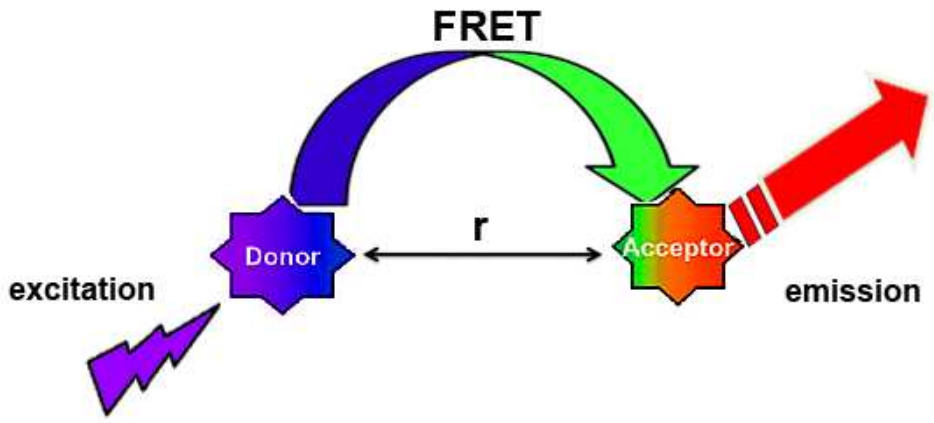

Figure 22. Schematic of the FRET process

In this mechanism, an electron in HOMO of the acceptor molecule is excited with energy released during the relaxation of electron in donor LUMO to its ground state. The acceptor must absorb energy at the emission wavelength of the donor (spectral overlap). The rate of energy transfer is dependent on many factors, such as the extent of spectral overlap, the relative orientation of the transition dipoles, and the distance between donor and acceptor molecules.[70] FRET usually occurs over distances comparable to the dimensions of most biological macromolecules, that is, about 10 to 100 Å.

A nice example is illustrated in Figure 23. Compound **20** is a kind of proton sensing agent acting via electron and energy transfer.[71] Piperazine here is a linker between anthracene and chalcone moieties. When anthracene is excited, energy transfer does not occur to the chalcone moiety because of electron transfer occuring from piperazine to the anthracene unit. However, when piperazine is protonated, the electron transfer is blocked and energy transfer takes place to chalcone moiety which is followed by emission at 510 nm.

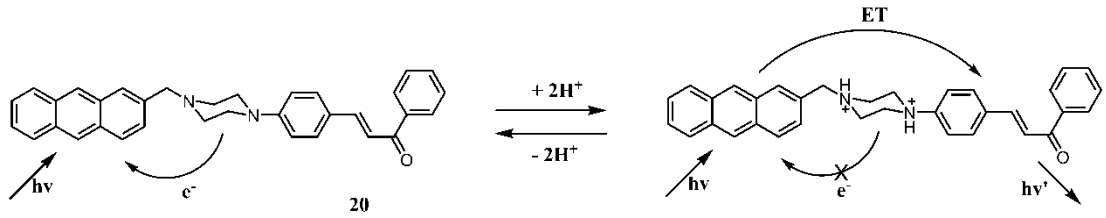

Figure 23. Electron and energy transfer in compound 20

Within the past 50 years, the use of Förster energy transfer has found applications in a highly diverse field, including light frequency conversion, cascade systems, artificial photosynthetic antenna, singlet oxygen generation and switching element in molecular machines.

1.8.2 Dexter type

If the donor and acceptor units are connected by a conjugated linker fragment, energy transfer may take place via several pathways which are through-space mechanism and some other pathways that may be collectively called as through-bond energy transfer mechanisms (Dexter type). The Dexter-type mechanism requires donor-acceptor orbital overlap, which can be provided either directly or by the bridge. Thus it is a short-range (<10 Aº) interaction and it diminishes exponentially with distance.[72] Overlap between the emission spectrum of the donor and the absorption of the acceptor is not required in through-bond energy transfer. Contrary to the Förster mechanism, it may not be possible to determine how much energy transfer proceeds via conjugated bi(multi)chromophoric systems. Yet the overall rates of energy transfer can be measured.

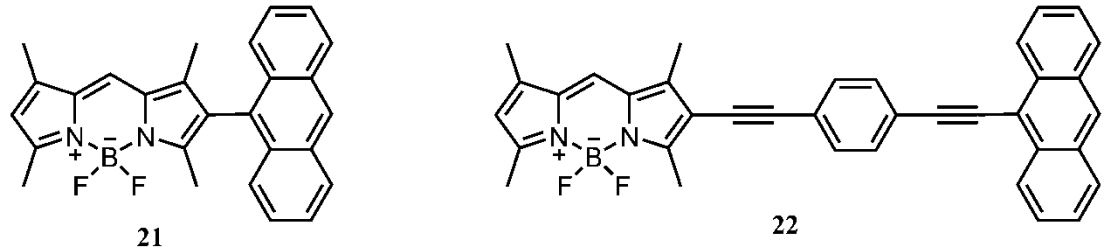

Figure 24. Through-bond energy transfer cassettes

Burgess et al synthesized a series of Anthracene-BODIPY cassettes in order to observe rates of energy transfer when the orientation of donor and acceptor moieties are changed.[48] Compounds **21** and **22** (Figure 24) clearly summarize the description of a truly cassette. **22** is not a truly cassette, because it's a fully conjugated system without an internal twist to break that conjugation. This is reflected in the slightly red-shifted and broader absorption spectrum. But in **21** the anthracene and the BODIPY are directly attached and steric interactions prevent the planarity of the structure which makes it a true cassette.

CHAPTER 2

EXPERIMENTAL

2.1 Instrumentation

All chemicals and solvents purchased from Aldrich were used without further purification. Column chromatography of all products was performed using Merck Silica Gel 60 (particle size: 0.040–0.063 mm, 230–400 mesh ASTM). Reactions were monitored by thin layer chromatography using fluorescent coated aluminum sheets.

^{1}H NMR and ^{13}C NMR spectra were recorded using a Bruker DPX–400 in $CDCl_3$ with TMS as internal reference. Splitting patterns are designated as s (singlet), d (doublet), t (triplet), q (quartet), m (multiplet), and p (pentet).

Absorption spectrometry was performed using a Varian spectrophotometer. Fluorescence spectra were determined on a Varian Eclipse spectrofluorometer. Solvents used for spectroscopy experiments were spectrophotometric grade. Mass spectrometry measurements were done at the Ohio State University Mass Spectrometry and Proteomics Facility, Ohio, USA.

2.2 Synthesis of compound 23

4-Iodobenzoylchloride (7.7 mmol, 2.05 g) and 3-ethyl-2,4-dimethyl pyrrole (15.4 mmol, 1.9 g) were dissolved in CH_2Cl_2 and refluxed for 3 h. After 3 h, Et_3N (5 mL) and $BF_3.OEt_2$ (5 mL) were added. Then bright yellowish fluorescence was observed. Crude product washed three times with water and dried over Na_2SO_4 and concentrated in vacuo. Then the crude product purified by silica gel column chromatography (eluent $CHCl_3$). First fraction which has bright yellow fluorescence was collected. Orange solid (2.53 g, 65 %).[73]

^{1}H NMR (400 MHz, CDCl3) δ 7.40-7.37 (m, 3H), 7.21-7.17 (m, 2H), 2.45 (s, 6H), 2.22 (q, 4H *J*= 7.5 Hz), 1.20 (s, 6H), 0.90 (t, 6H, *J*= 7.5 Hz)

^{13}C NMR (100 MHz, CDCl3) δ 153.7, 140.2, 138.4, 135.8, 132.7, 130.8, 128.9, 128.7, 128.3, 17.1, 14.5, 14.1, 12.5, 11.6

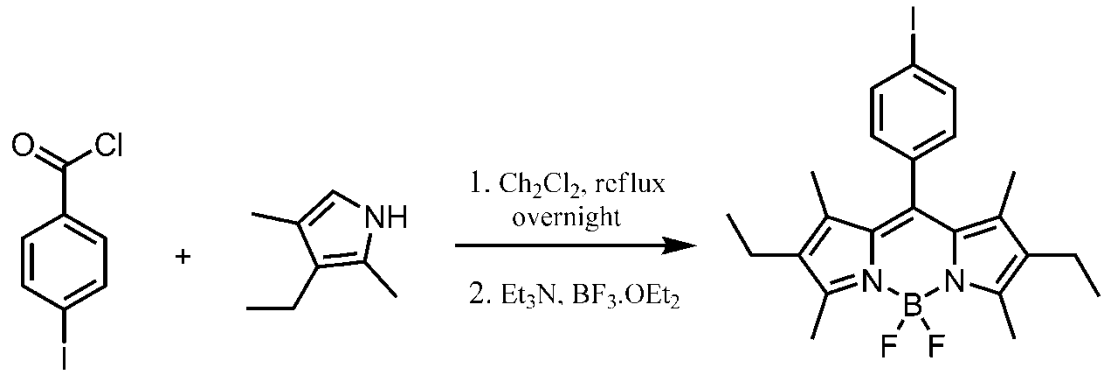

23

Figure 25. Synthesis of compound 23

2.3 Synthesis of compound 24

Compound **23** (1 mmol, 506mg) and 4-butoxy benzaldehyde (2.2mmol, 392mg; synthesized according to literature procedure[74]) were refluxed in a mixture of benzene (40 mL), glacial acetic acid (440 µL), and piperidine (530 µL). Water formed during the reaction, was removed azeotropically by heating overnight in a Dean-Stark apparatus. Crude product concentrated under vacuum, and then purified by silica gel column chromatography ($CHCl_3$ as eluent) the green colored fraction was collected (700mg, 84 %)

^{1}H NMR (400 MHz, CDCl3) δ 7.85 (d, 2H, *J*= 7.93 Hz), 7.66 (d, 2H, *J*= 16,7 Hz), 7.55 (d, 4H, *J*= 8.57 Hz), 7.21 (d, 2H, *J*= 16.77 Hz), 7.08 (d, 2H, *J*= 8.09 Hz), 6.92 (d, 4H, *J*= 8.56 Hz), 4.00 (t, 4H, *J*= 6.51 Hz), 2.60 (p, 4H, *J*= 8.5 Hz), 1.79 (m, 4H), 1.40 (s, 6H), 1.15 (t, 6H, *J*= 7.45 Hz), 1.00 (t, 6H, *J*= 7.35 Hz)

^{13}C NMR (100 MHz, CDCl3) δ 159.9, 151.0, 150.8, 138.3, 135.8, 133.8, 132.4, 130.8, 130.1, 128.8, 117.9, 114.8, 94.5, 67.9, 31.3, 19.2, 18.4, 14.0, 13.8, 11.9, 11.8

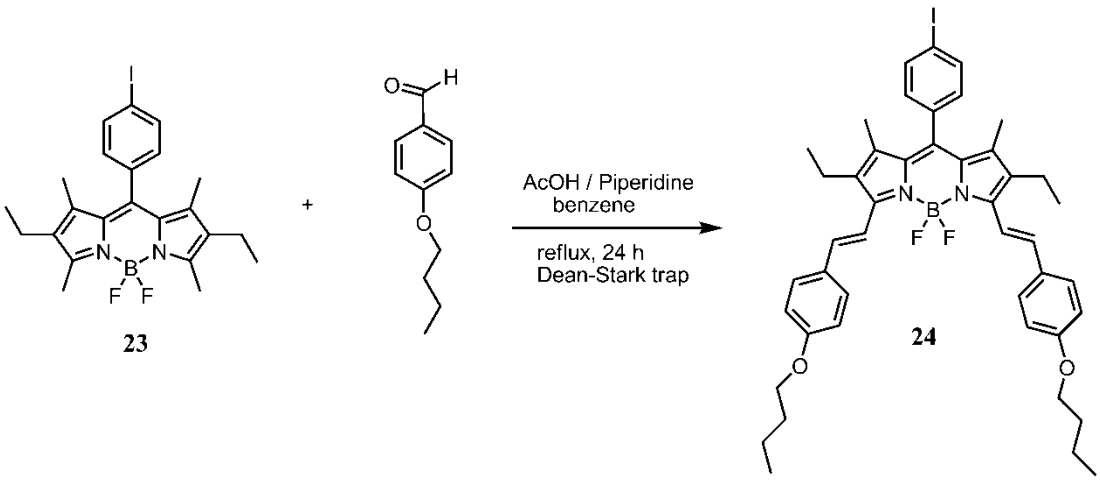

Figure 26. Synthesis of compound **24**

2.4 Synthesis of compound 25

Compound **24** (0.3 mmol, 248mg), $PdCl_2$ (0.06mmol, 10.6mg), CuI (0.12mmol, 23mg) and PPh_3 (0.24 mmol, 63mg) were added to the round bottomed flask which was previously flushed with Argon. As a solvent Et_3N (5 mL) and anhydrous THF (50 mL) were added. The solution was degassed with Argon for 15 min. The trimethylsilylacetylene (0.7mmol, 0.1mL) was then added. The reaction mixture was stirred overnight at room temperature. After completion of the reaction, solvent was removed in vacuo. The crude product purified by silica gel column chromatography (eluent: $CHCl_3$). Green solid (210mg, 87%)

^{1}H NMR (400 MHz, CDCl3) δ 7.50 (d, 2H, *J*= 15.8 Hz), 7.42 (d, 2H, *J*= 8.1 Hz), 7.35 (d, 4H *J*= 7.92 Hz), 7.10 (d, 2H, *J*=8.23 Hz), 7.02 (d, 2H, *J*= 16.1 Hz), 6.70 (d, 4H, *J*= 8.4 Hz), 3.80 (t, 4H, *J*= 6.42 Hz), 2.40 (m, 4H), 1.60 (m, 4H), 1.30 (m, 6H), 1.15 (s, 6H), 1.00 (t, 6H, *J*= 7.5 Hz), 0.80 (t, 6H, *J*= 7.3 Hz), 0.12 (s, 9H)

^{13}C NMR (100 MHz, CDCl3) δ 159.9, 150.8, 138.5, 136.8, 135.7, 134.4, 132.7, 130.2, 129.6, 128.3, 127.7, 123.8, 118.0, 114.9, 104.5, 95.7, 67.9, 31.4, 19.3, 18.5, 14.1, 13.9, 11.8, 0.0

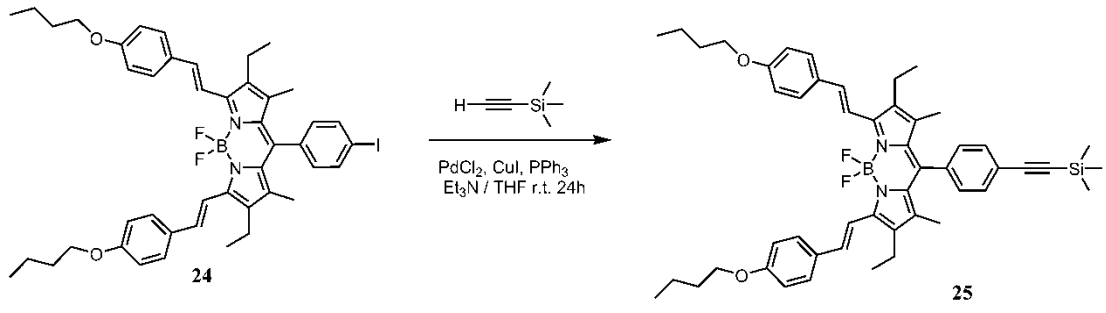

24 25

Figure 27. Synthesis of compound **25**

2.5 Synthesis of compound 26

NaOH (2mmol, 80mg) in 5 mL MeOH was added to a solution of **25** (1mmol, 800mg) in MeOH/CH_2Cl_2 (10/30 mL). The solution was stirred at r.t. for 1 hour, until the complete consumption of the starting material was observed by TLC ($CHCl_3$/Hex 1:1). Water (30 mL) was added and the solution was extracted with CH_2Cl_2 (30 mL). After evaporation, the organic layer was purified by column chromatography on silica (eluent: $CHCl_3$), yielding the desired compound **26** (680mg, 93%)

^{1}H NMR (400 MHz, CDCl3) δ 7.60 (d, 2H, *J*= 15.7 Hz), 7.50 (d, 2H, *J*= 8.13 Hz), 7.40 (d, 4H, *J*= 7.9 Hz), 7.20 (d, 2H, *J*= 8.1 Hz), 7.10 (d, 2H, *J*= 16.7 Hz), 6.80 (d, 4H, *J*= 8.3 Hz), 3.90 (t, 4H, *J*= 6.4 Hz), 3.10 (s, 1H), 2.50 (m, 4H), 1.70 (m, 4H), 1.40 (m, 6H), 1.30 (s, 6H), 1.10 (t, 6H, *J*= 7.3 Hz), 0.90 (t, 6H, *J*= 7.2 Hz)

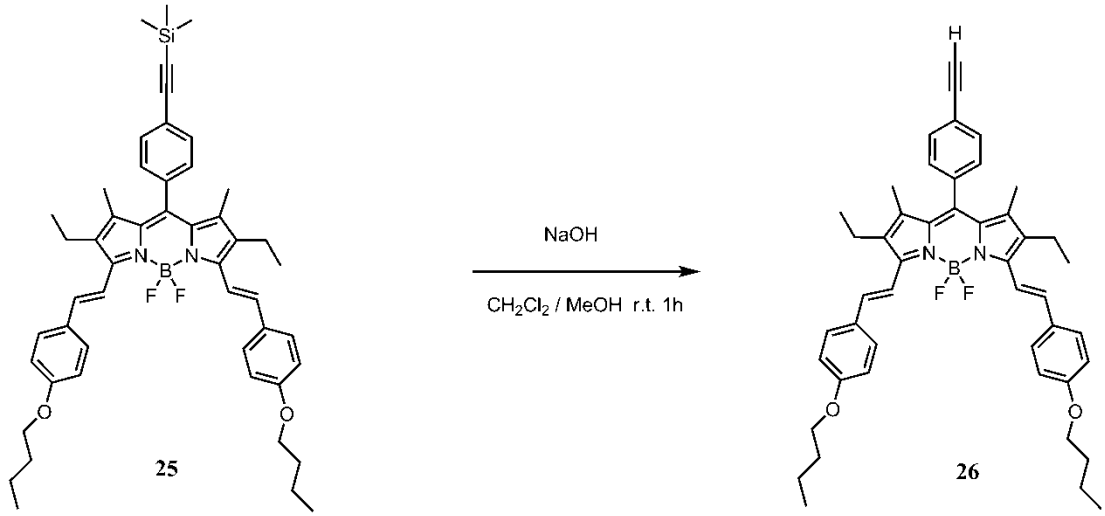

Figure 28. Synthesis of compound **26**.

2.6 Synthesis of compound 27

(2-(4-Idophenyl) ethynyl) trimethylsilane (0.4mmol, 120mg; synthesized according to literature procedure[75]) compound **26** (0.33mmol, 240mg), $PdCl_2$ (0.06mmol, 10.6mg), CuI (0.12mmol, 23mg) and PPh_3 (0.24mmol, 63mg) were added to the round bottomed flask which was previously flushed with Argon. As a solvent Et_3N (5 mL) and anhydrous THF (30 mL) were added. The reaction mixture was stirred overnight at room temperature. After completion of the reaction, solvent was removed in vacuo. The crude product purified by silica gel column chromatography (eluent: $CHCl_3$). Green solid (130mg, 44%)

^{1}H NMR (400 MHz, CDCl3) δ 7.60 (d, 2H, *J*= 15.6 Hz), 7.40 (d, 4H, *J*= 7.8 Hz), 7.40-7.10 (m, 10H), 6.80 (d, 4H, *J*= 8.4 Hz), 3.90 (t, 4H, *J*= 6.5 Hz), 2.50 (m, 4H), 1.70 (m, 4H), 1.40 (m, 6 H), 1.30 (s, 6H), 1.10 (t, 6H, *J*= 7.4 Hz), 0.90 (t, 6H, *J*= 7.4 Hz), 0.20 (s, 9H)

^{13}C NMR (100 MHz, CDCl3) δ 160.0, 150.8, 138.5, 136.8, 135.8, 133.9, 132.8, 132.3, 131.7, 131.5, 130.2, 129.2, 128.9, 123.8, 123.4, 123.0, 118.1, 114.9, 104.6, 96.6, 90.7, 90.4, 67.9, 31.4, 29.7, 19.3, 18.4, 14.1, 13.9, 11.8, 0.0

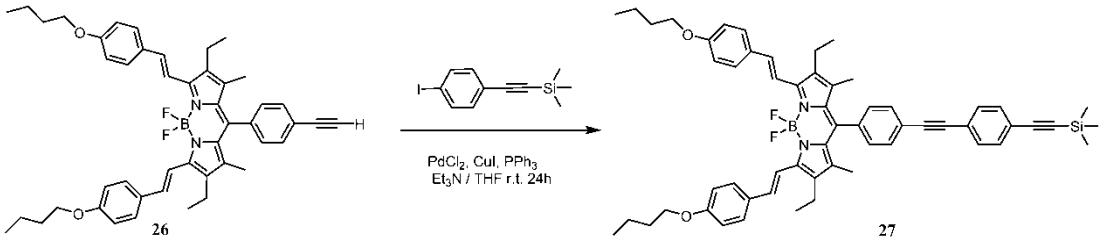

26 27

Figure 29. Synthesis of compound **27**

2.7 Synthesis of compound 28

NaOH (1mmol, 40mg) in 5 mL MeOH was added to a solution of **27** (0.5mmol, 450mg) in MeOH/CH_2Cl_2 (10/30 mL). The solution was stirred at r.t. for 1 hour, until the complete consumption of the starting material was observed by TLC ($CHCl_3$/Hex 1:1). Water (30 mL) was added and the solution was extracted with CH_2Cl_2 (30 mL). After evaporation, the crude product (**28**) was used in the next reaction without further purification. (330mg, 82%)

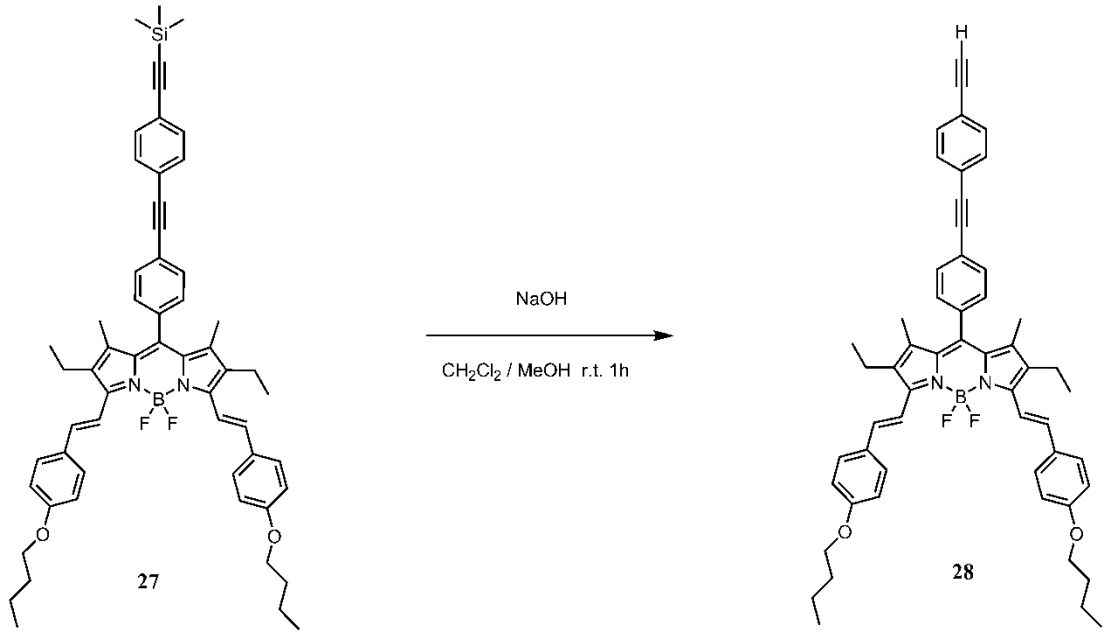

Figure 30. Synthesis of compound **28**

2.8 Synthesis of compound 29

Compound **23** (0.2mmol, 110mg), compound **26** (0.2mmol, 150mg), $PdCl_2$ (0.06mmol, 11mg), CuI (0.12mmol, 23mg) and PPh_3 (0.24mmol, 63mg) were added to the round bottomed flask which was previously flushed with Argon. As a solvent Et_3N (5 mL) and anhydrous THF (50 mL) were added. The mixture was heated at 60°C under Argon for 24 h, until the complete consumption of starting material was observed. The solution was evaporated to dryness and the product was purified by column chromatography on silica (eluent: $CHCl_3$), yielding the desired compound **29** (90mg, 41%)

^{1}H NMR (400 MHz, CDCl3) δ 7.64 (m, 4H), 7.60 (d, 2H, *J*= 15.9 Hz), 7.50 (d, 4H, *J*= 8.1 Hz), 7.25 (m, 4H), 7.15 (d, 2H, *J*= 16.2 Hz), 6.85 (d, 4H, *J*= 8.6 Hz), 3.90 (t, 4H, *J*= 6.5 Hz), 2.50 (m, 4H), 2.45 (s, 6H), 2.20 (m, 4H), 1.70 (m, 4H), 1.40 (m, 4H), 1.30 (s, 6H), 1.25 (s, 6H), 1.10 (t, 6H, *J*= 7.5 Hz), 0.90 (t, 12H, *J*= 6.7 Hz)

^{13}C NMR (100 MHz, CDCl3) δ 159.9, 154.1, 150.8, 139.2, 138.4, 138.2, 136.7, 136.2, 135.8, 133.8, 133.0, 132.7, 132.3, 130.6, 130.3, 130.1, 129.2, 128.8, 123.5, 117.9, 114.9, 90.1, 67.9, 31.3, 19.3, 18.4, 17.3, 17.1, 14.6, 14.08, 13.9, 12.6, 11.9, 11.7, 9.4

MALDI-TOF-MS calcd for $[M]^+$ 1102.609, found 1102.963.

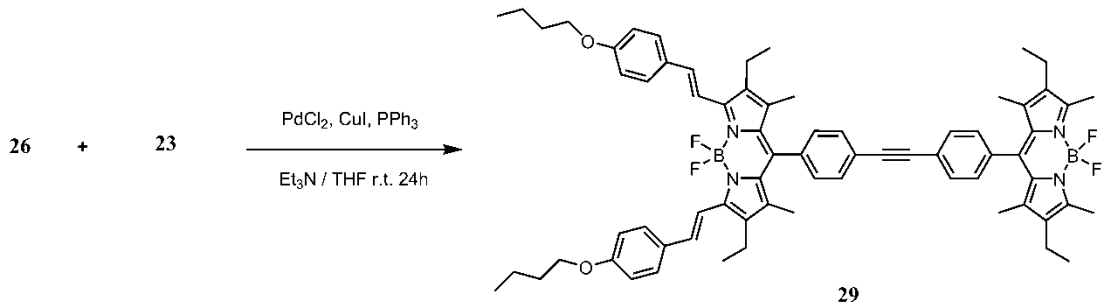

Figure 31. Synthesis of compound 29

2.9 Synthesis of compound 30

Compound **23** (0.25mmol, 127mg), compound **28** (0.25mmol, 200mg), $PdCl_2$ (0.06mmol, 11mg), CuI (0.12mmol, 23mg) and PPh_3 (0.24mmol, 63mg) were added to the round bottomed flask which was previously flushed with Argon. As a solvent Et_3N (5 mL) and anhydrous THF (50 mL) were added. The mixture was heated at 60°C under Argon for 24 h, until the complete consumption of starting material was observed. The solution was evaporated to dryness and the product was purified by column chromatography on silica (eluent: $CHCl_3$), yielding the desired compound **30** (140mg, 46%)

^{1}H NMR (400 MHz, CDCl3) δ 7.60 (m, 6H), 7.50 (s, 4H), 7.45 (d, 4H, *J*= 7.9 Hz), 7.30 (m, 4H), 7.20 (d, 2H, *J*= 18.3 Hz), 3.90 (t, 4H, *J*= 6.4 Hz), 2.55 (m, 4H), 2.47 (s, 6H), 2.25 (m, 4H), 1.70 (m, 4H), 1.45 (m, 4H), 1.30 (s, 6H), 1.26 (s, 6H), 1.10 (t, 6H, *J*= 7.2 Hz), 0.90 (t, 12H, *J*= 7.3 Hz)

^{13}C NMR (100 MHz, CDCl3) δ 158.9, 153.1, 137.4, 137.2, 135.1, 134.7, 132.8, 140.0, 131.7, 131.2, 130.7, 129.6, 129.1, 128.1, 127.7, 127.6, 122.6, 122.1, 116.9, 113.8, 89.9, 66.8, 30.3, 18.2, 17.4, 16.1, 13.6, 13.0, 12.8, 11.5, 10.9, 10.7

MALDI-TOF-MS calcd for $[M]^+$ 1202.640, found 1202.928.

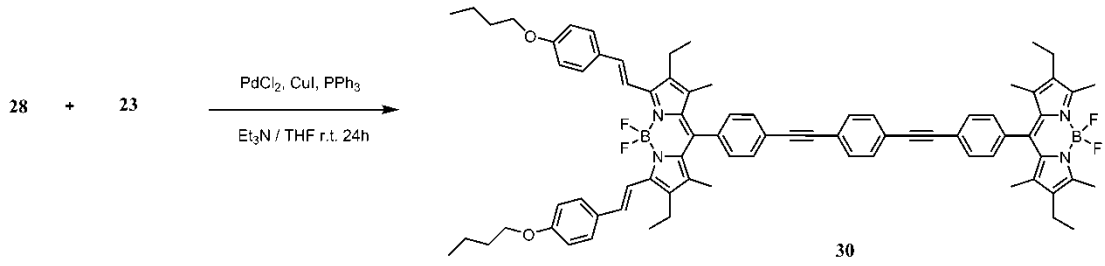

Figure 32. Synthesis of compound **30**

2.10 Synthesis of compound 31

Compound **29** (0.045mmol, 50mg) and p-dimethylaminobenzaldehyde (0.05mmol, 7.5mg) were refluxed in a mixture of benzene (40 mL), glacial aceticacid (0.5 mL) and piperidine (0.5 mL). Any water formed during the reaction, was removed azeotropically by heating overnight in a Dean-Stark apparatus. The solvent was removed in vacuo, then crude product was purified by Preparative thin layer chromatography (solvent: $CHCl_3$). Dark blue colored fraction was collected (15mg, 27%)

^{1}H NMR (400 MHz, CDCl3) δ 7.67 (m, 4H), 7.63 (d, 1H, *J*= 16.7 Hz), 7.53 (d, 4H, *J*= 8.4 Hz), 7.48 (d, 2H, *J*= 15.9 Hz), 7.32 (m, 4H), 7.20 (d, 1H, *J*= 16.4 Hz), 6.90 (d, 4H, *J*= 8.6 Hz), 6.70 (d, 2H, *J*= 15.9 Hz), 4.00 (t, 4H, *J*= 7.6 Hz), 3.00 (s, 6H), 2.60 (m, 4H), 2.52 (s, 3H), 1.80 (m, 4H), 1.50 (m, 4H), 1.40 (s, 6H), 1.35 (s, 6H), 1.10 (m, 9H), 0.90 (m, 9H)

^{13}C NMR (100 MHz, CDCl3) δ 159.9, 150.8, 138.4, 137.2, 136.6, 135.7, 133.8, 133.4, 132.7, 132.2, 131.2, 130.1, 129.2, 129.0, 128.8, 128.8, 123.6, 123.4, 117.9, 114.8, 112.4, 108.3, 90.2, 90.0, 67.9, 40.4, 31.3, 29.7, 19.2, 18.4, 17.1, 14.6, 14.0, 13.8, 12.6, 11.8, 11.7, 11.6

MALDI-TOF-MS calcd for $[M]^+$ 1233.683, found 1233.975.

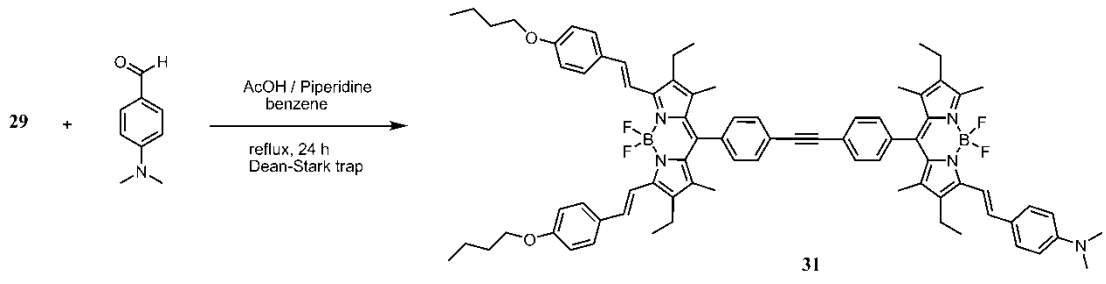

Figure 33. Synthesis of compound **31**

2.11 Synthesis of compound 32

Compound **30** (0.042mmol, 50mg) and p-dimethylaminobenzaldehyde (0.05mmol, 7.5mg) were refluxed in a mixture of benzene (40 mL), glacial aceticacid (0.5 mL) and piperidine (0.5 mL). Any water formed during the reaction, was removed azeotropically by heating overnight in a Dean-Stark apparatus. The solvent was removed in vacuo, then the crude product was purified by Preparative thin layer chromatography (solvent: $CHCl_3$). Dark blue colored fraction was collected (12mg, 20%)

^{1}H NMR (400 MHz, CDCl3) δ 7.61 (m, 6H), 7.60 (d, 1H, *J*= 16.7 Hz), 7.51 (m, 8H), 7.28 (m, 4H), 7.12 (m, 3H), 6.85 (d, 4H, *J*= 8.6 Hz), 3.90 (t, 4H, *J*= 7.6 Hz), 3.00 (s, 6H), 2.60 (m, 7H), 1.80 (m, 4H), 1.50 (m, 4H), 1.40 (s, 6H), 1.35 (s, 6H), 1.10 (m, 9H), 0.90 (m, 9H)

MALDI-TOF-MS calcd for $[M]^+$ 1333.714, found 1333.934.

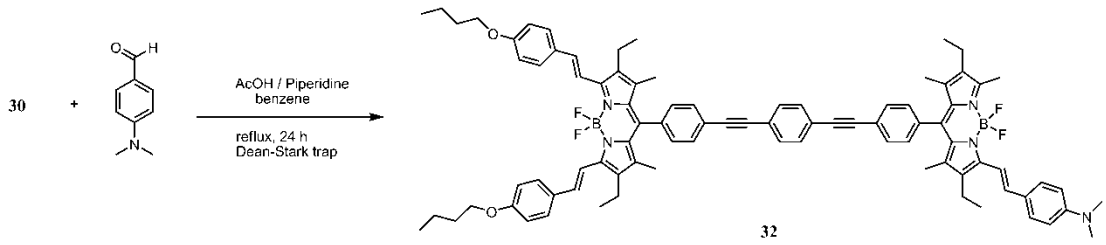

Figure 34. Synthesis of compound **32**

2.12 Synthesis of compound 33

Compound **29** (0.045mmol, 50mg) and 4-(1-aza-7,10-dioxa-4,13-dithiacyclopentadecyl) benzaldehyde (0.05mmol, 18mg; synthesized according to literature procedure[76]) were refluxed in a mixture of benzene (40 mL), glacial aceticacid (0.5 mL) and piperidine (0.5 mL). Any water formed during the reaction, was removed azeotropically by heating overnight in a Dean-Stark apparatus. The solvent was removed in vacuo, then the crude product was purified by Preparative thin layer chromatography (solvent: $CHCl_3$). Green colored fraction was collected (20mg, 31%)

^{1}H NMR (400 MHz, CDCl3) δ 7.65 (m, 4H), 7.58 (d, 1H, *J*= 15.8 Hz), 7.50 (d, 4H, *J*= 8.4 Hz), 7.42 (d, 2H, *J*= 16.6 Hz), 7.30 (m, 4H), 7.12 (d, 1H, *J*= 15.4 Hz), 6.85 (d, 4H, *J*= 8.4 Hz), 6.60 (d, 2H, *J*= 15.9 Hz), 3.90 (t, 4H, *J*= 6.9 Hz), 3.70 (m, 4H), 3.60 (m, 8H), 2.80 (m, 4H), 2.70 (m, 4H), 2.55 (m, 4H), 2.50 (s, 3H), 2.10 (m, 2H), 1.70 (m, 4H), 1.40 (m, 4H), 1.30 (s, 6H), 1.25 (s, 6H), 1.10 (m, 9H), 0.90 (t, 9H, *J*= 7.3 Hz)

^{13}C NMR (100 MHz, CDCl3) δ 158.9, 152.6, 150.2, 149.7, 146.4, 137.4, 136.2, 135.6, 135.1, 134.7, 132.8, 132.3, 131.7, 131.3, 130.8, 130.1, 129.1, 128.1, 128.0, 127.8, 124.8, 122.5, 118.9, 117.7, 116.9, 114.9, 113.8, 110.9, 89.1, 88.9, 73.2, 69.7, 66.8, 51.0, 30.3, 30.3, 28.6, 18.2, 17.4, 16.1, 13.6, 13.0, 12.8, 11.6, 10.8, 10.7, 10.6

MALDI-TOF-MS calcd for $[M]^+$ 1439.726, found 1440.009.

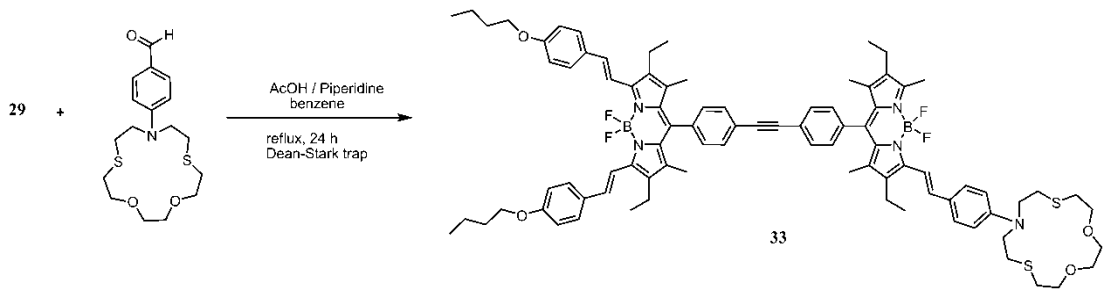

Figure 35. Synthesis of compound **33**

2.13 Synthesis of compound 34

Compound **30** (0.042mmol, 50mg) and 4-(1-aza-7,10-dioxa-4,13-dithiacyclopentadecyl) benzaldehyde (0.05mmol, 18mg; synthesized according to literature procedure[76]) were refluxed in a mixture of benzene (40 mL), glacial aceticacid (0.5 mL) and piperidine (0.5 mL). Any water formed during the reaction, was removed azeotropically by heating overnight in a Dean-Stark apparatus. The solvent was removed in vacuo, then the crude product was purified by Preparative thin layer chromatography (solvent: $CHCl_3$). Green colored fraction was collected (15mg, 30%)

^{1}H NMR (400 MHz, CDCl3) δ 7.60 (m, 4H), 7.50 (m, 9H), 7.25 (m, 4H), 7.15 (m, 3H), 6.85 (d, 4H, *J*= 8.4 Hz), 6.60 (d, 2H, *J*= 15.9 Hz), 3.90 (t, 4H, *J*= 6.9 Hz), 3.70 (m, 4H), 3.60 (m, 8H), 2.80 (m, 4H), 2.70 (m, 4H), 2.55 (m, 4H), 2.50 (s, 3H), 2.10 (m, 2H), 1.70 (m, 4H), 1.40 (m, 4H), 1.30 (s, 6H), 1.25 (s, 6H), 1.10 (m, 9H), 0.90 (t, 9H, *J*= 7.3 Hz)

^{13}C NMR (100 MHz, CDCl3) δ 156.9, 152.3, 151.2, 149.7, 146.4, 137.3, 136.3, 135.3, 135.1, 134.7, 132.5, 132.3, 131.7, 131.3, 130.8, 130.1, 129.6, 128.1, 128.0, 127.8, 125.8, 122.7, 118.9, 117.7, 116.9, 114.9, 113.8, 110.9, 89.1, 88.9, 73.2, 69.7, 66.8, 51.0, 30.3, 30.3, 28.6, 18.2, 17.4, 16.1, 13.6, 13.0, 12.8, 11.6, 10.8, 10.7, 10.7

MALDI-TOF-MS calcd for $[M]^+$ 1539.757, found 1538.6630.

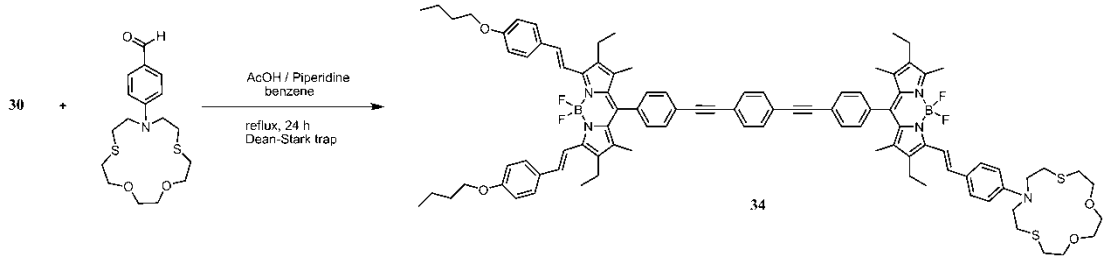

Figure 36. Synthesis of compound **34**

CHAPTER 3

RESULTS AND DISCUSSION

Due to the potential applications in cell physiology, analytical and environmental chemistry, design and synthesis of fluorescent chemosensors is an active field of supramolecular chemistry. Especially, chemosensors targeting heavy and transition metal cations, such as Hg (II), Pb (II), Ag (I), and Cu (II), are of great interest. Developing highly selective and sensitive fluorescent probes is stil a challenge and it's gaining importance as the research to that end advances. Up to now, large number of chemosensors for various cations has been reported. Most of them are PET type chemosensors, those working by causing spectral shifts in either absorbance or emission spectra (ICT type) are less common.

Recently boradiazaindacenes have become one of the most preferred fluorophores in the chemosensor design. Their magnificently rich chemistry and characteristic photophysical properties makes them invaluable.

Akkaya research group did a significant work by coupling ion sensing to resonance energy transfer. Previously, colleagues in our group reported BODIPY based modular ratiometric ICT chemosensors that were selective to Ag (I)[52] and Hg (II)[66]. In the first one they reported a dimeric BODIPY, which can be converted into an energy transfer cassette and furthermore into a ratiometric ICT based Ag (I) sensor, through simple structural modifications. In that design the two fluorophores were kept very close (a phenyl unit in between) to each other, so that the through-space energy transfer was nearly 100% efficient. Therefore it was a large pseudo-Stokes' shift chemosensor.

The second one which was designed as a Hg (II) selective chemosensor, was built from the same dimeric BODIPY unit as it was in the first example. But this time the distance between two fluorophores was changed (3 and 5 phenyl units as a spacer) and its affects on the RET (resonance energy transfer) efficiency was investigated. By completing this work, they introduced a new strategy in ratiometric chemosensor design in which the range of ratios can be significantly improved. If the chemosensor is designed as energy transfer dyad, and once the interchromophoric distance is carefully adjusted, binding of the analyte increases the spectral overlap between the donor emission and the acceptor absorption peaks. Thus, more efficient Forster type energy transfer in the bound state results in higher emission intensity for the analyte-bound chemosensor, effectively increasing the signal ratio for the two states. Binding of mercuric ion to the receptor unit shows ICT type behavior. As a result of this, absorbance of the acceptor unit was blue-shifted while the emission of the donor part remains to be same. This spectral change increases the spectral overlap, thus, causes spectacular change in the efficiency of the energy transfer. In other words, Hg (II) binding increases the spectral overlap, which increases the energy transfer from donor to acceptor, and due to this, dynamic range enhancement can be done.

Main feature of the two examples mentioned above is that in both of them, the receptor unit was attached to the energy acceptor (A) part of the chemosensor that was designed as an energy transfer dyad. This time, we decided to investigate the photophysical results when the receptor unit was tagged to the energy donor (D) part of the chemosensor. Binding of the analyte will decrease spectral overlap between the donor emission and acceptor absorption peaks. Therefore, the efficiency of the Förster type energy transfer will be diminished in the bound form. Our design principles are summarized in Figure 37.

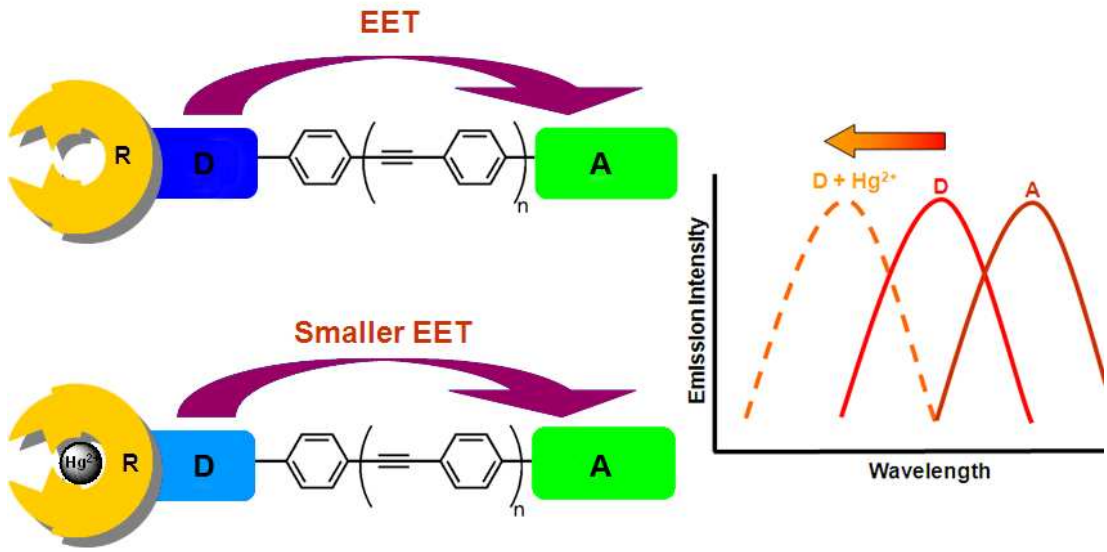

Figure 37. Design principle of the proposed System (n=1, 2)

To demonstrate feasibility of our approach, we targeted two generations of BODIPY dyads, with increasing interchromophoric distance (Figure 38). And the receptor unit we chose was Hg (II) selective one.

In ICT type chemosensors in which the cation receptor is an electron donating one, cation binding always causes blue shift in the absorption spectrum. In our system this will decrease the EET efficiency. We need to lower the EET efficiency to a certain level that appropriate cation modulation could be done. Therefore, we synthesized second generation of BODIPY dyad (compound **30**). By doing so, we aimed to take the advantage of increased interchromophoric distance that causes lowering of EET efficiency.

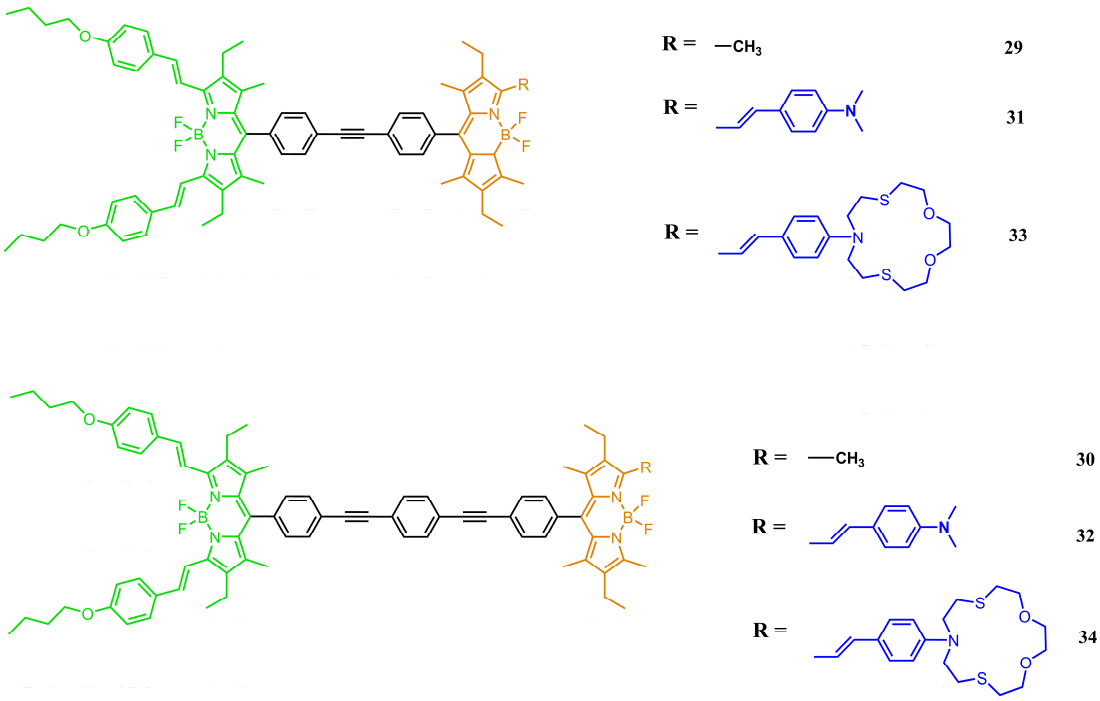

Figure 38. Target compounds

We also run energy minimization studies on these compounds by using Spartan'06 geometry optimization (Figures 39, 40). It's evident that we have through space interaction between donor and acceptor parts. The methyl groups next to the phenyl units ensure the perpendicular orientation of the phenyl rings, thus, prevents any through bond interaction between donor and acceptor moieties.

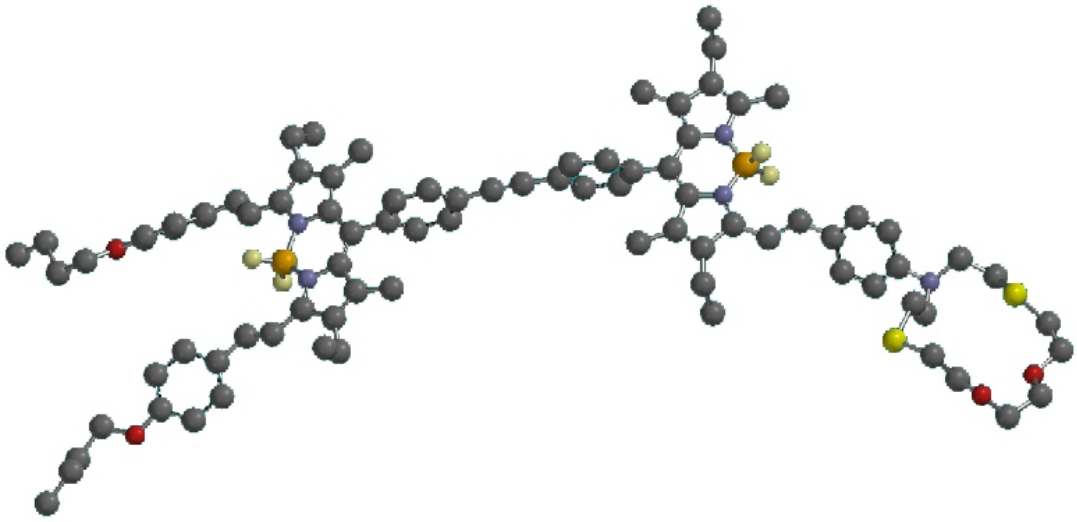

Figure 39. Energy minimized (Spartan'06 geometry optimization) structure of compound **33**. Calculated B-B distance 18.089 A°.

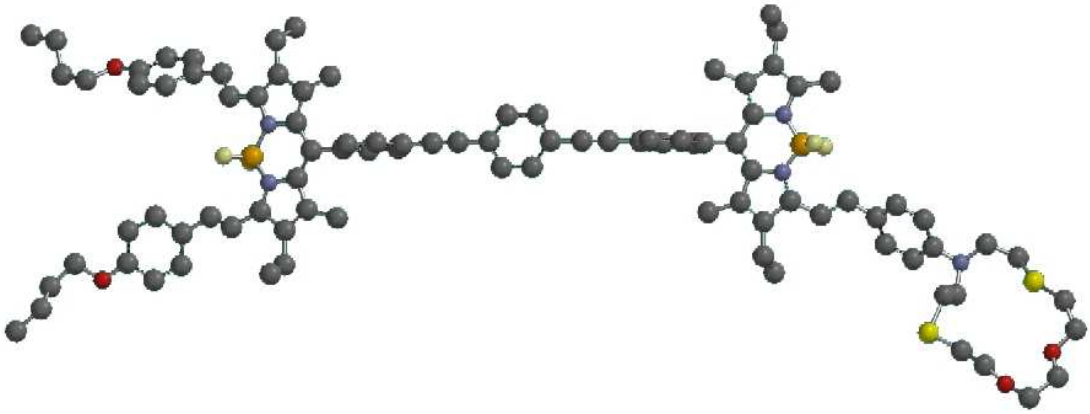

Figure 40. Energy minimized (Spartan'06 geometry optimization) structure of compound **34**. Calculated B-B distance 25.168 A°.

Existence of two distinct peaks at 520 and 660 nm in the absorption spectra of compounds **29** and **30** indicates the presence of two noninteracting chromophores in the mentioned molecules (Figure 31). The shorter wavelength absorption corresponds to the boradiazaindacene part, whereas the other one belongs to the modified BODIPY unit.

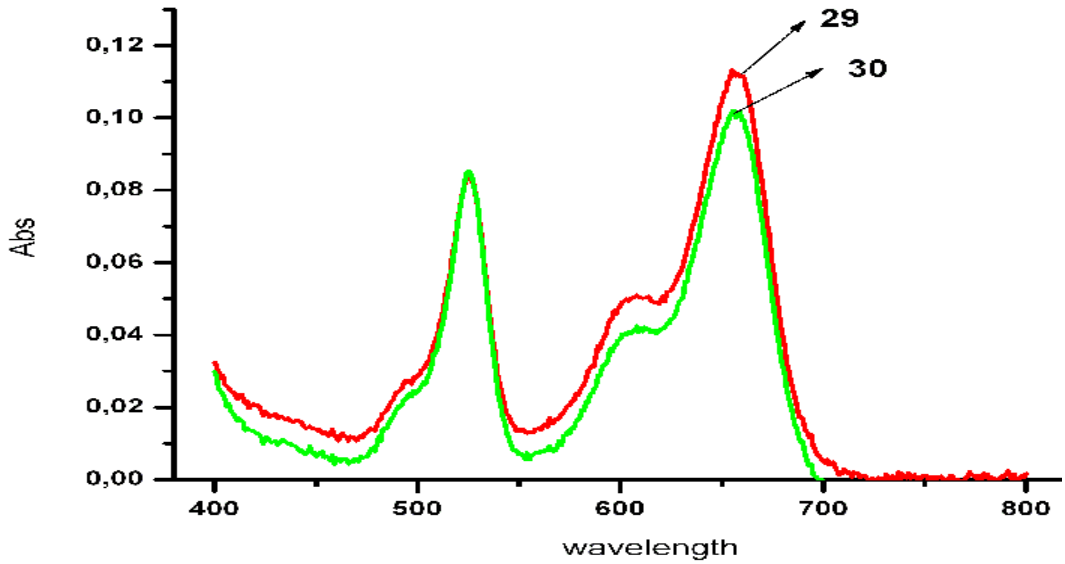

Figure 41. Absorption spectra of compounds **29** and **30** in THF.

The emission spectra of the same molecules (Figure 42) show that very effective energy transfer occurs in both of them. However, the efficiency of the energy transfer in compound **30** is less than that of compound **29**. This result correlates well with our expectations and theoretic definitions. Calculated B-B distance for compound **30** is 25.168 A°, and for **29** it is 18.089 A°. Increasing interchromophoric distance will decrease the energy transfer efficiency, as a result of this emission signal of the energy donor part increases.

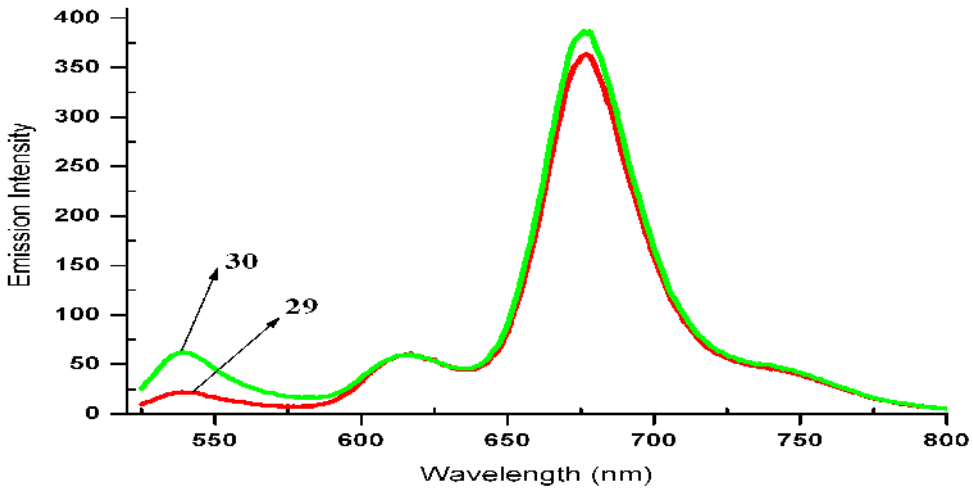

Figure 42. Emission spectra of compounds **29** and **30** in THF.

The methyl groups neighboring the BF_2 bridge are slightly acidic, and this property was exploited in the synthesis of compounds **31**, **32**, **33**, and **34**. The condensation reactions between compounds **29** and **30** and corresponding aldehydes were carried out in benzene, with azeotropic removal of water.

In order to obtain a cation responsive chemosensor, we took advantage of our modular design and switching to a dithiaazacrown-substituted benzaldehyde instead of 4-dimethylaminobenzaldehyde, we obtained compounds **33** and **34**. The specific dithiazacrown we selected, is reportedly selective for Hg(II) ions in a range of solvents. We made titration experiments for each of these compounds to see the affect of cation binding on the energy donor efficiency.

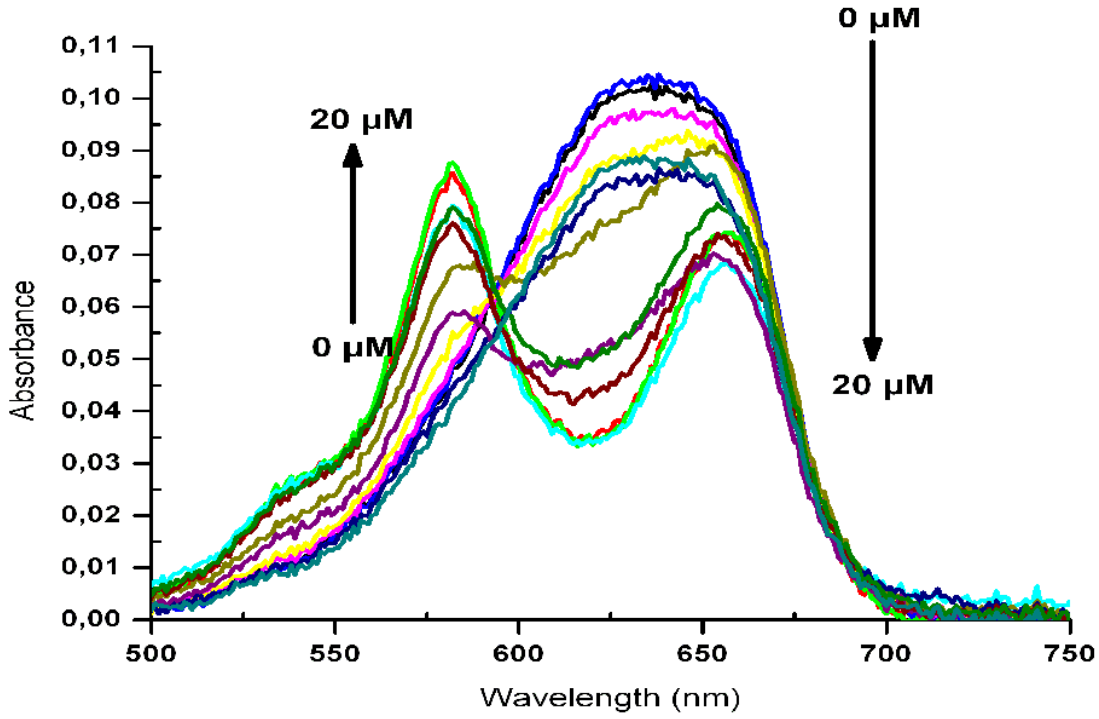

Figure 43. Absorbance spectra of compound **33** in the presence of increasing Hg(II) concentrations (0, 1.0, 2.0, 3.0, 4.0, 5.0, 10, 15, 20 µM)

Figure 43 shows the absorption spectra when the titration experiments are done for compound **33**. Since the absorption peaks of chromophores on compound **33** are very close, we see a broad peak locating in between 600 and 660 nm in the unbound form. Stock solutions are prepared in THF solution, the concentration of the dye kept at 1 μM. Stock solutions of the cations prepared by using the perchlorate salts as their THF solutions, then diluted with THF to obtain desired concentration of the cation. Bodipy dyad is titrated with Hg(II) at increasing concentrations (0, 1.0, 2.0, 3.0, 4.0, 5.0, 10, 15, 20 μM). Binding of the Hg(II) ion to the receptor part causes approximately 70 nm blue shift, due to the ICT type mechanism. And the receptor reaches its saturation point at 20 μM concentration.

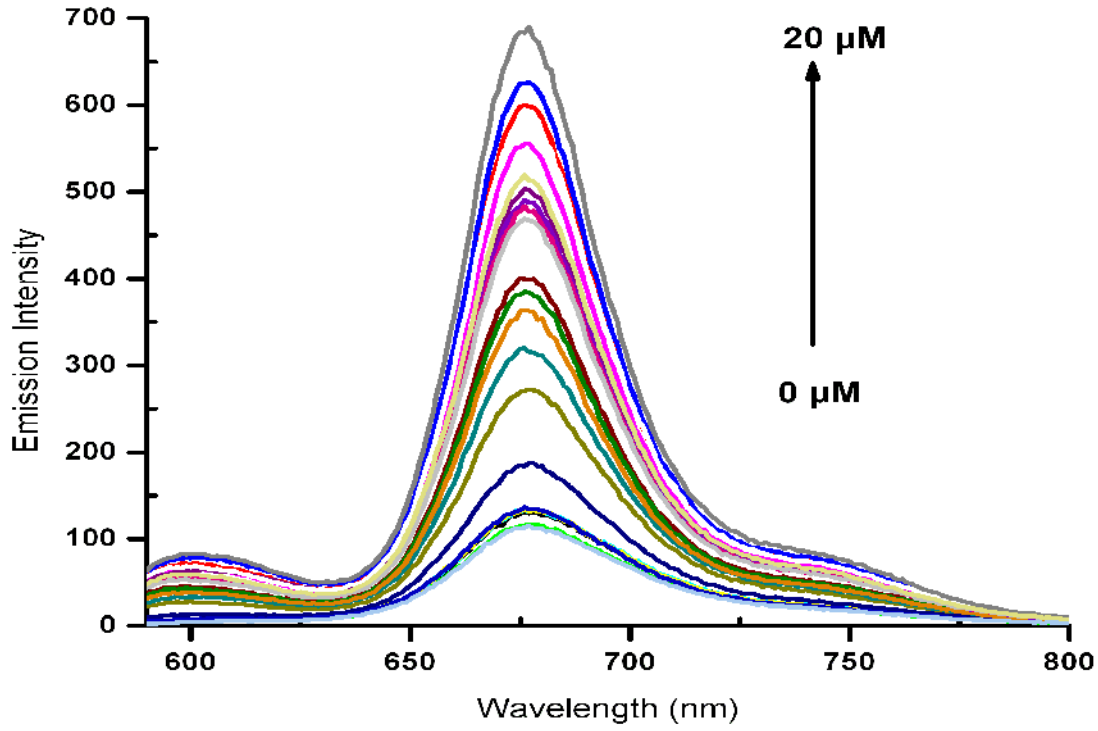

Figure 44. Emission spectra of compound **33** in the presence of increasing Hg(II) concentrations (0, 1.0, 2.0, 3.0, 4.0, 5.0, 10, 15, 20 μM)

Among the cations tested, the compound **33** showed high affinity towards Hg(II). In our case, Ag(I) ion is exceptional, it shows almost identical affinity with Hg(II). This is due to the hard-soft interaction and the shape of the macrocycle. But concentration of Ag(I) ion is quite low where the Hg(II) ion is quite abundant, so it doesn't cause much problem (Figure 45).

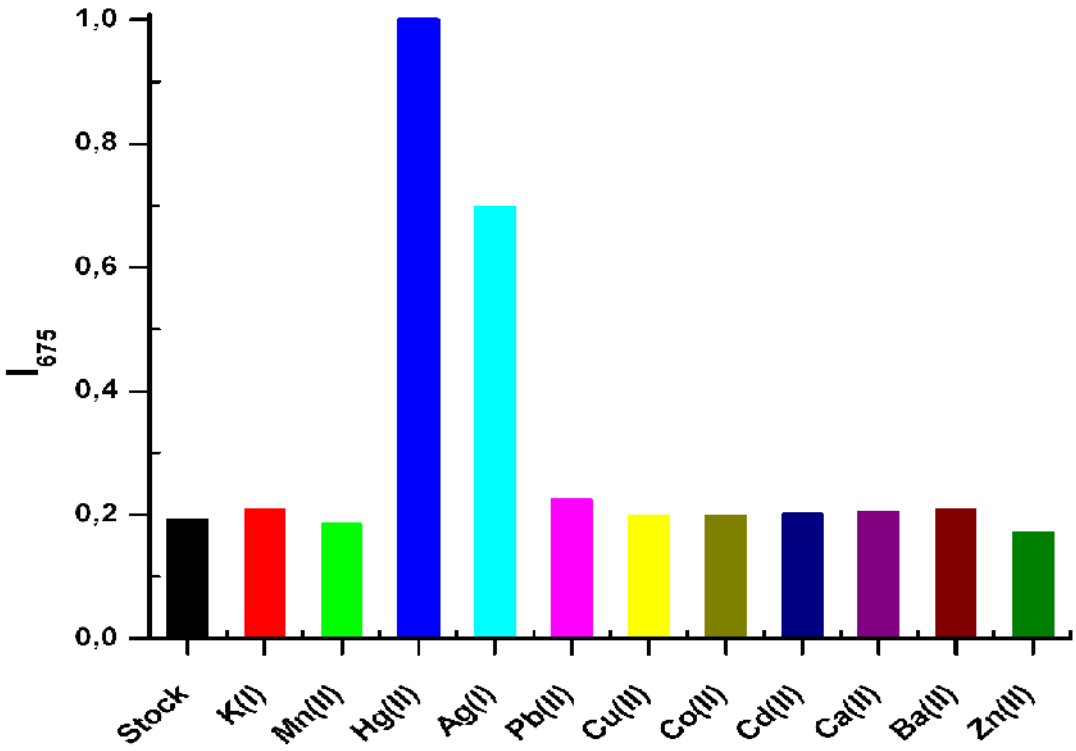

Figure 45. Emission ratios for the compound **33** obtained in the presence of different metal cations. The chemosensor was excited at 580 nm and ratio of emission data at 675 nm were calculated.

Also the emission experiments were carried out for the same solutions. Dye concentration is kept constant at 1.0 μM, and cation concentration in each solution is 50 μM. This value is 2.5 times higher than the saturation concentration of the chemosensor (Figure 46).

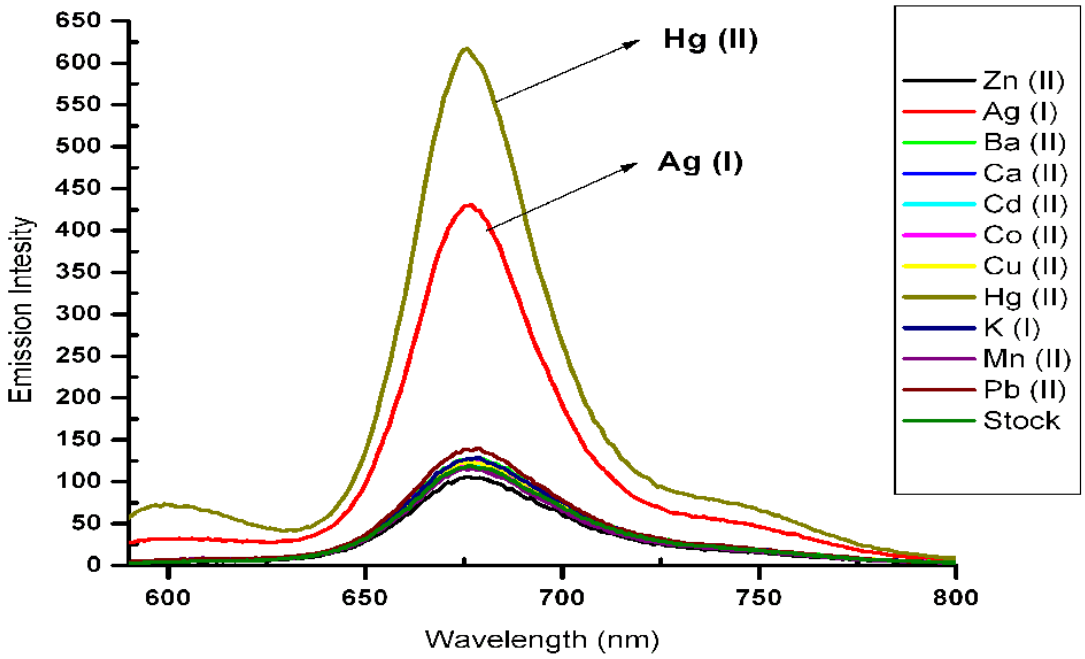

Figure 46. Emission spectra of compound **65** in the presence of various cations (cation concentrations 50 μM). Excitation wavelength 500 nm.

Finally, from the emission spectra of compounds **33** and **34** (bound and unbound form) it is difficult to make a judgment about the energy transfer efficiencies. We expected that bound form had lower energy transfer efficiency than the unbound form. Since the absorption of the acceptor part was so close to the emission of donor part (spectral overlap) nearly 100% efficient EET occurred in the unbound form. It's sure that after the cation binding the spectral overlap is diminished, and there should be a descent in the EET efficiency. In the initial state, there is larger overlap between donor emission and the acceptor absorbance, but in the bound state, overlap integral between donor emission and acceptor absorbance decreases which is directly proportional with the energy transfer efficiency, this is simply proof of our principle (Figure 47).

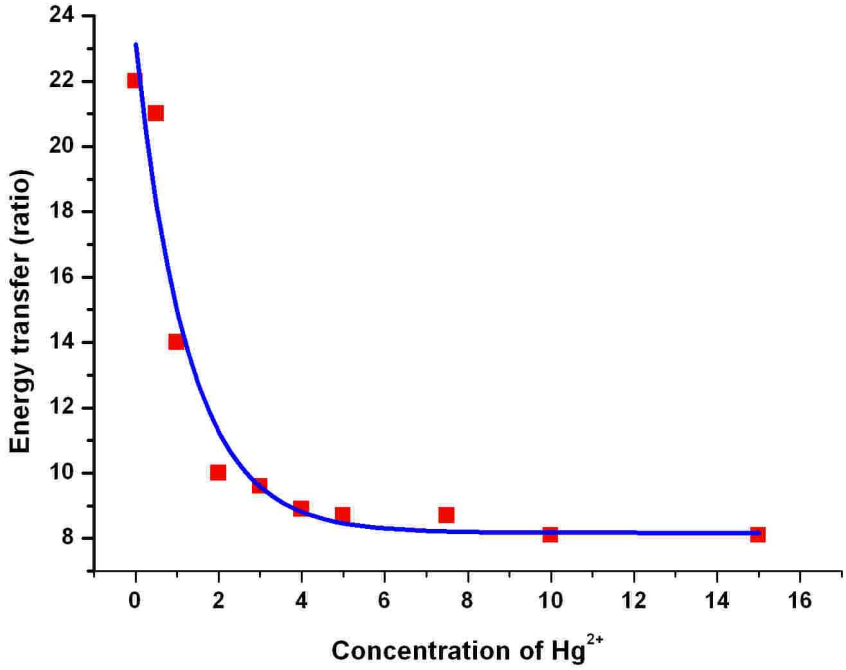

Figure 47. Decrease in the EET efficiency upon Hg(II) addition.

Our system is designed to work in organic media such as THF, but, chemosensors should also function in aqueous media for the signaling of the biologically important analytes. In our work we proposed that it's possible to design a ratiometric chemosensor via the modulation of energy donor chemosensor. This principle can easily be extended to aqueous media after appropriate structural modifications.

CHAPTER 4

CONCLUSION

In this study we have synthesized 2 different chemosensors for ratiometric assessment of ratiometric ion sensing. The results suggest that our original proposal was validated; the efficiency of energy transfer can be modulated from the side of energy donor chromophore. The work described here suggests paths for further improvements. It's apparent that the strategy described in this work would be more successful if chromophores with sharper absorbance and emission peaks were used instead of functionalized BODIPY derivatives. Nevertheless, this is a proof of principle study and the principle has been proved: namely it's possible to design a ratiometric chemosensor via modulation of energy donor efficiency.

It's expected that future work in our laboratory will adress such minor problems in near future and incorporation of solubility enhancing groups will no doubt result in practically useful chemosensors which can be used in various studies including cellular biology of biologically relevant cations.

REFERENCES

1. Lehn, J.M. *Supramolecular Chemistry: Concepts and Perspectives*, VCH, Weinheim, **1995**

2. Balzani, V.; Scandola, F. *Supramolecular Photochemistry*, Horwood, Chichester, **1991**

3. Vögtle F. *Supramolecular Chemistry An Introduction*, Wiley, Chichester, **1991**

4. Lindsey, J.S. *New J. Chem.*, **1991**, *15*, 153

5. Whitesides, G.M.; Mathias, J.P.; Seto, C.T. *Science.*, **1991**, *254*, 1312

6. Lehn, J.M. *Perpectives in Coordination Chemistry*, VCH, Basel, **1992**, p. 447

7. Lehn, J.M. *Proc. Natl. Acad. Sci*. USA **2002**, *99*, 4763-4768

8. Kang, J.; Rebek, Jr. *Nature* **1997**, *385*, 50 - 52

9. Kang, J.; Hilmersson, G.; Santamaría, J.; Rebek, Jr. *J. Am. Chem. Soc*. **1998**, *120*, 3650 – 3656

10. Kang, J.; Santamaría, J.; Hilmersson, G.; Rebek, Jr. *J. Am. Chem. Soc*. **1998**, *120*, 7389 – 7390

11. Manez, R.M.; Sancenon, F. *Chem. Rev.* **2003,** *103,* 4419–4476

12. Slone, R.V.; Benkstein, K.D.; Belanger, S.; Hupp, J.T.; Guzei, I.A.; Rheingold, A.L. *Coord. Chem. Rev.* **1998**, *171*, 221 – 243

13. Beer, P.D.; Szemes, F.; Balzani, V.; Sala, C.M.; Drew, M.G.B; Dent, S.W.; Maestri, M. *J. Am. Chem. Soc.* **1997,** *119*, 11 864 – 11875

14. Beer, P.D. *Chem. Commun.* **1996**, 689 – 696

15. Leung, K.C.F.; Nguyen, T.D.; Stoddart, J.F.; Zink, J.I. *Chem. Matter.,* **2006**, *18*, 5919

16. Feringa, B.L. *J. Org. Chem.,* **2007**, *72*, 6635

17. Nijhuis, C. A.; Huskens, J.; Reinhoudt, D. N. *J. Am. Chem. Soc.,* **2004,** *126*, 12266

18. Paul, D.; Suzumura, A.; Sugimoto, H.; Teraoka, J.; Shinoda, S.; Tsukube, H. *J. Am. Chem. Soc.* **2003**, *125*, 11478

19. Pauvert, M.; Laine, P.; Jonas, M.; Wiest, O. *J. Org. Chem.* **2004**, *69*, 543

20. Regehly, M.; Greish, K.; Rancan, F.; Maeda, H.; Bohm, F.; Roder, B. *Bioconjugate Chem*. **2007**, *18*, 494

21. Balzani, V.; Credi, A.; Raymo, F.M.; Stoddart, J.F. *Angew. Chem.* **2000,** *112*, 3484 – 3530

22. Valeur, B. *Molecular Fluorescence,* Wiley-VCH, Weinheim, **2002,** p. 10

23. Lakowicz, J.R. *Principles of Fluorescence Spectroscopy*, Plenum Press, New York, **1999**

24. De Silva, A.P.; Gunaratne, H.Q.N.; Gunnlaugsson, T.; Huxley, A.J.M.; Rademacher, J.T; Rice, T.E. *Chemosensors for Ion and Molecule Recognition,* Ed. Czarnik, A.W. Deseverge, J.P. NATO ASI Series, Series C; Mathematical and Physical Sceinces, Vol.*492*, pp 143-147, Kluwer Academic Publishers, **1997**

25. Metzger, A.; Lynch, V.M.; Anslyn, E. V. *Angew. Chem. Int. Ed. Engl,* **1997**, *36*, 862

26. Valeur, B. *Molecular Fluorescence*, Wiley-VCH: Weinheim, **2002**

27. Rurack, K.; Resch-Genger, U. *Chem. Soc. Rev*. **2002**, *31*, 116–127

28. Valeur, B.; Leray, I. *Coord. Chem. Rev.* **2000**, *205*, 3-40

29. De Silva, A.P.; de Silva, S.A. *J. Chem. Soc. Chem. Commun.* **1986**, 1709

30. De Silva, A.P.; Gunaratne, H.Q.N. and Sandanayake, K.R.A.S. *Tetrahedron Lett. 31*, **1990**, p. 5193

31. Fabbrizzi, L.; Lichelli, M.; Pallavicini, P.; Perotti, A. and Sacchi, D. *Angew. Chem. Int. Ed. Engl. 33*, **1994**, p. 1975

32. Turfan, B.; Akkaya, E. U. *Org. Lett*. **2002**, *4*, 2857–2859

33. Kim, S.K.; Lee, S.H.; Lee, J.Y.; Bartsch, R.A.; Kim, J.S. *J. Am. Chem. Soc.* **2004**, *126*, 16499–16506

34. Turfan, B.; Akkaya, E.U. *Org. Lett.* **2002**, *4*, 2857-2859

35. Mateeva, N.; Enchev, V.; Antonv, L.; Deligeorgiev, T.; Mitewa, M. *J. Incl. Phenom.* **1995**, *93*, 323

36. Martin, M.M.; Be´gin, L.; Bourson, J.; Valeur, B. *J. Fluoresc.* **1994**, *4*, 271

37. Treibs, A.; Kreuzer, F.-H. Justus Liebigs Ann. Chem. 1968, *718*, 208

38. López Arbeloa F.; Bañuelos J.; Martínez V.; Arbeloa T.; López Arbeloa I. *Int Rev Phys Chem*, **2005**, *24*, 339–374

39. Thoresen, L. H.; Kim, H.; Welch, M. B.; Burghart, A.; Burgess, K. *Synlett* **1998**, 1276

40. Wada, S.; Ito, S.; Uno, H.; Murashima, T.; Ono, N.; Urano, T.; Urano, Y. *Tetrahedron Lett*. **2001**, *42*, 6711

41. Ela, S.E.; Yilmaz, M.D.; Icli, B.; Dede, Y.; Icli, S.; Akkaya, E.U. *Org.Lett.* **2008**, *10* (15), 3299-3302

42. Hattori, S.; Ohkubo, K.; Urano, Y.; Sunahara, H.; Nagano, T.; Wada, Y.; Tkachenko, N.V.; Lemmetyinen, H.; Fukuzumi, S. *J. Phys. Chem. B*. **2005**, *109*, 15368

43. Rurack, K.; Resch-Genger, U. *Chem. Soc. Rev*. **2002**, *31*, 116

44. Metzker, M.L.; Lu, J.; Gibbs, R.A. *Science,***1996**, *271*, 1420–1422

45. Farber, S.A.; Pack, M.; Ho S.Y.; Johnson, I.D.; Wagner, D.S.; Dosch, R.; Mullins, M.C.; Hendrickson ,H.S.; Hendrickson, E.K.; Halpern, M.E. *Science*, **2001**, *292*, 1385–1388

46. Lammi, R.K.; Wagner, R.W.; Ambroise, A.; Diers, J.R.; Bocian, D.F.; Holten, D.; Lindsey, J.S. *J Phys Chem B*, **2001**, *105*, 5341–5352

47. Wan, C.-W.; Burghart, A.; Chen, J.; Bergström, F.; Johansson, L.B.A.; Wolford, M.F.; Kim, T.G.; Topp, M.R.; Hochtrasser, R.M.; Burgess, K. *Chem Eur J,* **2003**, *9*, 4430–4441

48. Harriman, A.; Izzet, G.; Ziessel, R. *J Am Chem Soc,* **2006**, *128*, 10231–10239

49. Karolin, J.; Johansson, L.B.-A.; Strandberg, L.; Ny, T. J. *Am. Chem. Soc.,* **1994**, *116*, 7801

50. Coskun, A.; Deniz, E.; Akkaya, E. U. *Tetrahedron. Lett*., **2007**, *48*, 5359

51. Coskun, A.; Yilmaz, M.D.; Akkaya, E. U. *Org. Lett*., **2007**, *9*, 607

52. Coskun, A.; Akkaya, E. U. *J. Am. Chem. Soc.,* **2005**, *127*, 10464

53. Atilgan, S.; Ekmekci, Z.; Dogan, A.L.; Guc, D.; Akkaya, E.U. *Chem. Commun.*, **2006**, 4398

54. Li, L.; Han, J.; Nguyen, B.; Burgess, K. *J. Org. Chem*., **2008**, *73*, 1963

55. Thivierge, C.; Bandichhor, R.; Burgess, K. *Org. Lett*., **2007**, *9*, 2135

56. Yogo, T.; Urano, Y.; Ishitsuka, Y.; Maniwa, F.; Nagano, T. *J. Am. Chem. Soc*., **2005**, *127*, 12162

57. Magos, L. *Physiol Toxicol Mercury,* **1997**, *34*, 321–370

58. Von Burg, R. *J Appl Toxicol,* **1995**, *15* (6), 483–493

59. Welz, B.; Sperling, M. *Atomic absorption spectrometry*, 3rd ed. Weinheim, Germany, Wiley, **1999**

60. Moreton, J.A.; Delves, H.T. *J. Anal. At. Spectrom*. **1998**, *13*(7), 659–665

61. Xiao-Bing Zhang; Can-Cheng Guo; Zhi-Zhang Li; Guo-Li Shen; Ru-Qin Yu; *Anal. Chem*. **2002**, *74*, 821–825

62. Qi-Yin Chen; Chuan-Feng Chen *Tetrahedron Lett.* **2005**, *46*, 165–168

63. R.G. Pearson *J. Am. Chem. Soc*. **1963**, *85*, 3533

64. Du, J.; Fan, J.; Peng, X.; Li, H.; Wang, J.; Sun, S. *J.Fluoresc*. **2008**, asap article

65. Nolan, E.M.; Lippard, S.J. *J. Am. Chem. Soc.*, **2003**, *125*, 14270-14271

66. Coskun, A.; Akkaya, E.U. *J. Am. Chem. Soc.,* **2006**, *128*, 14474-14475

67. Förster, T. *Ann. Phys*., **1948**, *2*, 55

68. Förster, T. Z. *Naturforsch*., **1949**, *4*, 321

69. Dexter, D.L. *J. Chem. Phys*., **1953**, *21*, 836

70. Lakowicz, J.R. *Principles of Fluorescence Spectroscopy*, 2nd ed., Kluwer/Plenum, New York, **1999**

71. Wang, P.; Wu, S. *J. Photochem. Photobiol. A*, **1998**, *118*, 7

72. Turro, N.J., *Modern Molecular Photochemsitry*, University Science Books, Sausalito, **1991**

73. Ulrich, G.; Ziessel, R. J. *Org. Chem*. **2004**, *69*, 2070–2083. (Ref.3b)

74. Sudeep, P.K.; Thomas, K.G.; George, M.V.; Barazzouk, S.; Kamat, P.V. *Org.Lett.* **2002**, *2*(1), 29-35

75. Hsung, R. P.; Babcock, J. R.; Chidsey, C. E. D.; Sita, L. R. *Organometallics*, **1995**, *14*, 480

76. Ishikawa, J. *Bull. Chem. Soc. Jpn.* **1995**, *68*, 3071-76

APPENDIX

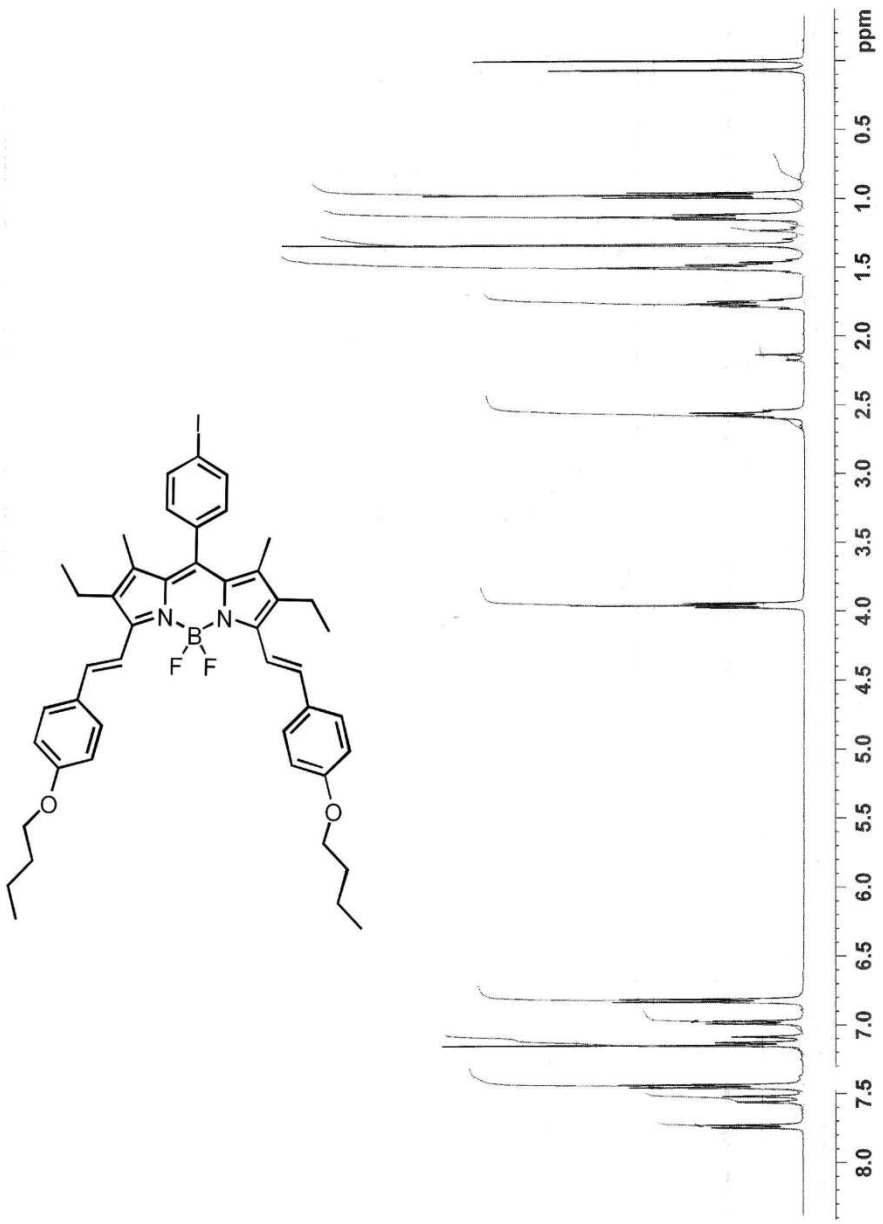

Figure 48. ^{1}H spectrum of compound **24**

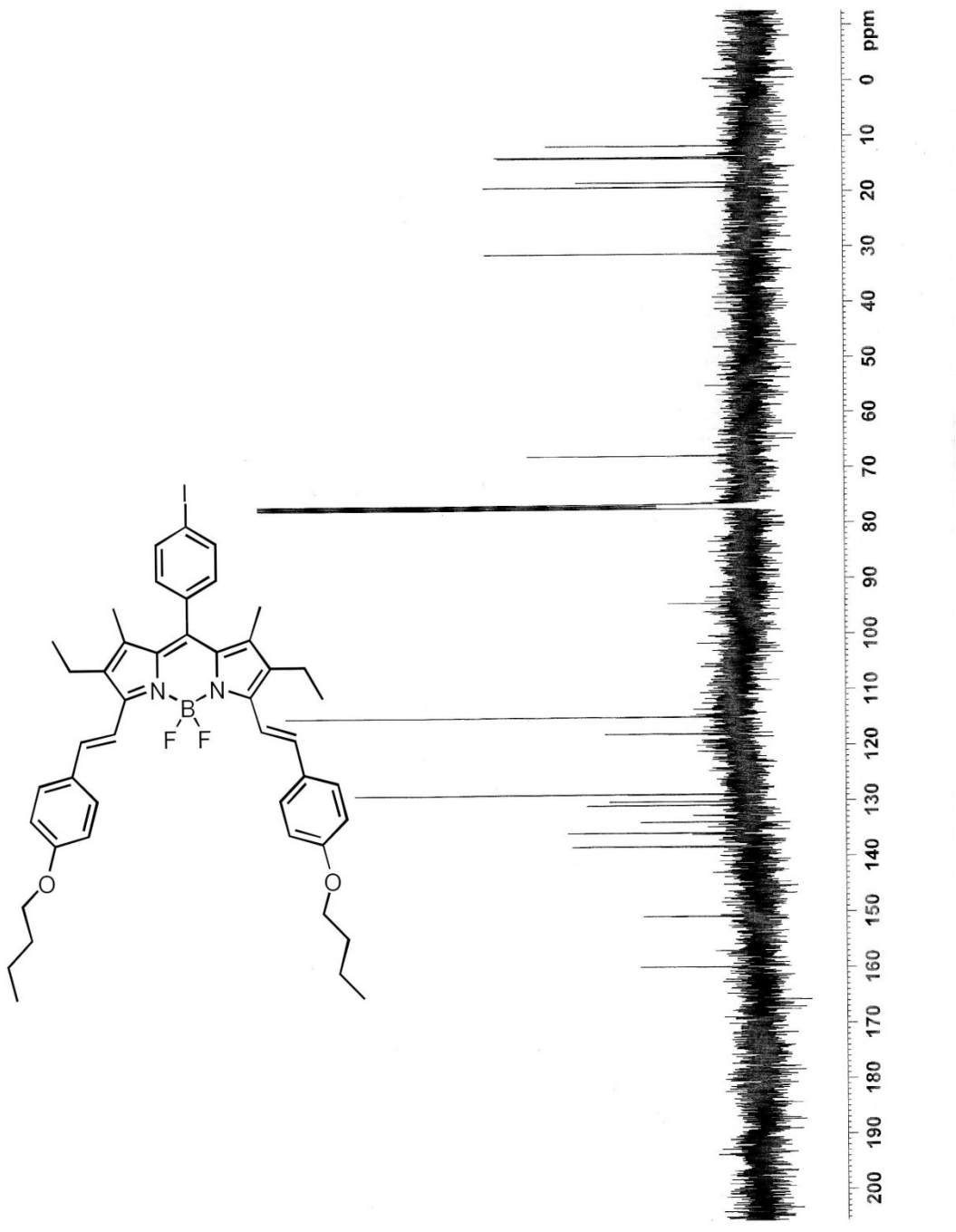

Figure 49. ^{13}C spectrum of compound **24**

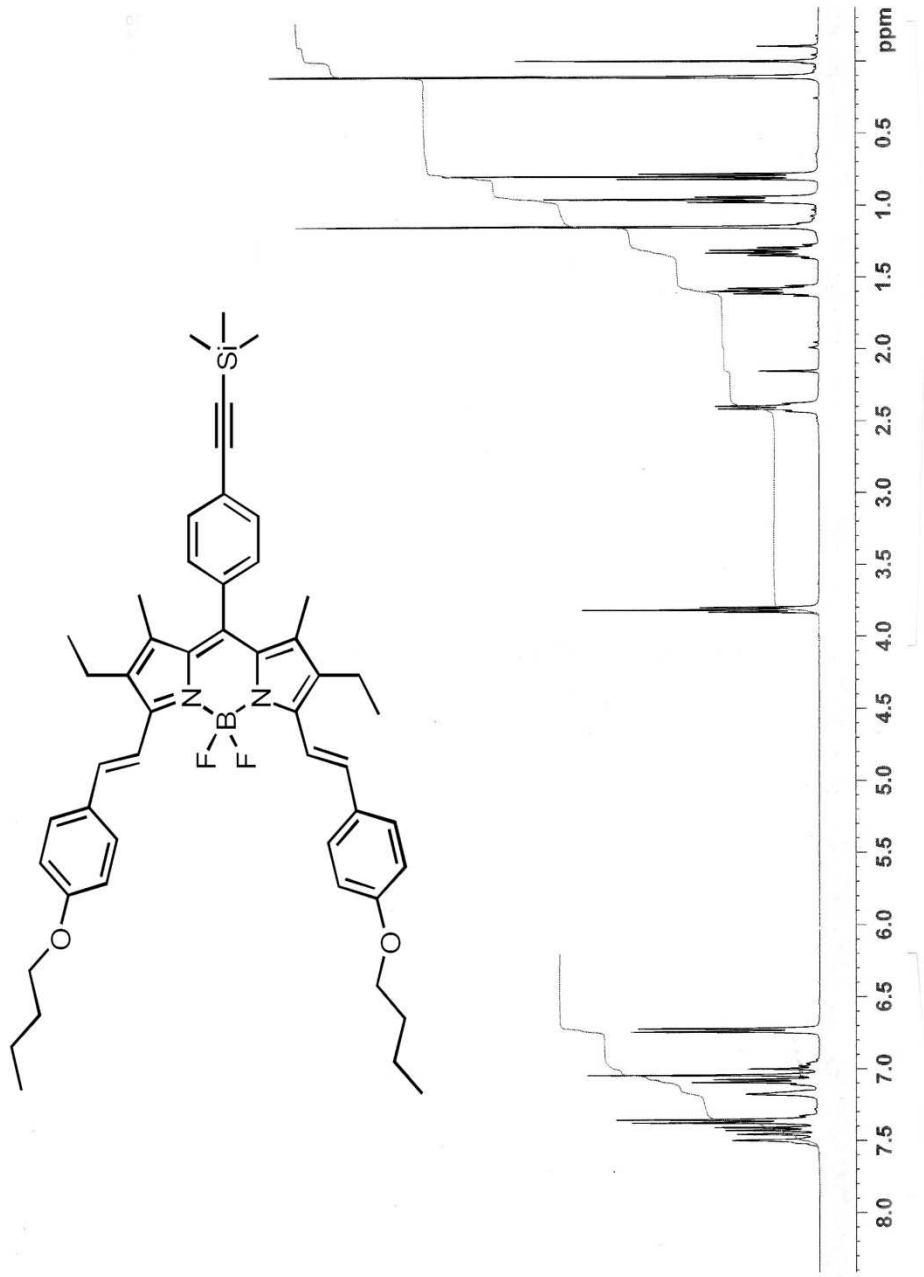

Figure 50. ^{1}H spectrum of compound **25**

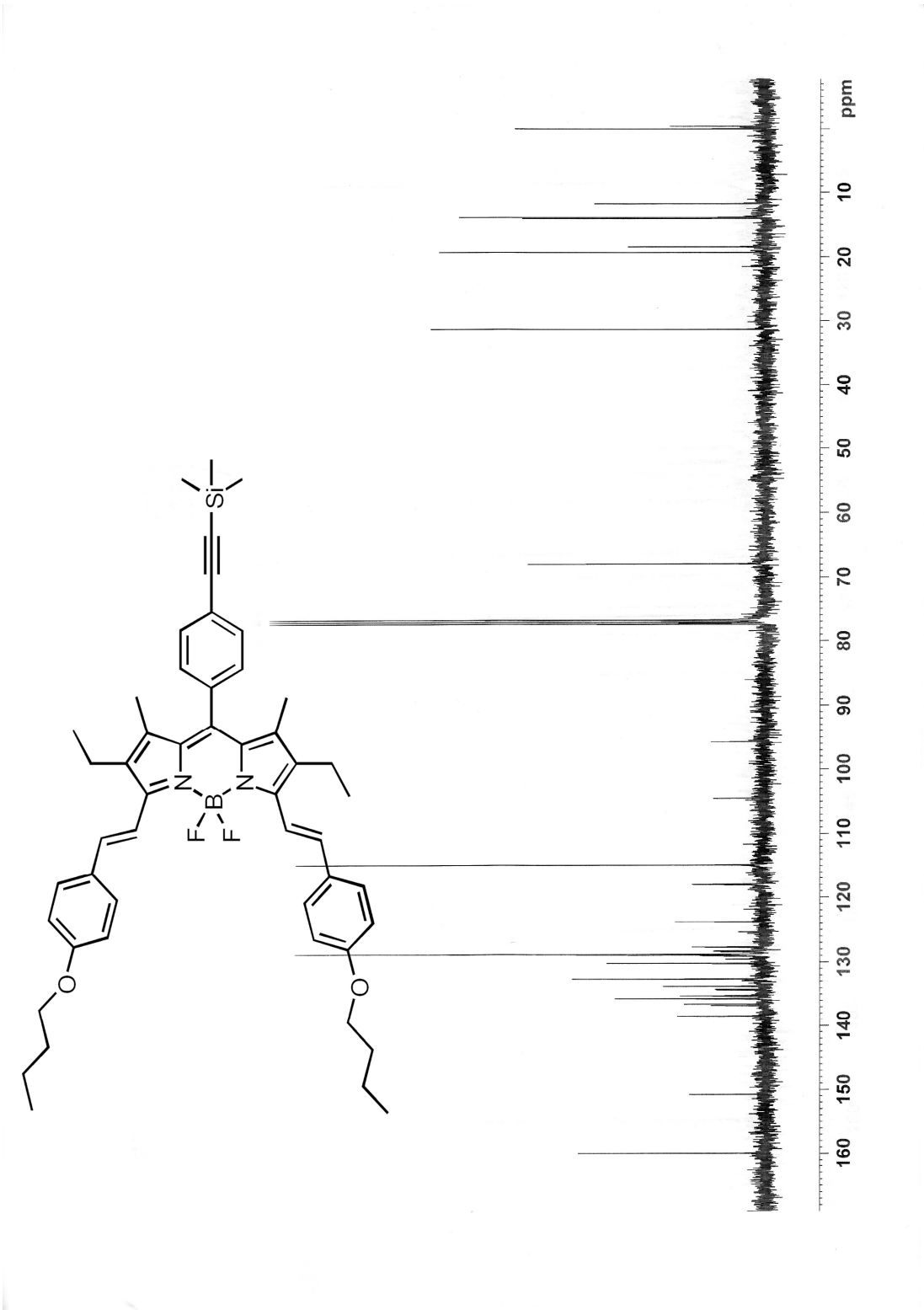

Figure 51. ^{13}C spectrum of compound **25**

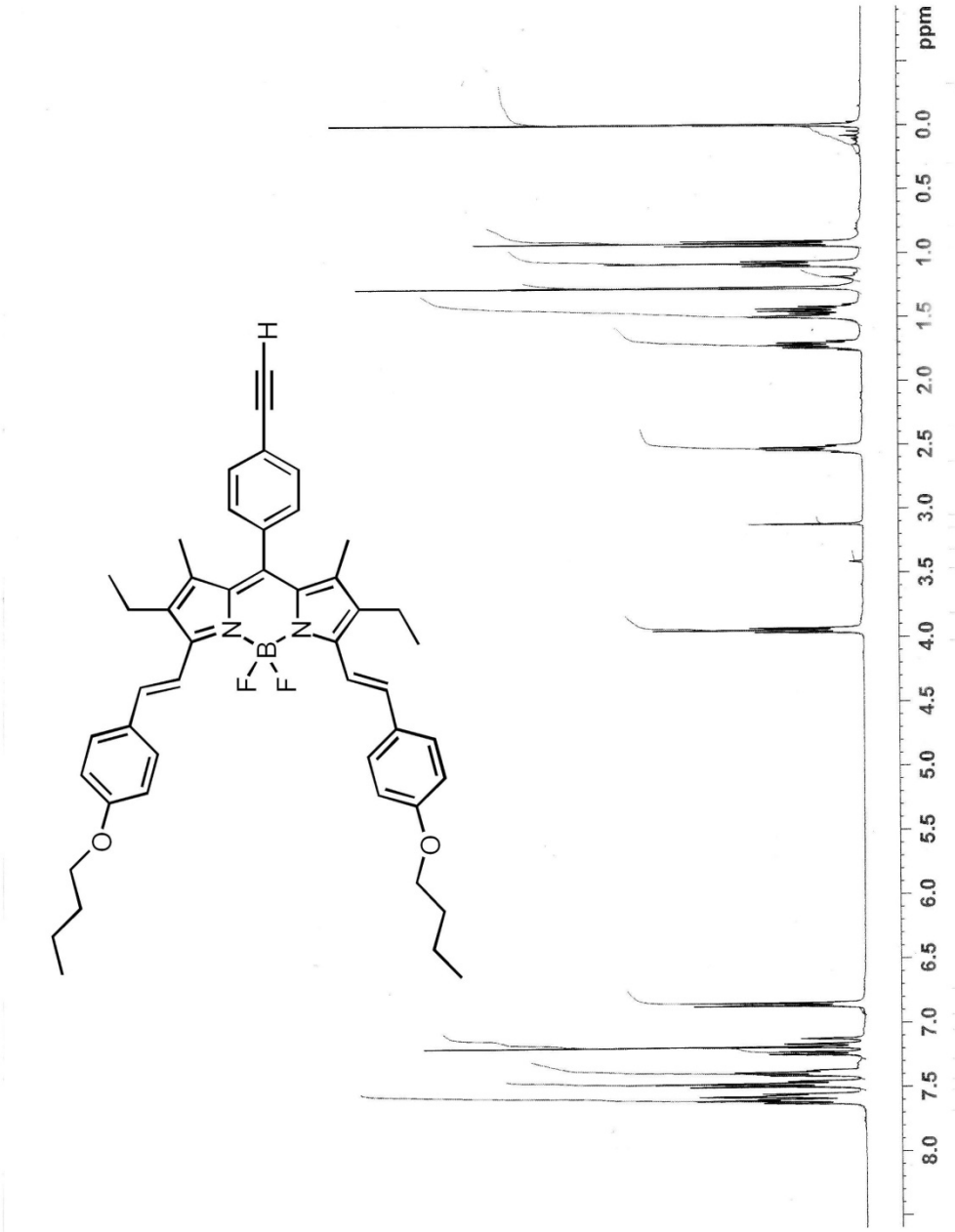

Figure 52. ^{1}H spectrum of compound **26**

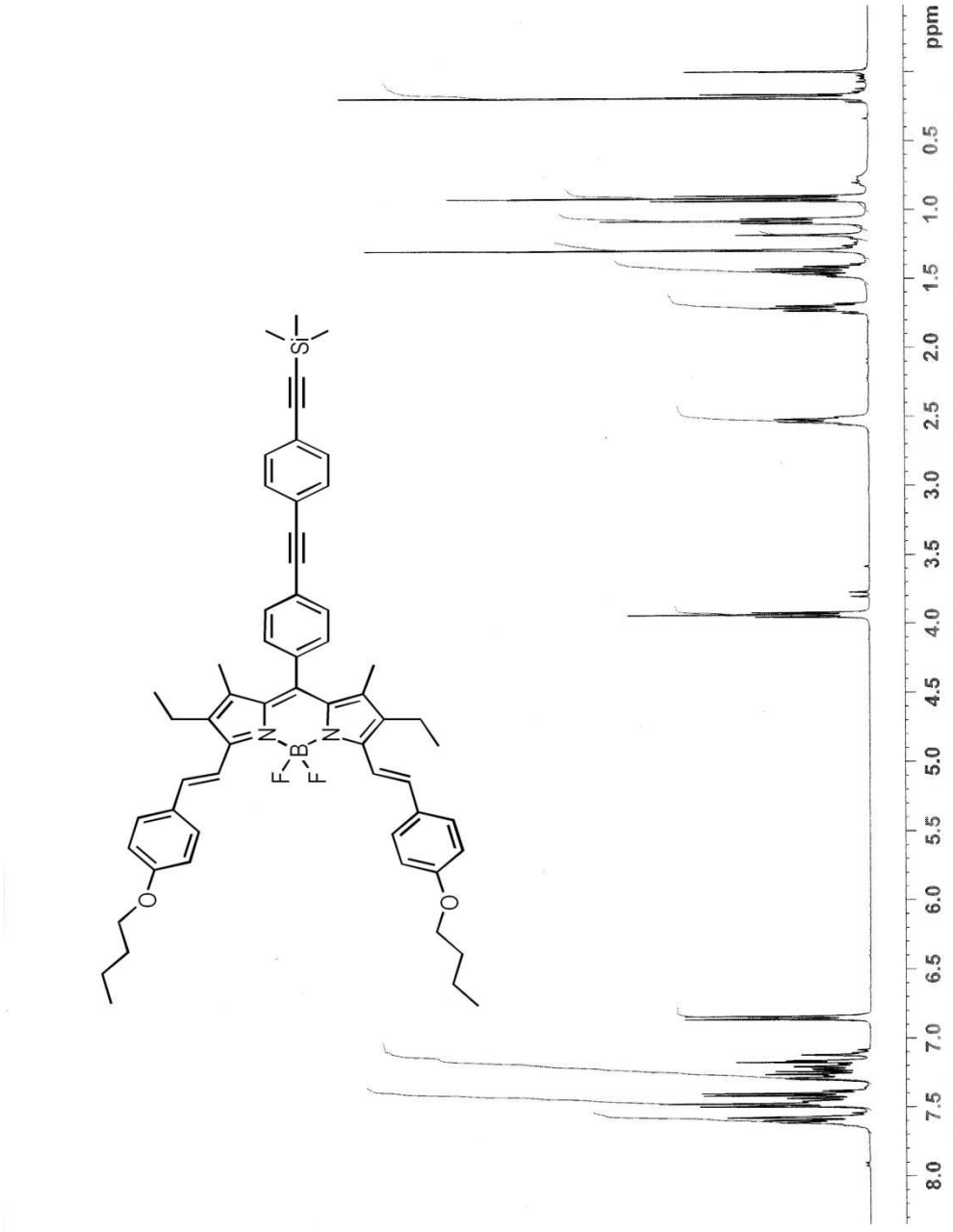

Figure 53. ^{1}H spectrum of compound **27**

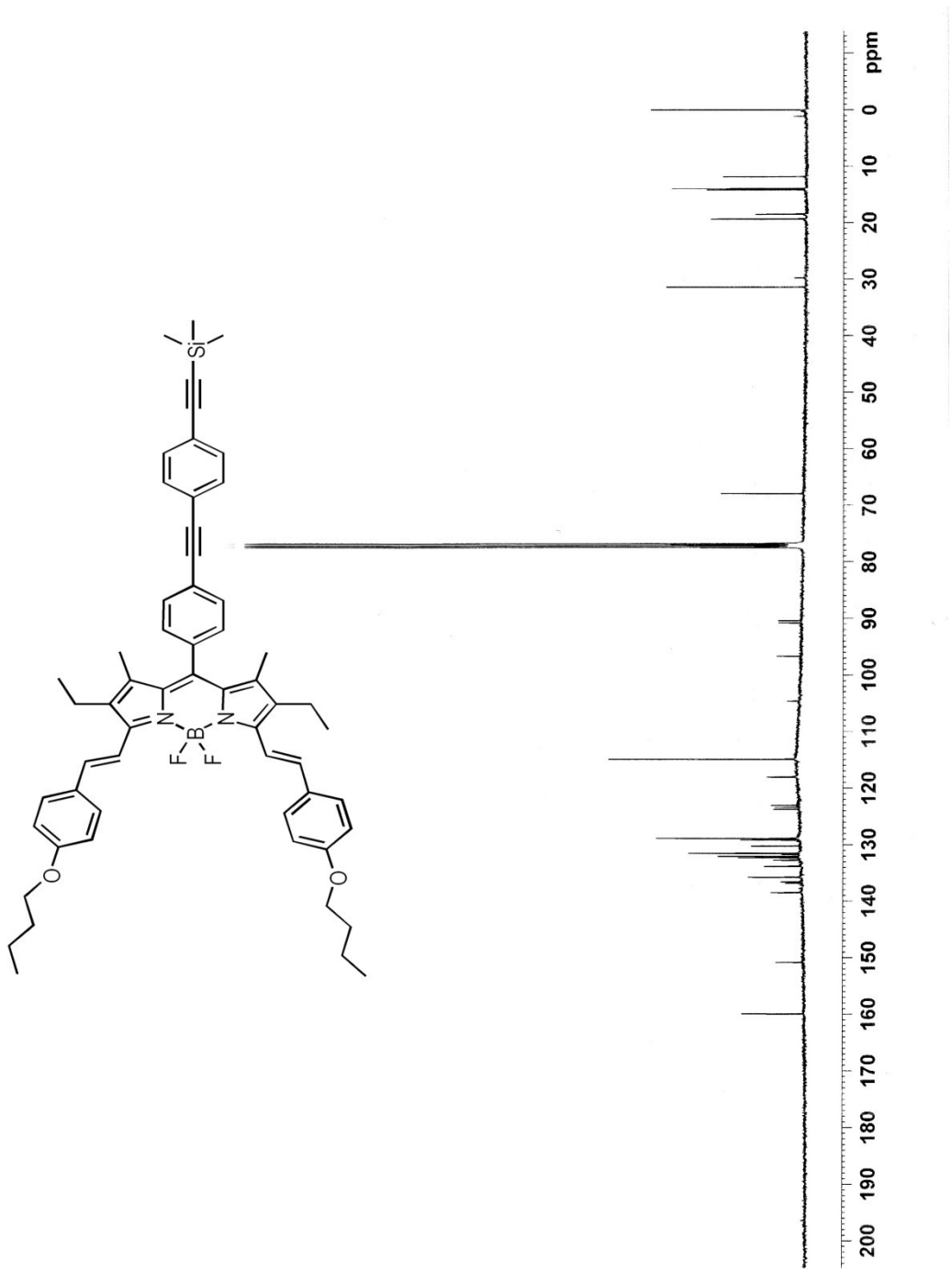

Figure 54. ^{13}C spectrum of compound **27**

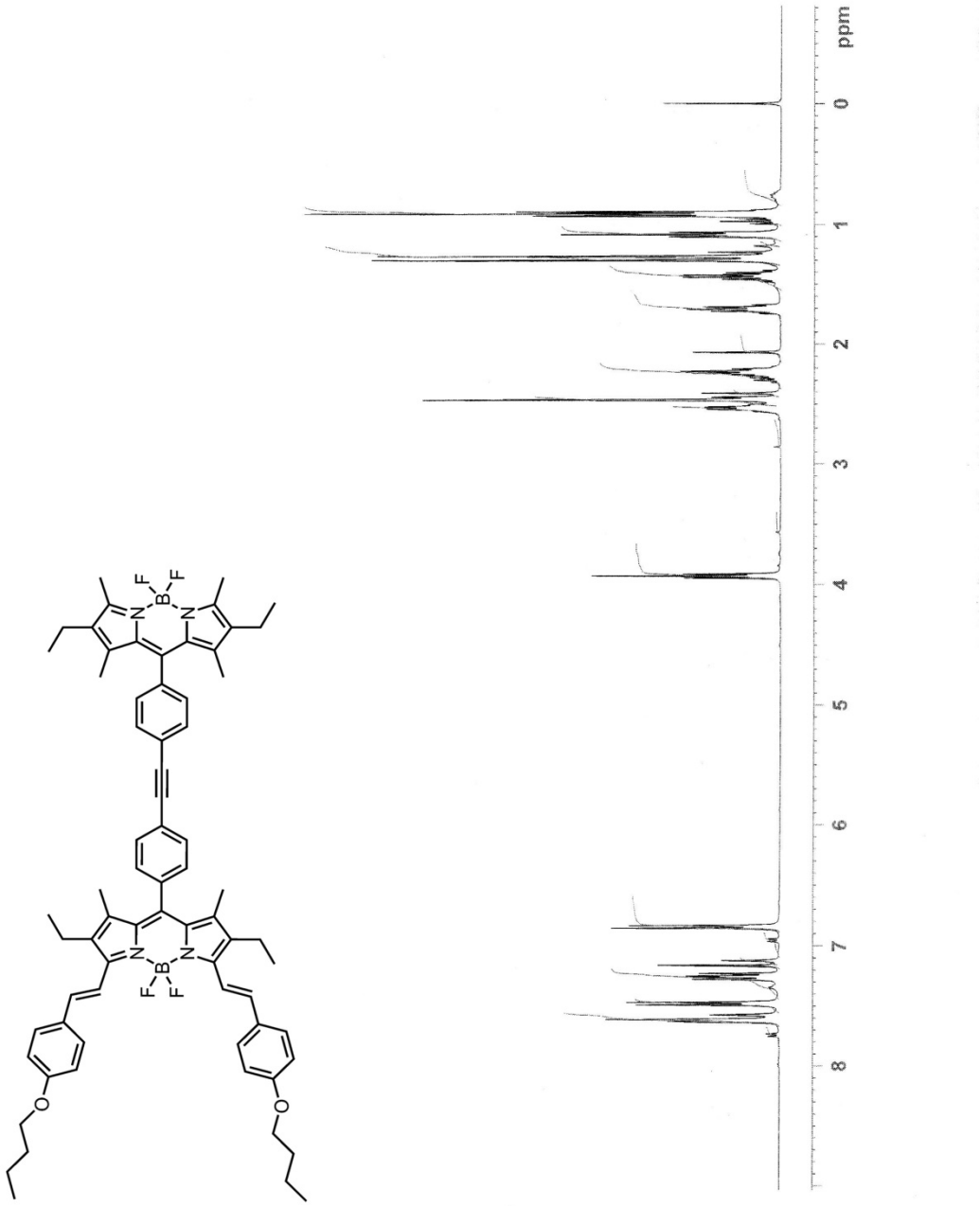

Figure 55. ^{1}H spectrum of compound **29**

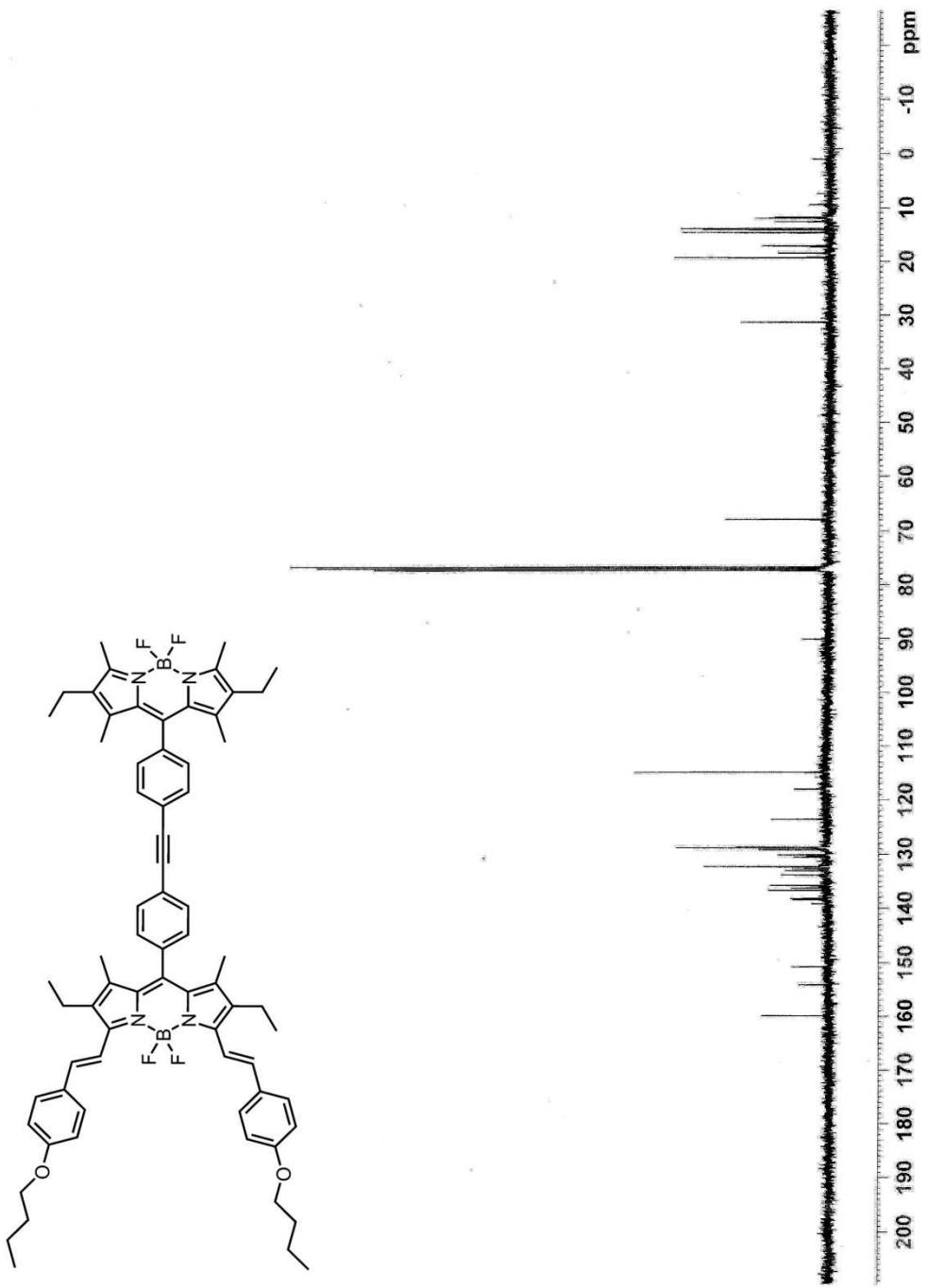

Figure 56. ^{13}C spectrum of compound **29**

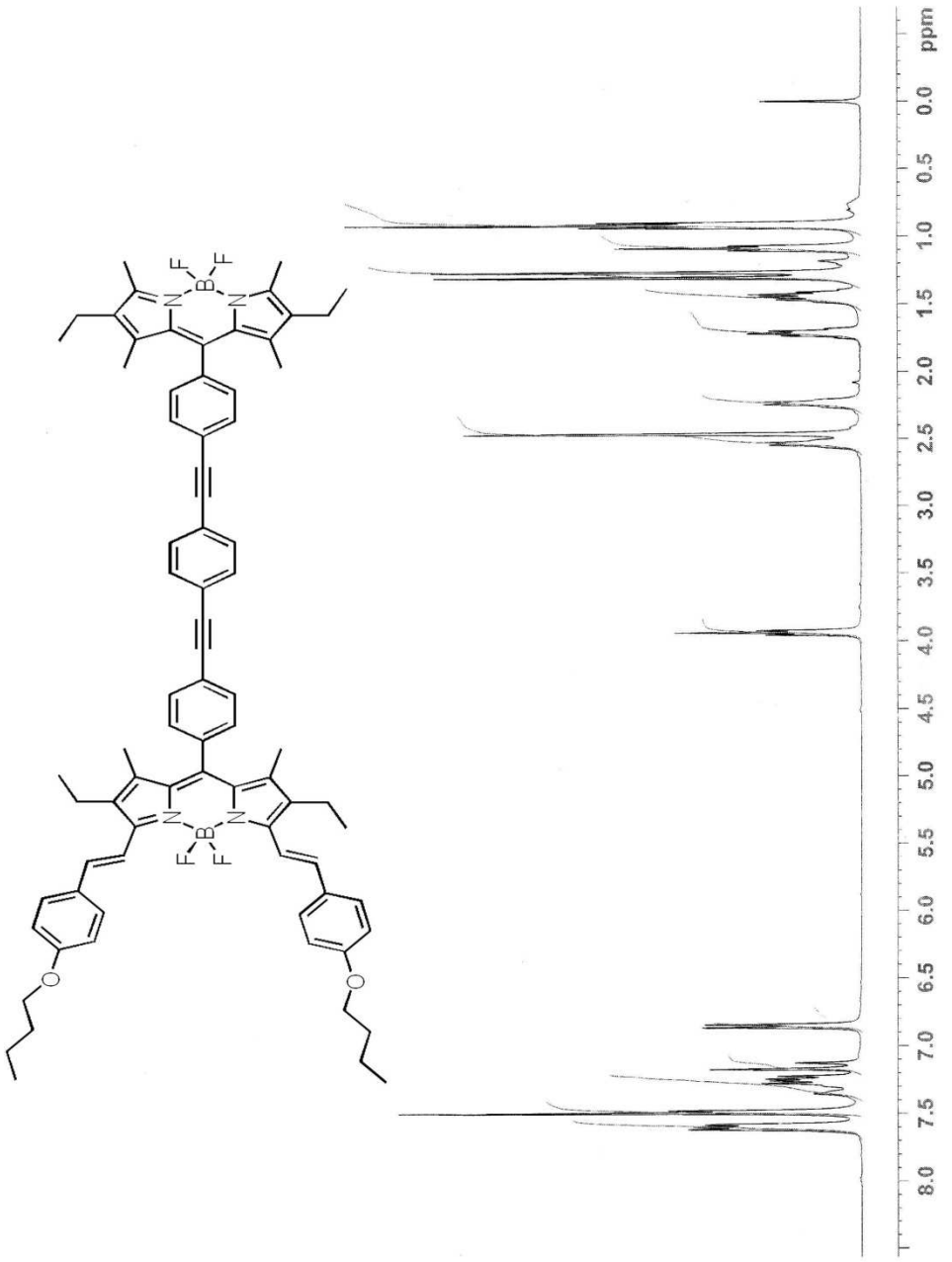

Figure 57. ^{1}H spectrum of compound **30**

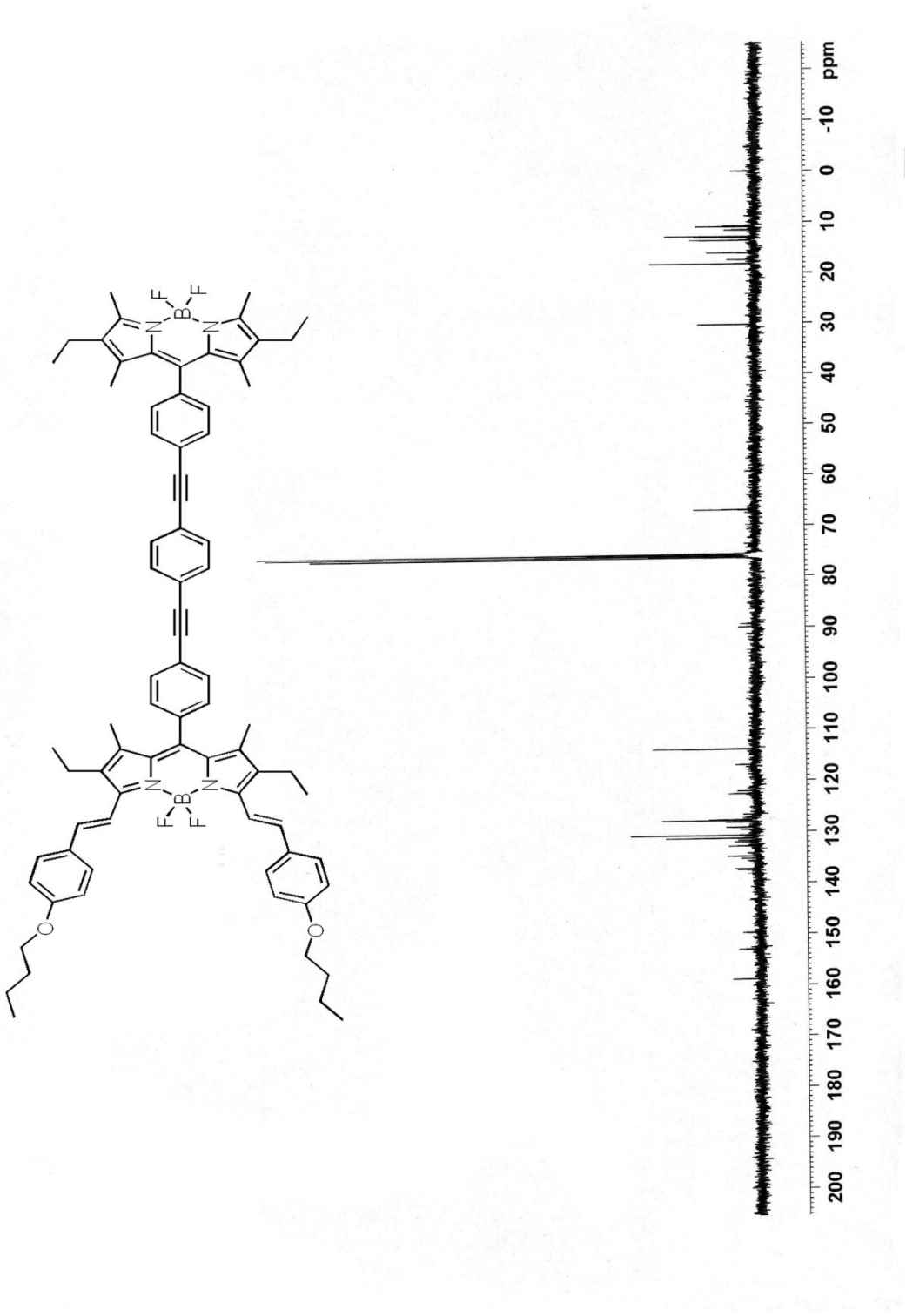

Figure 58. ^{13}C spectrum of compound **30**

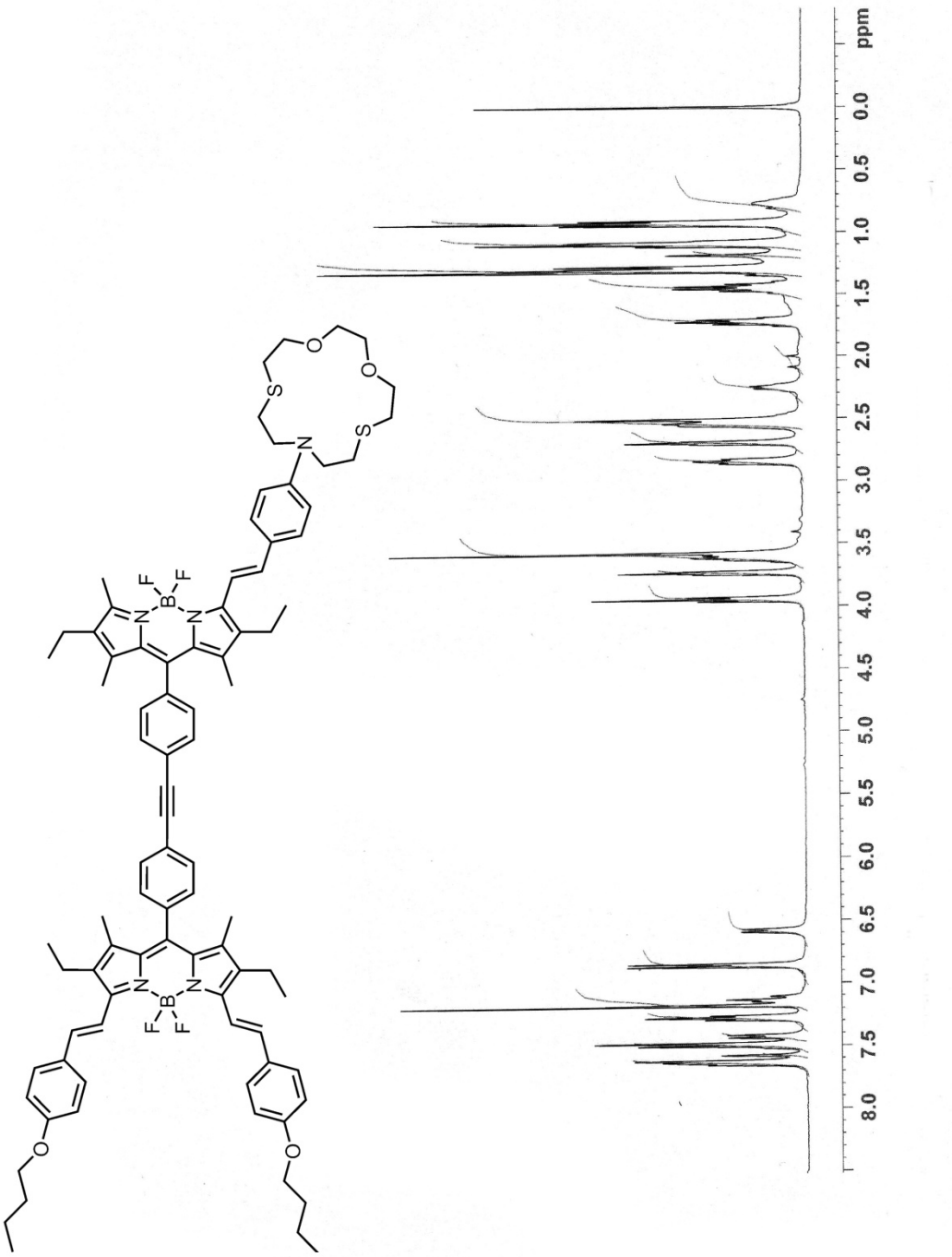

Figure 59. ^{1}H spectrum of compound **33**

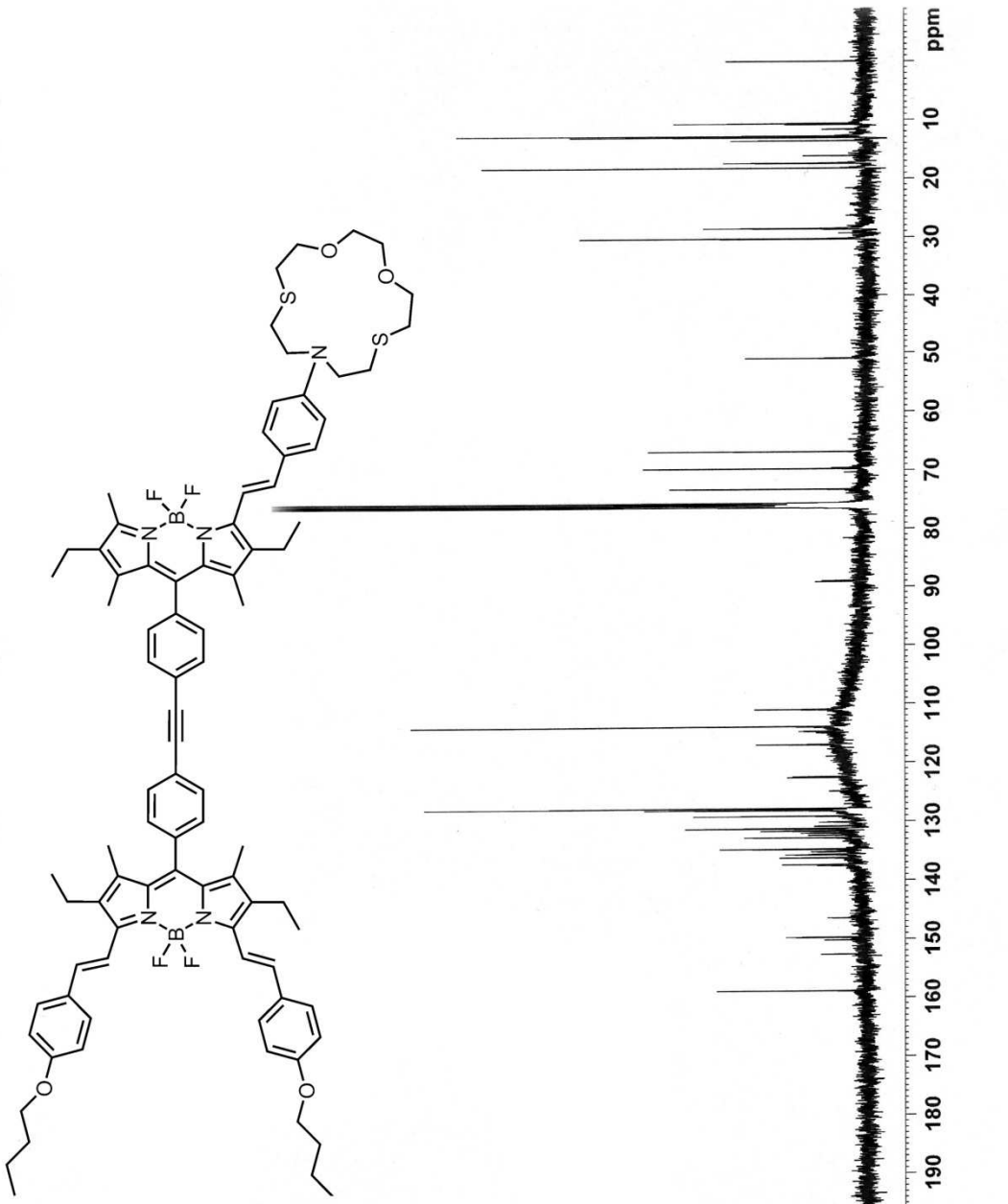

Figure 60. ^{13}C spectrum of compound **33**

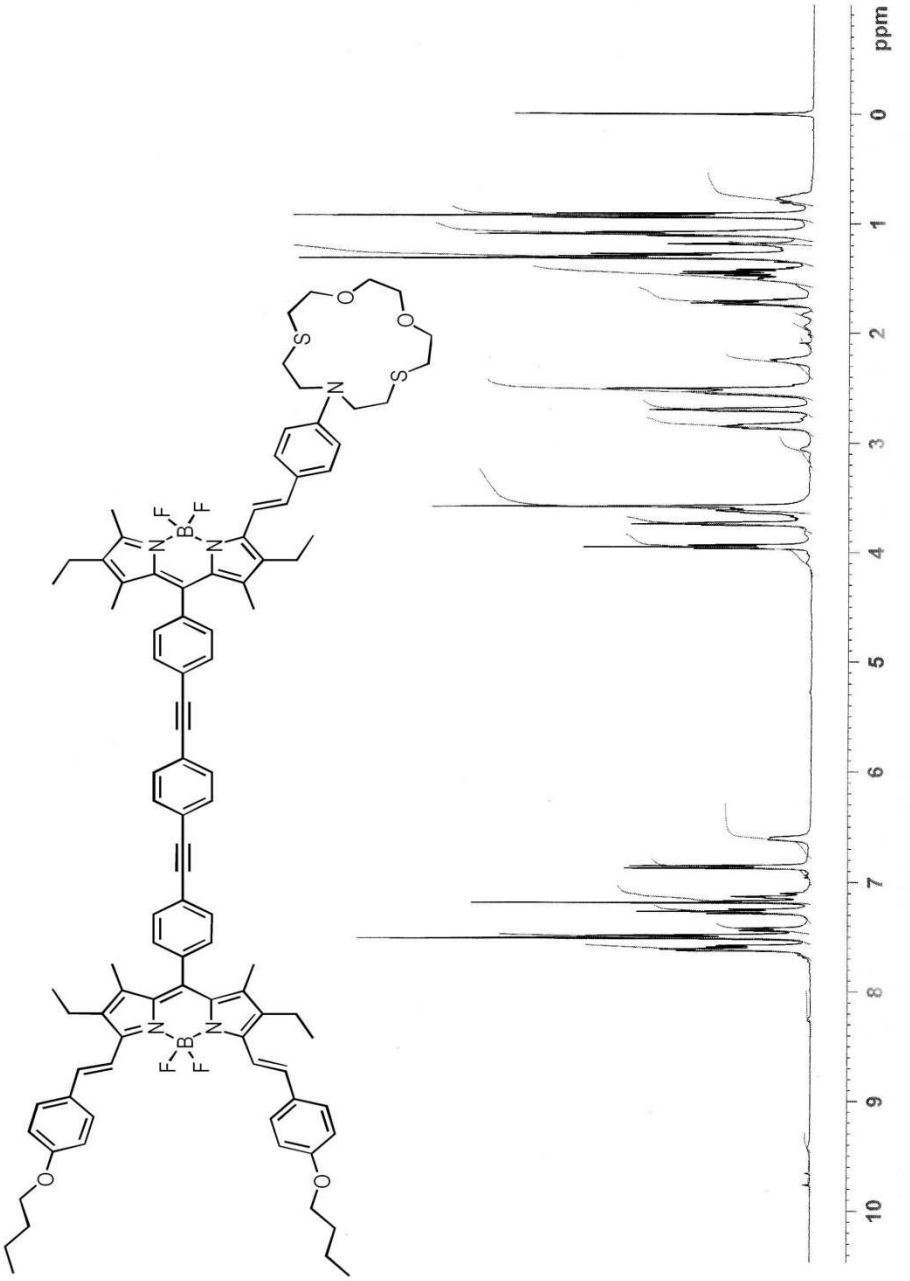

Figure 61. ^{1}H spectrum of compound **34**

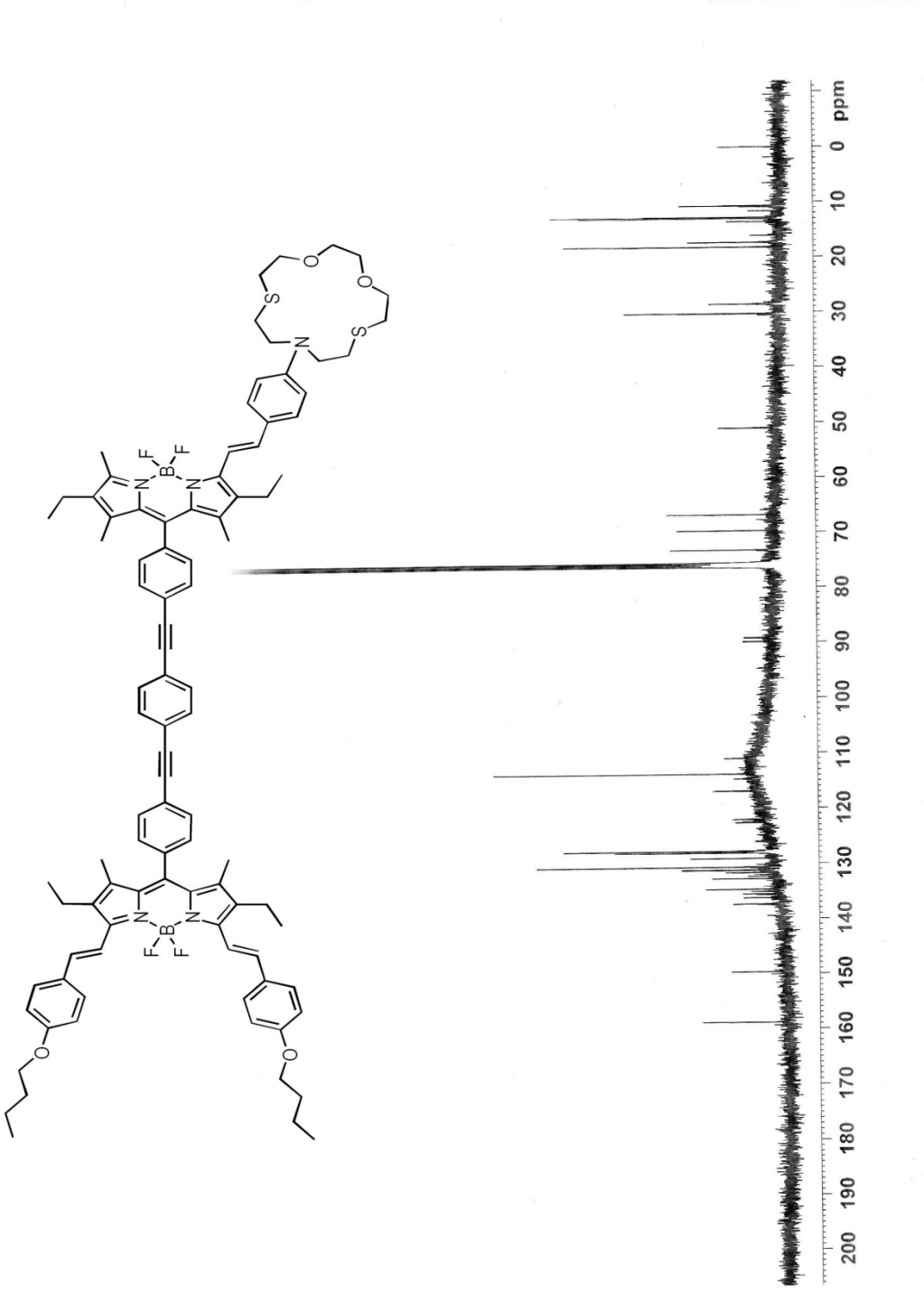

Figure 62. ^{13}C spectrum of compound **34**

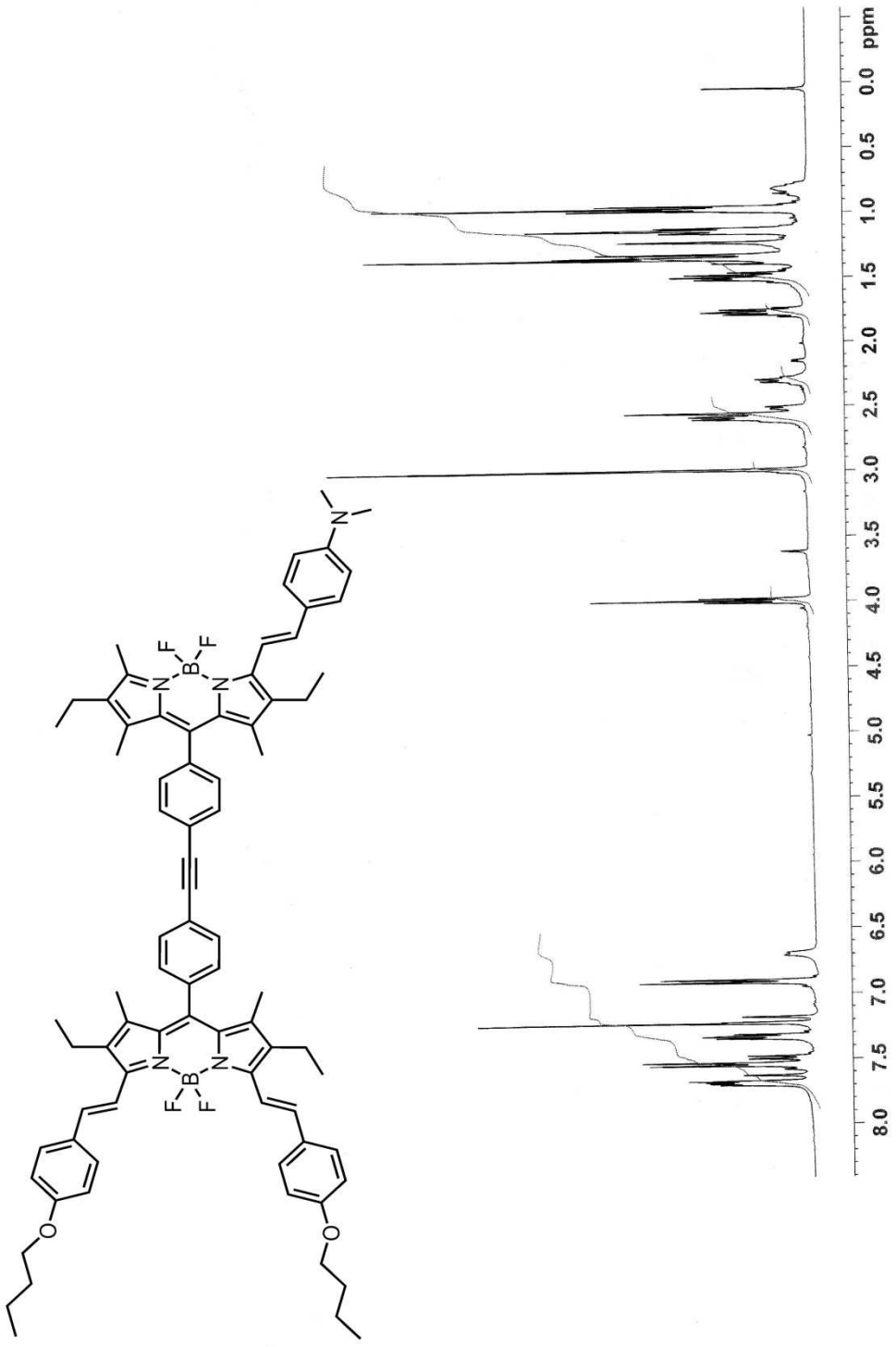

Figure 63. ^{1}H spectrum of compound **31**

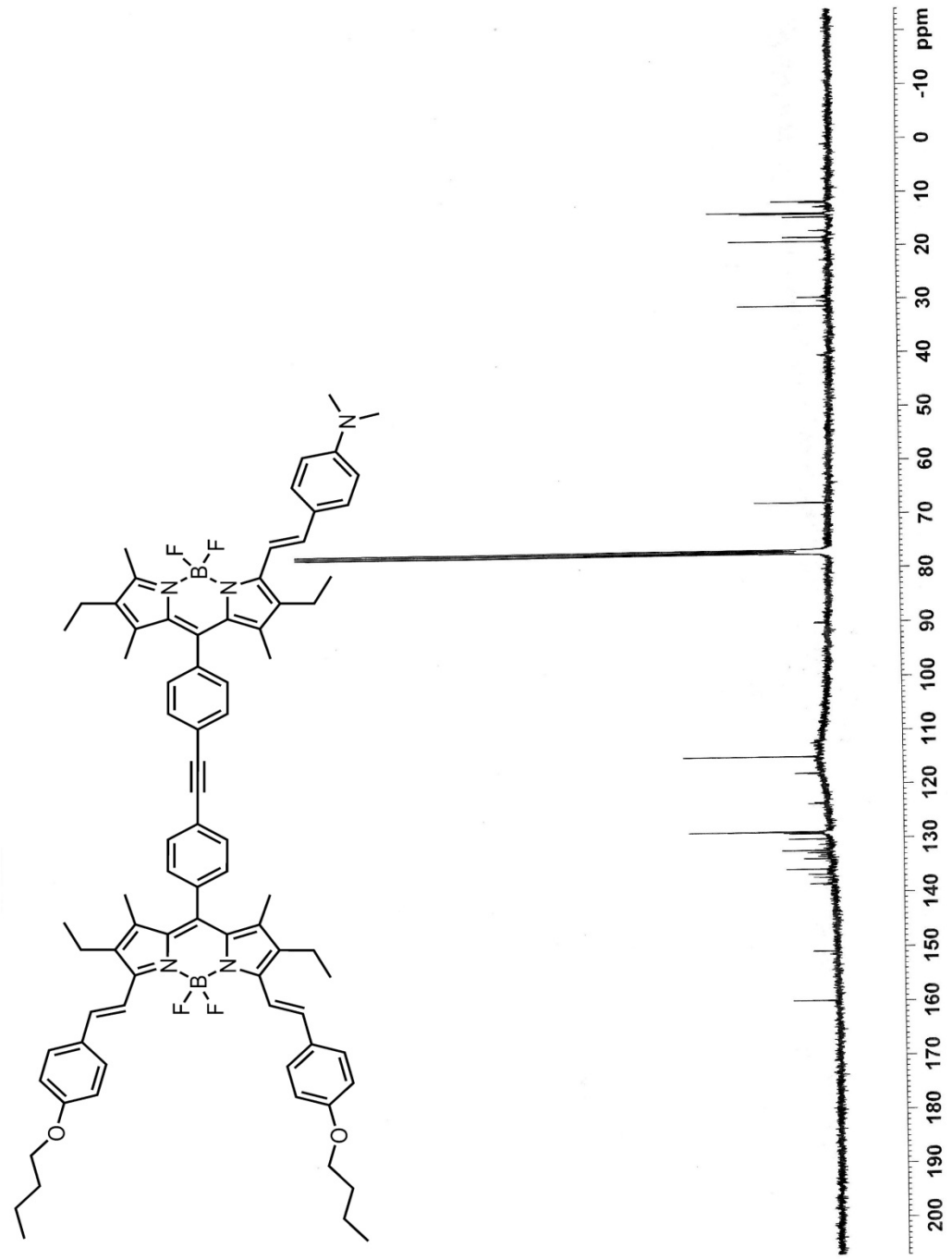

Figure 64. ^{13}C spectrum of compound **31**

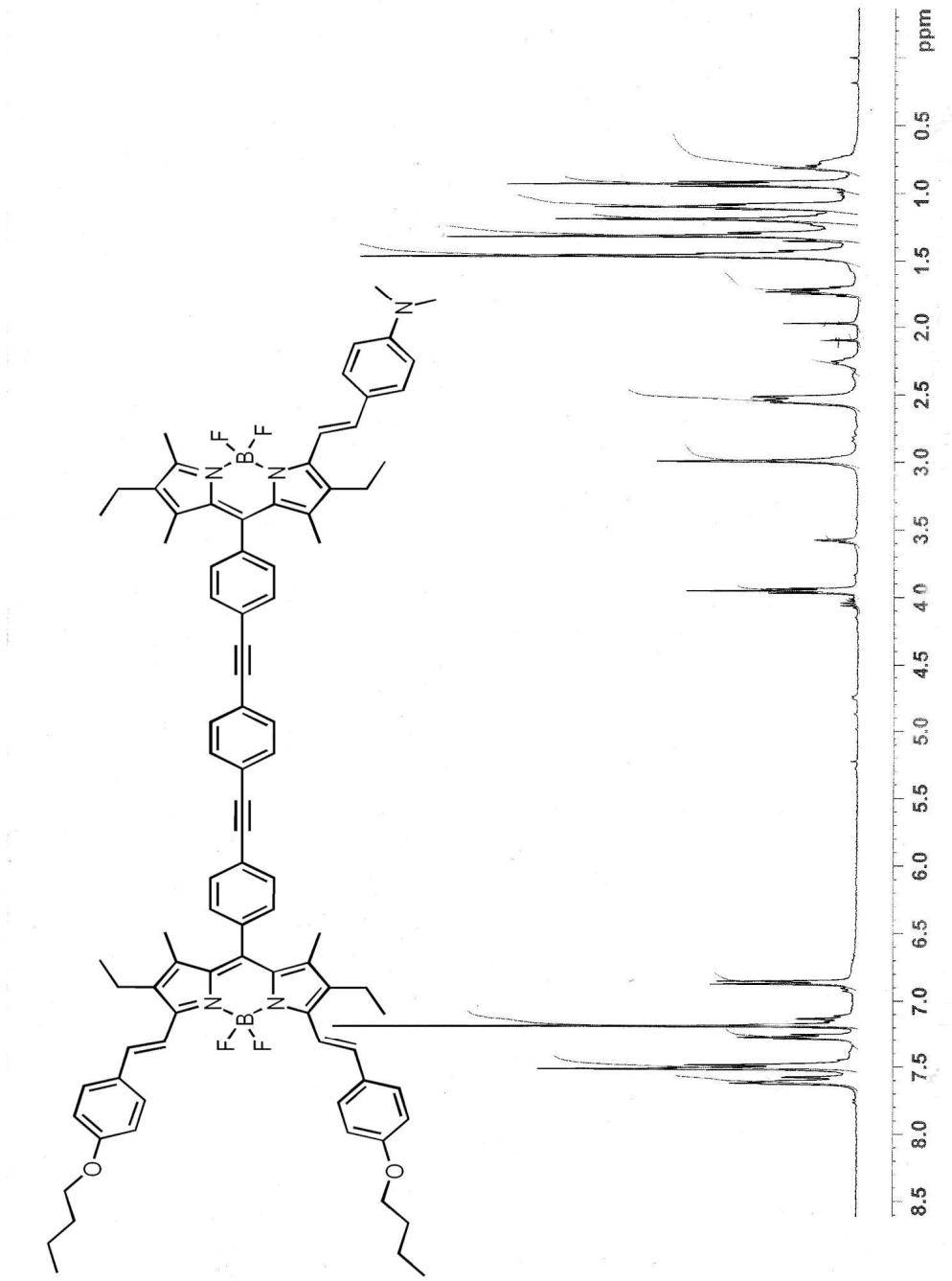

Figure 65. ^{1}H spectrum of compound **32**